GAS CHROMATOGRAPHY-MASS SPECTROMETRY ANALSYIS, *IN VITRO* ANTIBACTERIAL EFFICACY AND *IN SILICO* MOLECULAR DOCKING OF COMPOUNDS PRODUCED BY ENDOPHYTES ISOLATED FROM INDEGENOUS MEDICINAL PLANTS.

A dissertation submitted in partial fulfilment of the requirements for the degree of **Master in Science in Biotechnology**

By

Kudakwashe Nyambo (R1811081)

Supervisor: Professor Idah Sithole-Niang

UNIVERSITY OF ZIMBABWE

FACULTY OF SCIENCE

DEPARTMENT OF BIOCHEMISTRY

AUGUST 2020

ABSTRACT

Native medicinal plants have been traditionally used to treat various bacterial infections, fungal infections, cancers, viral infections and cardiovascular diseases. Endophytic bacteria residing inside the tissues of traditional medicinal plants are capable of producing the therapeutically important bioactive compounds. The bioactive compounds can be used as alternative therapeutic agents thus helping to combat antimicrobial resistance in pathogenic bacteria. Currently bioactive compounds extracted from endophytic bacteria isolated from medicinal plants native to Zimbabwe has not been evaluated computationally. Therefore, this study aimed to characterise and evaluate the bioactive compounds secreted by endophytes isolated from native Zimbabwe trees for control of clinically important bacteria. Acetone, methanol and ethyl acetate extracts from 24 endophytes were evaluated for antimicrobial efficacy against *Escherichia coli* and *Staphylococcus aureus* by agar well diffusion assay. Total genomic DNA was extracted from the endophytic samples expressing potent antimicrobial activity. Amplification of 16 S rRNA gene was used to confirm that the endophytic isolated are bacteria. Amplification of RAPDs using the M13 forward primer was used to differentiate the endophytic bacteria. Gas chromatography-mass spectrometry (GC-MS) was used to identify the endophytic compounds present in the extracts and a SwissADME online tool was used to evaluate the pharmacokinetic properties of the most abundant endophytic compounds. The bioactivity spectrum of the selected endophytic compounds was predicted by a PASSonline tool. Potential bacteria protein targets namely lumazine synthase, tryptophan synthase subunit beta and UDP-N-acetylglucosamine 1-carboxyvinyltransfrase were selected for molecular docking to evaluate the specificity and affinity of the selected endophytic compounds to the potential drug targets. M13 RAPDs analysis indicated that the endophytic bacteria are not the same. Endophytic acetone extracts from sample 1, 3, 9 and 17 exhibited the strongest antimicrobial efficacy against *E. coli* and *S. aureus.* Sulfonamide derivates, pyrazolo(3,4-d)pyrimidine derivatives, indolizine derivatives, quinone derivatives, furan derivatives, organic acids, fused uracils, aroma compounds and phenolic compounds were identified by gas chromatography-mass. The diverse compounds identified by GC-MS could be responsible for potent antimicrobial activity against *E. coli* and *S. aureus.* Predicted solubility of the endophytic compounds ranged from soluble to very soluble in water, with only eicosane, 2-(1-Fluorovinyl)-5-nitropyridine, octadecane and hexadecane displaying poor solubility. Most of the abundant endophytic compounds satisfied the Lipinski's rule of five. Compounds that had predicted function of phobic treatment were all predicted to cross the blood-brain barrier. 3-Amino-2,2,4-trimethylhexane, octadecane, 2-(1H-Imidazol-2-yl)acetic acid, 2-Piperidinone and 5H,10H-Dipyrrolo[1,2-a:1',2'-d]pyrazine-5,10-dione, octahydro-, (5aS,10aS)- were the most abundant endophytic compounds in all endophytic samples and were selected for *in silico* molecular docking against potential antibacterial drug targets namely lumazine synthase, tryptophan synthase and UDP-N-acetylglucosamine 1-carboxyvinyltransfrase. Prediction of bioactivity spectrum of 3-Amino-2,2,4-trimethylhexane, octadecane, 2-(1H-Imidazol-2-yl)acetic acid, 2-Piperidinone and 5H,10H-Dipyrrolo[1,2-a:1',2'-d]pyrazine-5,10-dione, octahydro-, (5aS,10aS)- indicated that they have higher chances of exhibiting antimicrobial, and, anticancer and could also be useful in the treatment of phobic disorders. 5H,10H-Dipyrrolo[1,2-a:1',2'-d]pyrazine-5,10-dione, octahydro-, (5aS,10aS)- exhibited strong binding affinities to all three potential drug targets. The binding affinity of 5H,10H-Dipyrrolo[1,2-a:1',2'-d]pyrazine-5,10-dione, octahydro-, (5aS,10aS)-is -1.3 kcal/mol was slightly weaker than the binding affinity of ampicillin, when they were docked with lumazine synthase. The analysis of the binding affinities results indicates that 5H,10H-Dipyrrolo[1,2-a:1',2'-d]pyrazine-5,10-dione, octahydro-, (5aS,10aS)- is a potent inhibitor of lumazine synthase and UDP-N-acetylglucosamine 1-carboxyvinyltransfrase which are critical for the survival of bacteria.

5H,10H-Dipyrrolo[1,2-a:1',2'-d]pyrazine-5,10-dione, octahydro-, (5aS,10aS)- was selected as lead compound for the development of an antibacterial drug. This study shows the potential of endophytic compounds as drugs scaffolds and can help in combating antibacterial resistance.

DEDICATION

To my parents: Abraham and Dorothy Nyambo; brothers: Peter, Patrick and Tendai; sisters: Violet and Christine.

Give instruction to a wise man and he will yet be wiser: teach a just man, and he will increase in learning – ***Proverbs 9 v 9***

ACKNOWLEDGEMENTS

It has been a period of intense learning for me, not only in the scientific arena but also on a personal level. Writing this thesis has had a significant impact on me. I want to reflect on the people who have supported and helped me so much in making this dream a reality. First, I would like to express gratitude to Almighty God for the Abundant **GRACE, IN ALL THINGS AT ALL TIMES**, that carried me through my studies.

I would particularly like to single out my supervisor professor Idah Sithole-Niang and thank her for the guidance and invaluable contributions made to this study. She provided me with the tools that I needed to choose the right direction and complete my thesis. To personnel in the Molecular biology lab in the Biochemistry Department (Mr Zharo). I thank him for excellent assistance in making laboratory facilities available for to me conduct my research.

To colleagues that assisted me in various ways and those that deserve mention are Dr P. Nyambo, Dr M. Musokwa, Mr P. Jambwa, Dr T.N Mudhimba, Mr B. Muzambwe.

I would also like to thank my parents for their wise counsel, support, encouragement, love and sympathetic ear. I know this will make you proud. This is the product.

Thank you very much to everyone and may the Almighty God richly bless you all.

'*And God is able to make all grace abound toward you; that ye, always having all sufficiency in all things, may abound to every good work'*: **-2 Corinthians 9:8**

Contents

List of Tables

List of Figures

List of Appendices

CHAPTER 1

1. Introduction

1.1 Endophytes

The emergence of multidrug-resistant pathogens, along with the continuous isolation of already known compounds is a calamity to public health worldwide (Annunziato, 2019; Matar *et al*., 2020). Also, it has consequently led to a shift to semi-synthetic drugs in-order to combat the microbial resistance to drugs and widen the activity spectrum (Spengler, 2019). Due to the increase in antibiotic resistance mechanisms, medical practitioners are significantly hindered in defining the effective (appropriate) treatment regimens of the antimicrobial arsenal and have turned to last-resort drugs (third line alternatives) (Verma and Gange, 2014). Some drugs, for example, colistin possesses a profile with detrimental side effects (Gajdács and Albericio, 2019) which compromises the safety and quality of life of the patients. In low resource settings, they might struggle in procuring the drugs as they are expensive (WHO, 2017). It was estimated that 10 million deaths could occur and the global Gross Domestic Product (GDP) could suffer $100 trillion lose by 2050 if the antimicrobial resistance if not effectively addressed (Clift, 2019). Microbial natural products alternatively resemble a wide-ranging area for the discovery of novel therapeutic compounds (Mohamed *et al*., 2020). In some research papers (Avedissian *et al.*, 2019; Mast and Stegmann, 2019; McLean *et al.*, 2019; Robertsen and Musiol-Kroll, 2019; Tan *et al*., 2019), they emphasised microbial bioactive secondary metabolites as targets for discovery and development of new drugs, mostly anticancer, antibiotics, antifungals, antiparasitic. The plant endo-biome is a principal player in global biogeochemical cycles. Research has been carried out to manipulate various pathways responsible for the synthesis and secretion of bioactive and novel molecules for plant disease development, to promote plant secondary metabolite production, and to ease chemical inputs (Kowalski *et al.*, 2018; James F White *et al.*, 2019; James F. White *et al.*, 2019).

Plants do not exist alone as single entities, but instead, they are intimately associated with microbes living inside the endo-sphere (plant tissues) (Harrison *et al.*, 2019) and those residing in the neighbourhood (Hardoim *et al.*, 2015). Every living plant constitute of vast and diverse niches of endophytic fungi, bacteria and actinomycetes (Fouda *et al.*, 2015), hence, the term endophyte was coined to describe microbes which reside asymptomatically intra or intercellular in plant tissues (Rosenblueth and Martínez-romero, 2006; Lubna *et al.*, 2018). Usually, plants were only thought to synthesise some bioactive products, but in fact, endophytes which have colonised the plant are also capable of synthesising the same potent bioactive secondary metabolites (Harrison *et al.*, 2019). The genetic flexibility and adaptability of endophytes have enabled the production of a wide array of valuable secondary metabolites in response to the natural stimuli (Chadha *et al.*, 2015). It is beyond question that endophytes are a vibrant and reliable source of natural products mostly structurally unique bioactive secondary compounds which can potentially be utilised in agricultural, industrial and modern medicinal applications (Brader *et al.*, 2014; Sibanda and Mabandla, 2018). For example, paclitaxel (Taxol), podophyllotoxin, camptothecin and hypericin and other novel compounds which have great potential pharmaceutically have been isolated from endophytes (Pansanit and Pripdeevech, 2018).

Endophytes are known to be the treasure of a wide range of extracellular enzymes which include, chitinases, lipases, amylases, cellulases and proteases, pectinases and laccase (Fouda *et al.*, 2015)., which can be utilised in numerous industrial processes, for instance, baking, brewing, textile, confectionaries, paper, pulp and leather, removal of stains, bioremediation and biosensing. The gummosis process is thought to be a consequence of the association of endophytes in most gum-yielding trees (Ibanez *et al.*, 2017).

A study by (Palanichamy *et al.*, 2018) revealed the ability of endophytes to yield bioactive metabolites which exhibited broad-spectrum potency against *Escherichia coli (E. coli),*

Staphylococcus aureus (*S. aureus*), *Corynebacterium diphtheriae*, *Salmonella typhi* and *Proteus mirabilis*. Extracts from the fungal isolate MGTMMP031 which was obtained from *Vitex negundo* plant exhibited potency against both Gram-negative and Gram-positive pathogens. In another investigation of antimicrobial activity of endophytic extracts obtained from *Ocimum* species (*Tulsi*), isolates P14T1 and P13T5 were potent against *Candida albicans* and *Pseudomonas aeruginosa*. The extracts obtained from the isolates (P14T1 and P13T5) exhibited 22 mm and 21 mm zones of inhibition, respectively (Pavithra *et al*., 2014). *Aspergillus versicolor* is an endophytic fungus that was isolated from the roots of *Asteraceae*. Compound 5 obtained from the extracts of the endophytic fungus (*Aspergillus versicolor*) exhibited antimicrobial capacity against *E. coli*, *Bacillus cereus* and *Staphylococcus aureus*. The zones of inhibition showed by Compound 5 against *E. coli*, *Bacillus cereus* and *Staphylococcus aureus* were 24.5, 19.8 and 14.3 mm respectively, and the MICs value were 3.9, 3.7 and 4.3 µg/ml, respectively, contrasted to ciprofloxacin MICs which were 3.5, 2.8 and 3.1 µg/ml, respectively (Ibrahim and Asfour, 2020).

Currently, a few plant species colonised by endophytes have been explored particularly in Zimbabwe in addition to the genetic diversity of endophytes. Thus, only a small fraction of endophytes has been studied for the discovery of novel bioactive compounds.

The methods used in the laboratory for culturing endophytic species have limitations that restrict the diversity studies. This presents a vast, mostly untapped, resource for bioactive compounds which can be readily studied as more and more plants species are exploited, and new cultivation techniques are developed. This study will seek novel drug scaffolds and enzymes that could be useful in medicinal and industrial applications, respectively.

1.2 The rationale for exploring endophytes as potential sources of novel compounds

The rationale for exploring endophytic microorganisms from native Zimbabwean medicinal plants as potential sources for novel biotherapeutics and enzymes is because they are a relatively unexplored area in biochemical diversity. The perusal of literature on the genomic mining strategies of the natural microbial product showed that microorganisms remarkably have a larger hidden capacity of synthesising bioactive secondary metabolites than previously obtained under *in vitro* laboratory conditions (Kusari *et al*., 2012). This provides the need to harness microbial natural products research for drug discovery and industrial use. Also, the efficient extraction method enhances the understanding of the diversity of chemical compounds produced by endophytes. Precisely, the fortification provided by endophytes to the host plant by a wide array of antimicrobial compounds enhances the attractiveness of these compounds in the medical field. For any potential drug, the toxicity to higher organisms has to be addressed. Natural products isolated from endophytes are therefore fascinating as they are produced inside a eukaryotic system without causing any harm. Thus, the host plant has naturally functioned as a selection system. Endophytes exhibit lower generation time and subsequently higher growth rates as compared to plants which have lower growth rates (Yasser *et al.*, 2019).

1.3 Main Objective

Thus, the broad aim of this study was to evaluate the potential of the under-explored new endophytes isolated from native Zimbabwean medicinal plants to produce bioactive compounds. To attain this goal, the following were the specific objectives:

1. To isolate bacterial and fungal endophytes and to purify and cultivate the isolates in liquid broth.

2. To isolate genomic DNA and perform 16S rRNA gene amplification and M13 RAPDs to confirm bacterial origin.
3. To extract bioactive compounds from liquid culture using different organic solvents and screen for antibacterial activity using agar plate assays.
4. To identify bioactive metabolites by using Thin Layer Chromatography (TLC) and Gas Chromatography (GC) Mass spectrometry.
5. To evaluate the pharmacokinetics, biological activity spectrum, and molecular interaction of the endophytic compounds using computational tools.

1.4 Hypothesis

1. Molecular analysis can be used to identify bacterial and fungal endophytes from native plants from Zimbabwe.
2. Agar well diffusion assay can be used to determine the antimicrobial efficacy of endophytic extracts.
3. Chromatographic methods and computational tools can be used to identify and characterise bioactive endophytic extracts.

CHAPTER 2

2. Literature review

2.1 Antimicrobial Resistance

Antimicrobial resistance prevalence has reached an alarming level globally and thus, poses a severe threat to environmental, animal and human health (Mashe *et al.*, 2019; UNICEF, 2019; Chen and Lu, 2020; Saeed *et al.*, 2020). For instance, infections which are caused by methicillin-resistant *Staphylococcus aureus* (MRSA) are characterised by high mortality and high morbidity in humans (Wang *et al.*, 2018). Zimbabwe is currently facing growing antimicrobial resistance to HIV, sexually transmitted infections, meningitis, urinary tract infections, tuberculosis, diarrhoea and malaria (Ministry of Health and Child Care, Ministry of Agriculture, Mechanisation and Irrigation and Ministry of Environment, Water, and Climate, 2017). A study was done in Zimbabwe by Mashe *et al.*, (2019) revealed that resistance to ciprofloxacin by *Salmonella enteric (S. enteric)* increased to 22% in 2017 from 4.2% in 2014, while resistance to cephalosporin by *E. coli* increased to 34.9% from 20.3% between 2012 and 2017 (Mhondoro *et al.*, 2019). Thus, in Zimbabwe, there is a need to bio prospect and advance conventional approaches to mitigate AMR.

Historically, Africa is considered to be the cradle of *Homo sapiens* and is an invaluable sanctuary of possibly the oldest and most diversified healthcare systems which are yet to be fully utilised (Nankaya *et al.*, 2020; Traoré *et al.*, 2020; Zouaoui *et al.*, 2020). Approximately, 50% of the African population uses ethnomedicinal remedies for the treatment of various diseases (Shoko, 2018), while, 80% of the southern hemisphere population still relies on the traditional approach to medicine based on herbal drugs (Agrawal *et al*., 2017). The Traditional Medicine Strategy (2014-2023) of the World Health Organization (WHO) supports the incorporation of traditional medicine into modern healthcare practices and strategies (Packer *et al.*, 2019). Thus, the historical background and vast knowledge possessed by tribal people

about the use of ethnomedicinal plants should be reliably preserved because it is beneficial in the discovery of bioactive compounds (Chinnasamy and Arumugam, 2018). A medicinal plant is any plant that possesses components that can be utilised directly or indirectly for medicinal purposes, while, botanical formulations, herbs, herbal extraction/ preparations and finished products are categorised as herbal medicines (Ngarivhume *et al.*, 2015; Jamshidi-Kia *et al*., 2018).

2.1.1 Medicinal plants found in Zimbabwe and used in this study

2.1.1 *Piliostigma thonningii*

Piliostigma thonningii, commonly known as *Musekesa* in Shona, belongs to the *Leguminosae* family which possesses economic and ethnomedical functions/properties. Traditionally the pharmacological decoction is prepared by using the roots, bark, seed and or leaves of the *P. thonningii.* The decoction is utilised in the treatment of toothache, diarrhoea, arresting nose bleeding, snake bites, skin infections, hepatitis B and C and HIV infection (Dasofunjo *et al.*, 2013; Afolayan *et al.*, 2018). Phytochemical analysis of ethanol extracts of *P. thonningii* leaves has revealed the presence of numerous essential compounds which include tannins, flavonoids, cardiac glycosides, terpenoids and saponins (Olakunle, 2011; Tijjani, 2018).

2.1.2 *Colophospermum mopane*

Colophospermum mopane, also known as *Mopane* is a notable drought-resistant species of the savanna forests (Madzibane and Potgieter, 1999). In southern Africa, *C. mopane* is used for firewood and medicinally for the treatment of numerous human and animal diseases. For instance, impotence, kidney stones, syphilis (Madzibane and Potgieter, 1999; Makhado *et al.*,

2009), and diseases which are caused by *S. aureus* and *E. coli*. The phytochemical profile of *C. mopane* parts comprises of flavonoids, tannins, diterpenes, anthocyanidins and polyphenols (Mudzengi *et al.*, 2017).

2.1.3 *Vernonia amygdalina*

Vernonia amygdalina (*V. amygdalina*)(*Nyatex*) is a small shrub belonging to the *Asteraceae* family that is usually named "Bitter African leaf" (Kadiri and Olawoye, 2016). It has been used for ethnomedical remedies in Africa, particularly for the treatment of infertility, malaria, tumours, diabetes, sexually transmitted diseases and gastrointestinal infections. Research on the phytochemical composition of the roots and bark of *V. amygdalina* revealed the presence of flavonoids, alkaloids, saponins, terpenoids and hydrocyanic acids. Alkaloids, saponins, tannin extracts from *V. amygdalina* were shown to exhibit antifungal properties (Adebola *et al.*, 2020). Ethyl acetate extracts of endophytes isolated from *V. amygdalina* also exhibited antimicrobial potency against *S. aureus* and *E. coli* (Praptiwi *et al.*, 2020).

2.1.4 *Lannea discolour*

Lannea discolour (L. discolour) is a medicinal tree found in the South Central region of Zimbabwe and is commonly known as *Mugan'acha* (Grey, 2019). The root extracts of *L. discolour* are utilised for the treatment of sore eyes and infertility, while the fibre extracts are utilised for the treatment of menstrual disorders, gastrointestinal disorders, viral infections and bacterial infections (Maroyi, 2013; Maroyi, 2019). Phytochemical analysis of the *Lannea* species revealed the presence of flavonoids, cyclohexene derivatives, tetracyclic and pentacyclic triterpenes, and phenolic lipids (Maroyi, 2019).

2.1.5 *Pterocarpus angolensis*

Pterocarpus angolensis (*P. angolensis*) commonly referred to as *Mubvamaropa* or *Mukwa* in Shona is a large tall tree which stands 18-19 m. *Pterocarpus angolensis* possesses exceptional timber properties; thus, it is utilised as raw material for furniture and building industries (Abubakar and Majinda, 2016). Traditionally, different parts of *P. angolensis* are used in the preparation of decoctions for treatment of skin problems, gastrointestinal, respiratory and urinal-genital problems (Abubakar and Majinda, 2016; Alaribe and Motaung, 2019).

2.1.6 *Strychnos pungens*

Mutamba (*Strychnos pungens*) is an indigenous tree to subtropical Africa belonging to the *Loganiaceae* family (Nitcheu-Ngemakwe *et al.*, 2017). Phytochemical analysis of *Monkey orange* has revealed that it possesses a high total antioxidant capacity owing to the alkaloids, flavonoids, glycosides and phenolics bases (Rajesh *et al.*, 2011; Isa *et al.*, 2014; Nitcheu-Ngemakwe *et al.*, 2017). Traditionally, monkey orange fruits are utilised in the treatment of sexually transmitted diseases, bronchitis and as a snake antidote (Nitcheu-Ngemakwe *et al.*, 2017).

2.1.7 *Sclerocarya birrea*

Marula subspecies *caffra* is an economically, culturally, and ecological relevant indigenous tree located in sub-Saharan Africa (Gadd, 2002; Gouwakinnou *et al.*, 2011; Nitcheu-Ngemakwe *et al.*, 2017)**.** Rural African societies use the *Marula* stem-bark decoctions for the treatment of inflammation of the spleen and skin, liver diseases, dysentery, blood circulation

problems, gonorrhoea, syphilis, proctitis and boils (Ojewole, 2004; Fotio *et al.*, 2009; Ojewole *et al.*, 2010; Gouwakinnou *et al.*, 2011; Gaertin *et al.*, 2020). In an investigation of acetone and methanol extracts of the inner bark, outer bark and leaf were observed to be potent against the proliferation of *S. aureus, E. coli, P. aeruginosa and E. faecalis* (Ojewole *et al.*, 2010). *Marula* has been utilised in the food industries to increase the shelf life of products because it inhibits enzymes and proliferation of microbes that are responsible for causing product spoilage (Hall, O'Brien and Sinclar, 2002). Phytochemical studies of acetone, methanol and aqueous extracts of the stem bark have revealed the presence of alkaloids, flavonoids, tannins, oleic acid, saponins, triterpenoids, ascorbic acid, steroids, coumarins, sesquiterpene hydrocarbons, β-sitosterol and amino acids (Fotio *et al.*, 2009; Ojewole *et al.*, 2010).

Traditional medicinal plants are highly valued and are credibly utilised in the treatment of both primary health care and chronic disease which include cancer, heart diseases, diabetic wound, AIDS and osteoporosis (Husain, 2013)(Table 2.1). Bioactive metabolites have been extracted from medicinal plants and elucidated (Chaachouay *et al.*, 2019; Calzetta *et al.*, 2020; Hao and Xiao, 2020; Hernández Bautista *et al.*, 2019; Khan *et al.*, 2019; Mohotti *et al.*, 2020; Zouaoui *et al.*, 2020). However, the content of the metabolites was observed to be too low in some plants. This implies that other sources of medicinal plants should be considered (Hao and Xiao, 2020).

Table 2.1: Medicinal plants found in Zimbabwe and used in the current study.

Common name	Scientific name	Method of extraction	Plant tissue	Diseases cured	Reference
Musekesa	*Piliostigma thonningii*	Solvent extraction	roots, bark, seed and or leaves	diarrhoea, intestinal complications hepatitis B and C and HIV infection	(Dasofunjo *et al.*, 2013)
Mopane	*Colophospermum mopane*	Solvent extraction	Bark	impotence, kidney stones, syphilis	(Makhado *et al.*, 2009)
Nyatex	*Vernonia amygdalina*	Solvent extraction	roots and bark	malaria, tumours, diabetes, sexually transmitted diseases and gastrointestinal complications	Adebola *et al.*, 2020; Kemal *et al.*, 2020
Mugan'acha	*Lannea discolour*	Solvent extraction	roots and fibre	viral infections, bacterial infections, sore eyes and infertility	(Maroyi, 2013; Maroyi, 2019)
Mukwa	*Pterocarpus angolensis*	Solvent extraction	Bark	skin problems, fertility complications, gastrointestinal, respiratory and urinal-genital problems	(Abubakar and Majinda, 2016; Alaribe and Motaung, 2019)
Mutamba	*Strychnos pungens*	Solvent extraction	Bark, fruit	sexually transmitted diseases, snake antidote and bronchitis	(Nitcheu Ngemakwe *et al.*, 2017).
Marula	*Sclerocarya birrea*	Solvent extraction	Bark and leaf	inflammation of the spleen and skin, liver diseases, dysentery, blood circulation problems, gonorrhoea, syphilis, proctitis, boils and gangrenous rectitis	(Ojewole *et al.*, 2010; Gouwakinnou *et al.*, 2011; Gaertin *et al.*, 2020)

2.2 The plant Microbiota

The plant microbiota has been known to be a significant determinant in the functioning of the plant holobiont, thus, guaranteeing rapid and efficient nutrient supply, seed germination and growth support, resistance against abiotic factors, pathogen defence and production of bioactive metabolites (Grosch *et al*., 2018). The composition and structure of plant microbiomes have been intensively studied (Turner *et al*., 2013; Tkacz and Poole, 2015; Vogel and Bai, 2016) and virtually all plant tissues are known to harbour microbial community (Turner *et al*., 2013). Thus, the host plant phenotype is thought to extend and include plant microbiome. The host's secretory system plays an essential role in establishing the broadening of the phenotype with microbial life (Hardoim *et al.*, 2015).

Abiotic and biotic challenges are thought to have influenced the co-evolution of endophytes, thus, the linear correlation between the host medicinal plant and endophytes in production of secondary metabolites (Palanichamy *et al.*, 2018). The ability of endophytes to synthesise plant growth hormones, for instance, ethylene, auxins, gibberellins, abscisins and cytokinins were suggested to be some of the evidence of transfer of genetic systems between the plant and the endophytic microbes (Li *et al.*, 2018). The metabolites synthesised by endophytes enable them to compete with co-existing endophytes, to colonise the host and repel pathogens and for the acquisition of nutrients (Goyena, 2019). Different classes of secondary metabolites often are restricted to organisms, or group of organisms, or typical individual species within a phylogenetic set (Sanchez and Demain, 2011). Thus, the microbial community in medicinal plants along with traditional and ethnobotanical knowledge can be useful in the isolation of bioactive compounds. (Ramawat, 2008).

2.3 Ecological Functions of endophytes

Endophytes virtually determine the health and productiveness of a plant (Wang *et al.*, 2019; Pelo *et al*., 2020). Numerous endophytic bacteria first compete in the rhizosphere before plant entry and are facultative plant colonisers. In this regard, the endophytic bacteria might possess a diverse, active arsenal of metabolites (Brader *et al.*, 2014). Thus, it is assumed that endophytes exhibit superior phenotypic plasticity, hence, can express extensive colonisation, virulence, saprophytic, latency or pathogenicity (Obasa *et al*., 2017) (Figure 2.1). Some endophytes particularly fungi residing in leaves occupy (epiphyllous net) and utilise all available nutrients, therefore, inhibiting the proliferation of potential pathogens as they are denied access to nutrients (Nan *et al.* 2018). While other endophytes secrete bioactive secondary metabolites which include protein toxins, antibiotics and exoenzymes, ultimately enhancing disease resistance of plants (Bell *et al.*, 2019). These compounds produced by endophytes might not only harbour antimicrobial potential but also participate in interspecies and intraspecies signalling processes (Brader *et al.*, 2014)

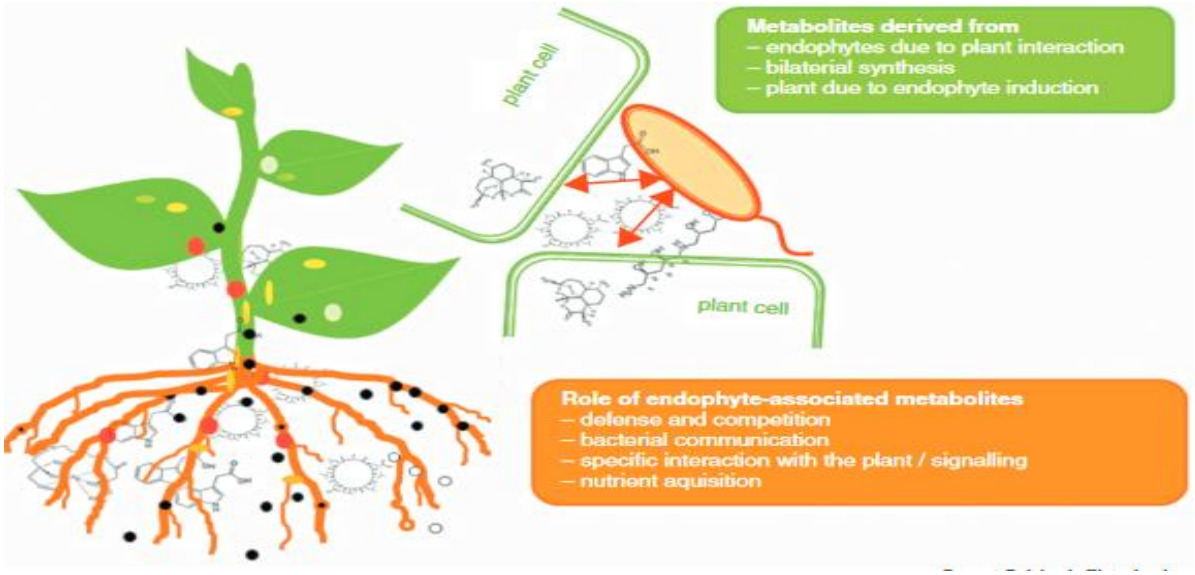

Figure 2.1: Interaction between host plant and endophyte. Adapted from (Brader *et al*., 2014)

The study by Sessitsch *et al.,* (2012) corroborated the presence of all known protein secretion systems responsible for translocation across the cytoplasmic membrane and outer membrane in endophyte metagenome. However, some of the elements (T3SS) of type III secretion system were not present in the endophytic metagenome, implying that they are not highly conserved in the endophytes. Pathogenic and symbiotic bacteria utilise a type III secretion system to directly insert effector proteins into the host cytoplasm, consequently modulating the host's reaction. In this regard, findings from their research support the hypothesis that endophytes are substantially different from pathogens and that endophytes lack type III secretion system in their genome. Endophytes are presumed to utilise the Type IV conjugal DNA-protein secretion system in colonising host plants and DNA conjugation. Thus, Type IV conjugal DNA-protein secretion system, genomic loci coding for ribulose bisphosphate carboxylase/ oxygenase and nitrogen fixation proteins are prominently discovered in endophytes than rhizosphere bacteria (Hardoim *et al.,* 2015).

2.4 Bioactivity of secondary compounds obtained from endophytes according to their chemical class

It is beyond question that a microbial community of chemically analysed endophytes are an excellent source and secrete a potent class of bioactive secondary compounds which are medically and ecologically significant (Nan *et al.,* 2018). The biological model of action of secondary metabolites produced by endophytic microorganisms is mainly by inhibiting or killing other species, thus, are acknowledged to be pharmacologically active (antifungal, larvicidal, antiprotozoal, anti-inflammatory, antibacterial and antioxidant activities) hence the tremendous effect on the society (Figueiredo *et al.,* 2009; Ma *et al.,* 2019; Manganyi *et al.,* 2019; Wang *et al.,* 2019; Kim *et al.,* 2020; Mohamed *et al*., 2020; Naama-amar *et al.,* 2020;

Nuankeaw *et al.*, 2020; Pelo *et al.*, 2020). The relationship between the host plant and endophyte is characterised by balanced antagonism; thus, endophytes protein secretion systems usually regulate the outcome of the association between plant and bacterium (Sessitsch *et al.*, 2012) (Figure 2.2). The secondary metabolites exhibit a great diversity of structures, and the most abundant classes include alkaloids, terpenoids and flavonoids. Terpenoids and polyketides are the most frequently purified from endophytes (Mousa and Raizada 2013). The processes in red (Figure 2.2) are associated with entry into the roots, proliferation and establishment inside the roots. The processes in brown are responsible for bio-controlling, plant-growth-promoting and phytoremediation; while processes in blue are related to metabolic adaptations. Lastly, the question mark in red symbolises effector proteins of the protein secretion system and the transfer of fixed nitrogen to the plant which are not known (Sessitsch *et al.*, 2012).

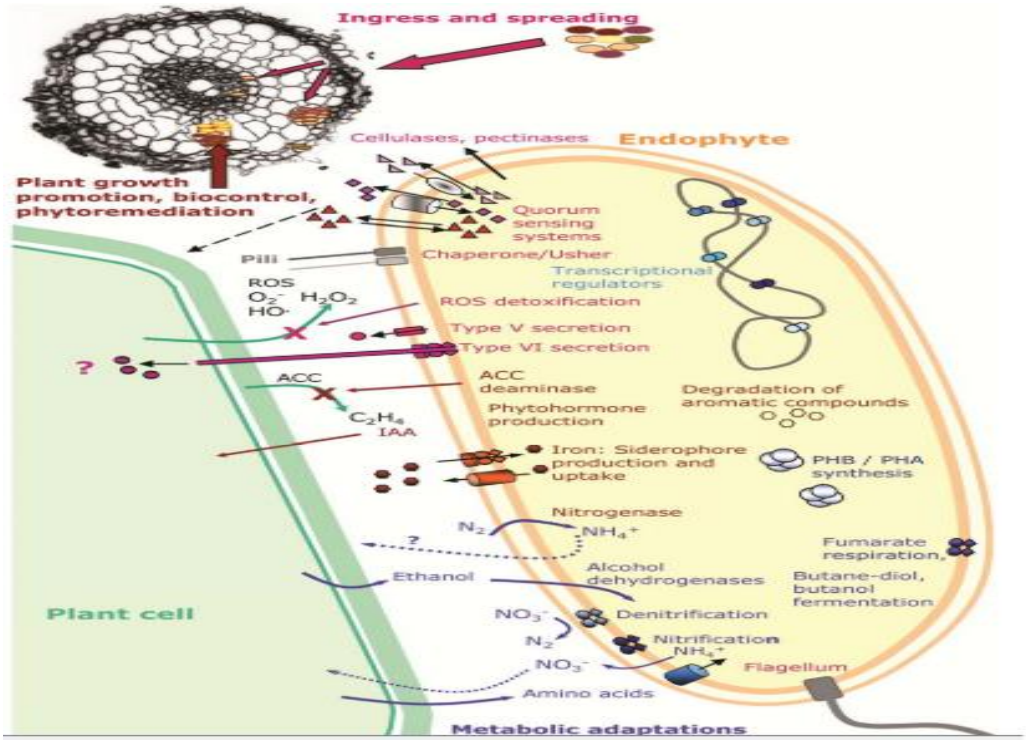

Figure 2.2: Host plant cell interaction with endophyte as obtained from the plant-endophyte metagenome. Adapted from (Sessitsch *et al*., 2012).

A study by Takarova, (2018) on endophytes isolated from Zimbabwe medicinal plants (*P. thonningii, C. mopane, V. amygdalina, L. discolour, P. angolensis, S. pungens* and *S. birrea*) did not characterise the metabolites secreted by endophytes but instead focused on the isolation of the endophytes and antimicrobial assays of crude extracts. Thus, there is an imperative prerequisite to qualitatively and quantitively characterise the secondary metabolites according to their chemical classes and assess their potential use in medicinal therapeutics and industrial purposes. Endophytes residing in different parts of a plant are different as well as the secondary metabolites they produce (Porras-alfaro and Bayman, 2011) (Figure 2.3). Bioactive compounds are grouped into two classes, i.e. soluble and volatile compounds depending upon biological and physiological properties. These classes include alkaloids, indole and isocoumarin derivatives, peptides, pyrrolizidines, aliphatic compounds, flavonoids, phenols, terpenoids, quinines, phenylpropanoids, glycosides, tetralones, polyketides, coumarins, lignans and steroids (Zaferanloo, 2014; Hardoim, 2019; Manganyi *et al.*, 2019; Uche-Okereafor *et al.*, 2019; Cui *et al.*, 2020).

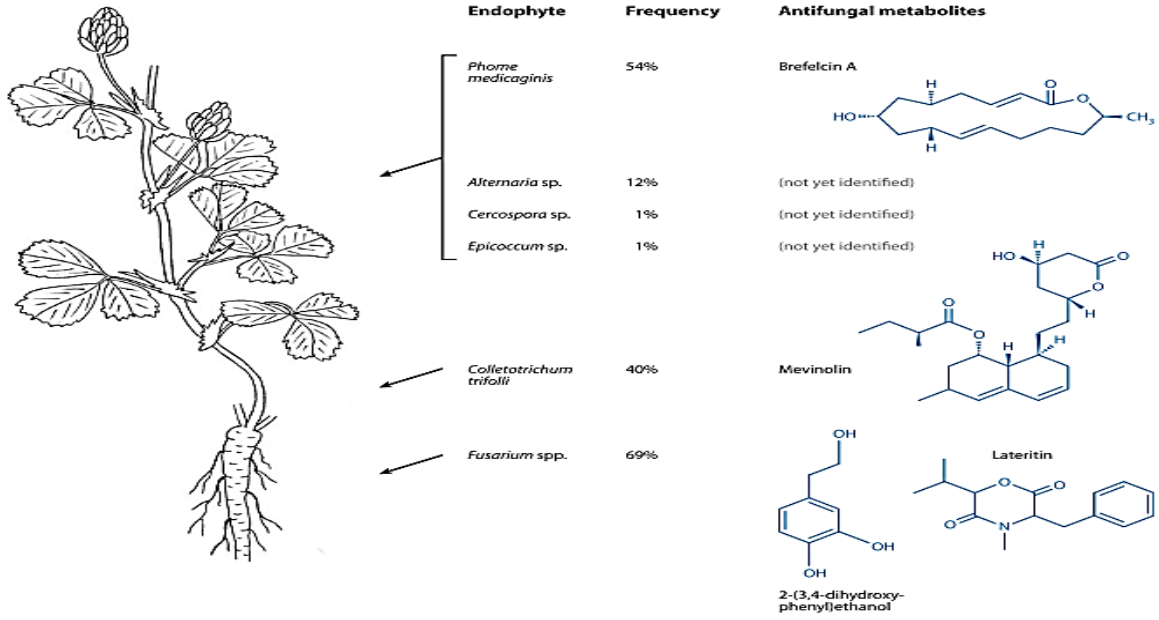

Figure 2.3:The secondary metabolites observed *in vitro*, not in an Alfalfa plant. Adapted from (Porras-alfaro and Bayman, 2011).

2.4.1 Alkaloids

Alkaloids are a broad heterogeneous group of organic bases which are constituted either by secondary, tertiary or cyclic amines (Makkar *et al*., 2007). A wide range of structurally diverse pharmacologically bioactive alkaloids have been commonly extracted from microorganisms and have been shown to exhibit bioactivity at very low dosage (Kishimoto *et al.*, 2016; Sanchez and Demain, 2011). For instance, a secondary metabolite phomoenamide was extracted from a culture of *Phomopsis sp.* and exhibited potent activity against *Mycobacterium tuberculosis* with a MIC of 6.25 µg/ml (Zaferanloo, 2014). Alkaloids are responsible for the protection of grasses from pathogenic fungi. Research has extensively documented that *Epichlo¨e* endophytes are responsible for synthesising alkaloids that are beneficial to the plant defence against pathogenic fungi (Nan *et al.* 2018). Some alkaloid compounds have been found through research to possess cytotoxic activity, for example, vincristine a drug used in chemotherapy treatment of acute lymphoblastic nephroblastoma and leukaemia. For example, camptothecin was extracted from an endophytic (*Entrophospora infrequens)* culture and exhibited cytotoxic activity. Bio-activity of camptothecin $C_2OH_{16}N_2O_4$ was performed using human cancer lines (HEP-2 for liver cancer, A-549 for lung cancer, OVCAR-5 for ovarian cancer), and the comparison against an authentic standard showed comparable activity (Kaul *et al.*, 2012).

2.4.2 Peptides

Antimicrobial peptides (AMPs) are amphipathic molecules which possess cationic amino acids (hydrophilic positive charges) and hydrophobic charges, which, enables them to successively bind at numerous sites on the biological membranes (Jiménez *et al.*, 2018). Examples of AMPs which are clinically used are colistin, polymyxin B, gramicidin S, nisin and daptomycin (Mantravadi *et al.*, 2019). The mode of action of AMPs is mainly due to interaction of the

negatively charged phospholipid head-on bacterial membranes and the positive charges of AMPs consequently internalising the peptide, thus, destroying intercellular targets (Jiménez *et al.*, 2018). AMPs have a numerous advantage over conventional antibiotics which include: multidrug-resistant microorganisms are less likely to develop resistance against AMPs, for example, polymyxin B shows incredible efficacy activity against *Pseudomonas aeruginosa*; AMPs can regulate the immune response; AMPs exhibit a wide antimicrobial range against various pathogens including fungi, viruses and protozoa (Avedissian *et al.*, 2019). The limitations associated with the use of AMPs as antimicrobials include;

- manufacturing costs are considerably high,
- poor bioavailability (polymyxin is intrathecally, intravascularly, topically or aerosolised administered (Avedissian *et al.*, 2019).
- can be lysed by proteases (Mantravadi *et al.*, 2019).

Some examples of peptides produced by endophytes include leucinostatin A, cryptocandin, and echinocandin A (Hardoim, 2019). An endophyte *Cryptosporiopsis quercina* which exist in *Tripterigium wiflordii* produced a novel antimycotic lipopeptide, cryptocandin, which displayed potent activity against *Candida albicans* and *Trichophyton sp*. which are essential human pathogens (Brader *et al.*, 2014). Furthermore, endophytic peptides Leuesnostatin A which is produced by *Acremonium sp.* existing in *Taxus baccata* displayed antibacterial activity against *Pythium ultimum* (Zaferanloo, 2014). The use of HPLC to quantify antimicrobial polypeptides is difficult because antimicrobial polypeptides have low UV absorption, the chromatographic profiles of the components are overlapping, and they have limited native fluorescence. In this regard, ultra-performance liquid chromatography-tandem mass spectrometry (UPLC-MS/MS) and liquid chromatography-tandem mass spectrometry (LC-

MS/MS) can be used as they possess superior specificity, sensitivity and accuracy of mass-spectrophotometry-based approaches (Avedissian *et al.*, 2019).

2.2.3 Flavonoids

Flavonoids are ubiquitous polyphenolic secondary compounds in green flora except for Anthocerotae, and they are frequently present as glycosides or in an esterified form (Aboody and Mickymaray, 2020; Nishiumi *et al.*, 2011). The flavonoid chemical configuration comprises of two benzene rings which are linked by three carbon ring (C6-C3-C6), i.e. rings A and B are interlinked by ring C. A wide array of chemical derivatives are distinguished by substitution pattern variations, hence, flavonoids can be classified into diverse subclasses which are flavones, flavanones, isoflavones, anthocyanins, chalcones and flavonols. Usually, flavonoids are brightly coloured due to the conjugated double bonds (Nishiumi *et al.*, 2011) (Figure 2.4).

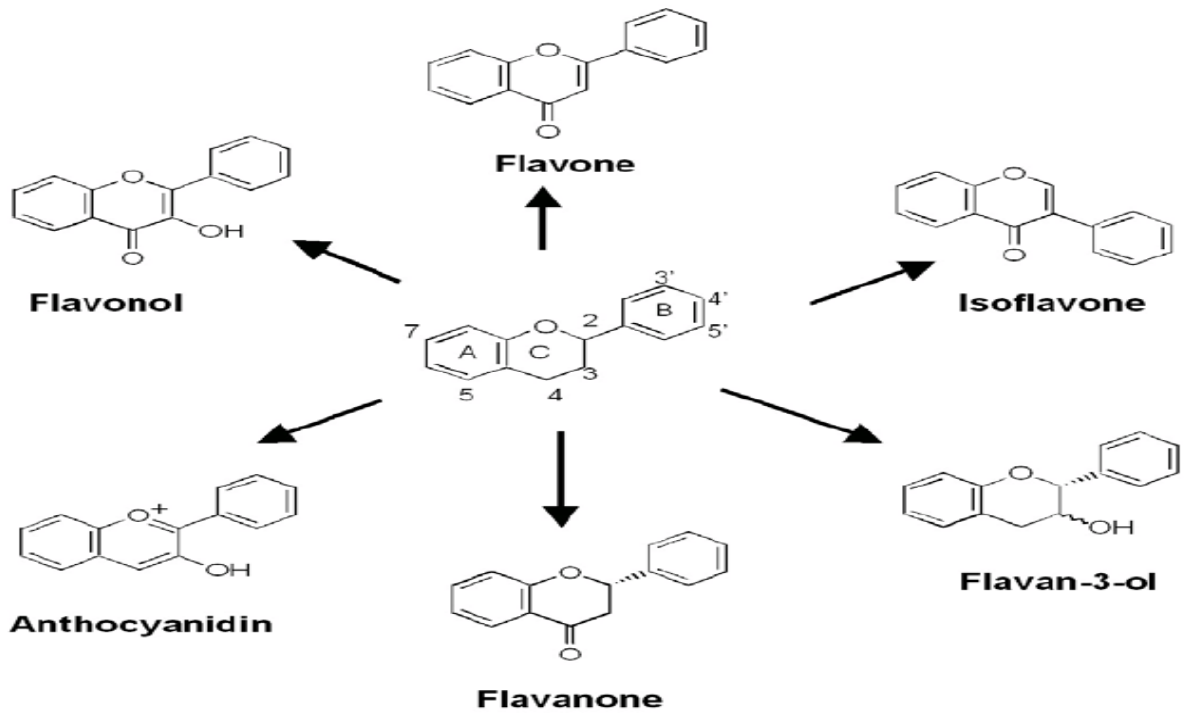

Figure 2. 4: Basic chemical structure of flavonoids. Adapted from (Nishiumi et al., 2011)

Research on the vast potential, bioavailability and profitable bioactive advantages possessed by flavonoids has received considerable attention (Nishiumi *et al.*, 2011). *In vivo* and clinical assays demonstrated numerous pharmacological properties which are exhibited by flavonoids. These properties include antiviral/ bacterial, neuroprotective, antithrombotic, renoprotective, anti-diabetic, anti-ageing, anti-inflammatory, anticancer and cardioprotective activities (Aboody and Mickymaray, 2020; Wang *et al*., 2018).

Flavonoids which possess antimicrobial activity have been extracted from *Nodulisporium sp.* an endophytic fungus which resides in *Juniperus cedre* (Zaferanloo, 2014). Studies have elucidated that therapeutic activities against *E. coli*, *Hepatitis C* virus, *Canine distemper* virus and *Influenza* virus are due to chemical conformations in particular patterns of glycosylation, methoxylation and hydroxylation. Viral/bacterial activity is immensely reduced due to methoxylation, which increases membrane fluidity. Two poly-methoxy flavonoids have been shown in a study to exhibit decreasing anti-*E.coli* activity as compared to associated aglycones (Wang *et al*., 2018). Furthermore, flavonoids are capable of controlling biological systems by inhibiting a broad spectrum of enzymes which are lipase, hydrolase, aldose reductase, xanthine oxidase, alkaline phosphatase, cyclooxygenase, hyaluronidase, aryluslphatse, cAMP phosphodiesterase, Ca +2 ATPase and several kinases (Aboody and Mickymaray, 2020).

2.2.4 Phenols and phenolic acids

Phenolic compounds are broadly distributed in nature and endophytes are also capable of synthesising phenol and phenolic acids. Microorganisms produce diverse chemical configurations of phenolic compounds, including simple phenols, for instance, catechols and hydroxybenzoic acid derivatives, flavonoids and stilbenes which have intermediate molecular weight. Long-chain high molecular weight polymers include condensed tannins, lignins and catechol melanins (Sanchez and Demain, 2011). Many studies have elucidated the potential

and effectiveness of phenol and phenolic acids as antibiotics. A typical example is Pestalachloride A and B, which were isolated from *Pestalotiopsis adusta* endophyte. Pestalachloride A and B showed significant antifungal activity against plant pathogens (Zaferanloo, 2014).

Polyphenols are potent against bacteria due to non-specific hydrogen bonding and hydrophobic interactions with the microorganism's cell membrane, cell wall, enzymes, adhesion molecules and cell envelope transport proteins. For instance, the lipid bilayer of both gram-negative and gram-positive bacteria interact with gallic acid, consequently increasing cell permeability, impeding cell motility, adhesion, sporulation and proliferation, ultimately disrupting the cell function (Kozubek *et al.*, 2001; Rasooly *et al.*, 2019). Thus, phenolic compounds secreted by endophytes show exceptionally potent antioxidant activity (Finkel *et al.*, 2017; Maroyi, 2019). Research work has demonstrated that hamamelitannin prevents the formation and production of biofilms and toxins, respectively, thus acting as a quorum sensing inhibitor of *Staphylococci* (Rasooly *et al.*, 2019). Some examples of phenolic compounds that have been extracted from endophytes include cytonic acid, p-coumaric acid, 2-methoxy-4-hydroxy-6-methoxymethyl benzaldehyde, p-hydroxy phenylacetic acid, p-hydroxybenzoic acid and colletotric acid (Hardoim, 2019). Separation of the phenolic compound on silica is influenced by the polarity of the chemicals being analysed; thus, the phenolic compounds adsorb more strongly to the silica as the number of hydroxyl groups increase (Sanchez and Demain, 2011).

2.2.5 Quinones

Quinones are bioactive secondary metabolites secreted by endophytes and exhibit broad range efficacy against a series of bacteria. For instance, altersolanol A and 3-O-methylalaternin were isolated from a crude extract of an endophyte (*Ampelomyces sp*) and were shown in a study to exhibit potent activity against Gram-negative bacteria namely, *S. epidermidis*, *S. aureus* and *E.*

faecalis (Zaferanloo, 2014). Another research revealed the ability of an endophyte (*Pestalotiopsis microsporum*) obtained from *Torreya taxifolia* to synthesise Torreyanic acid ($C_3H_{44}O_{12}$). Torreyanic acid was shown to be an exceptionally potent cytotoxic agent, and its mode of action is characterised by triggering apoptosis. Furthermore, it was revealed that torreyanic acid is 5-10 times more efficient in protein kinase C sensitive cell lines (Kaul *et al.*, 2012).

2.2.6 Saponins

Saponins are a class of pharmacologically active secondary metabolites synthesised in abundance by plants and endophytes (Afab *et al.*, 1996; Wu *et al.*, 2013; Troisi *et al.*, 2015; Ashour *et al*., 2019; Almubayedh and Ahmad, 2020; Zeng *et al.*, 2020). The primary chemical configuration of saponins is constructed by at least one glycosidic link at C-3 between sapogenin (steroid or triterpene) and sugar moiety (pentose, uronic acids or hexose) (Zeng *et al.*, 2020). Triterpenoid saponins are usually extracted from dicotyledons. The saponins interact with the cell membranes due to their lyobipolar properties thus are biological detergents (Afab *et al.*, 1996; Guclu-Ustundag and Mazza, 2007; Ashour *et al.*, 2019)(Figure 2.5). Saponins have been shown to have broad range medicinal properties and biological characteristics for instance, antibacterial, anti-inflammatory, anticancer, antiviral, antifungal, insecticidal and hemolytic factor(Guclu-Ustundag and Mazza, 2007; Weng *et al.*, 2011; Zeng *et al.*, 2020; Zhang *et al.*, 2020). Research on the antimicrobial efficacy of saponins revealed potent antibacterial activity against Gram-negative and Gram-positive bacteria with zones of inhibition diameter ranging from 22.6 and 28.4 mm (Jin *et al.*, 2017).

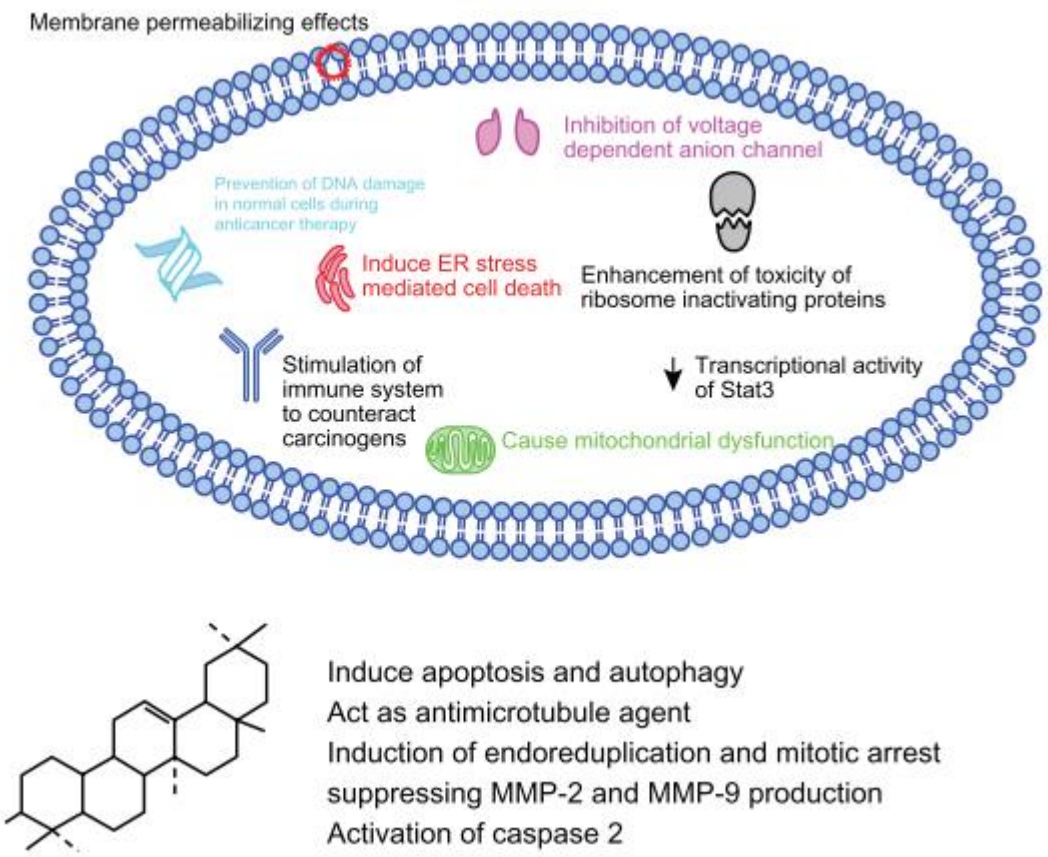

Figure 2.5:Cytotoxic activity of saponins. Adapted from (Weng *et al*., 2011)**.**

2.2.7 Terpenoids

Fundamentally, terpenoids are hydrophobic natural products which are structurally diverse and their basic building blocks are constructed from C5 isoprene units linked in a head to a tail pattern (Sanchez and Demain, 2011). Terpenoids are synthesised from enzymatic resections of sugars, amino acids and vitamins; thus, they are regarded as secondary metabolites (Fajardo *et al.*, 2016). The number of isoprene units that constitute a terpenoid determines the chemical class, for example, C5, C10, C20, C25, C30, C40 are respectively known as monoterpenes, sesquiterpenes, diterpenes, sestertepenes, triterpenes and tetraterpenes. These derivatives enhance the efficacy of terpenes against a series of microbes (Pansanit and Pripdeevech, 2018).

Terpenes non-specifically interact with bio-membranes. The interaction leads to an increase in membrane fluidity, unrestrained efflux of metabolites and ions, modulating of membrane proteins and receptors or even to cell leakage and eventually apoptosis (Figure 2.6). In this notion, terpenes are thus are capable of eliciting a broad-spectrum antimicrobial activity (Wink, 2010). Taxol/ paclitaxel is an exceptionally potent anticancer agent diterpenoid which was first isolated from the bark of the *PacificYew* (*Taxus brevifolia*). Taxol is a mullion dollar drug that is being utilised in the treatment of breast and ovarian cancer (Kaul *et al.*, 2012).

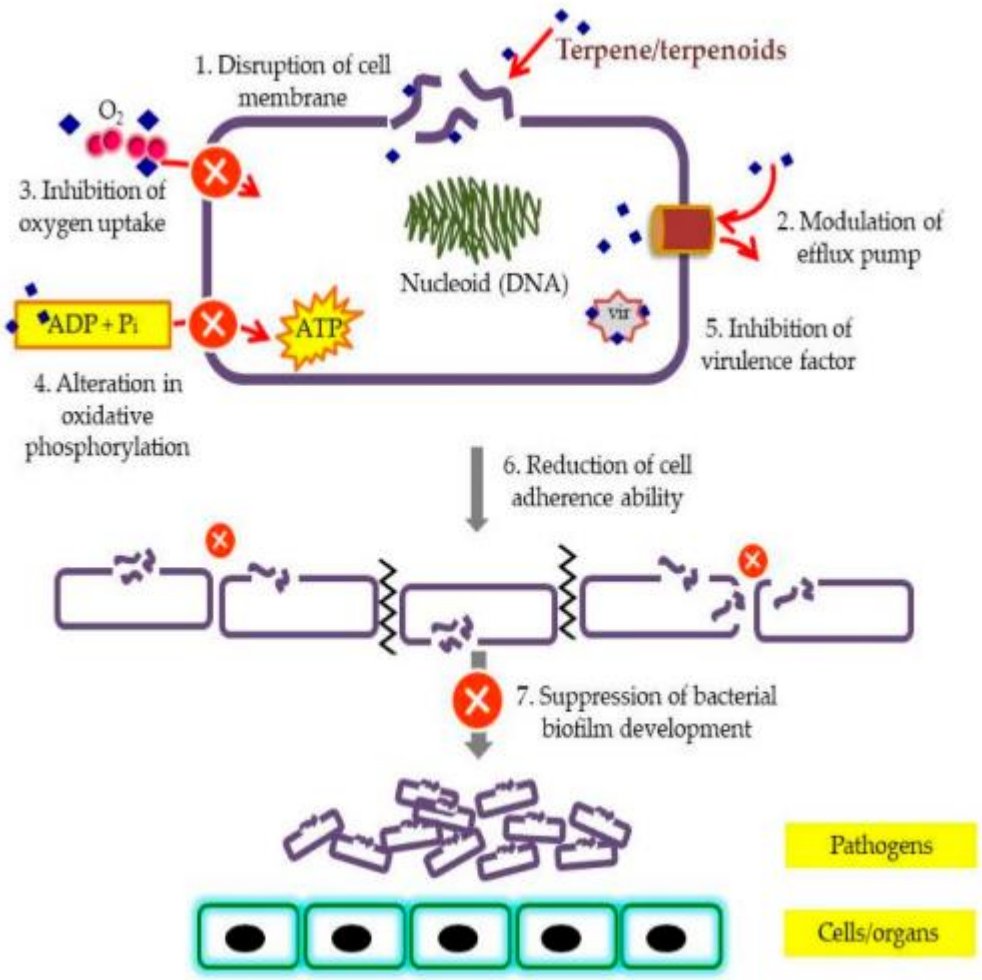

Figure 2.6: The hypothesised terpene/ terpenoids mode of action. Adapted from (Mahizan *et al.*, 2019).

2.3 Endophytic secondary metabolites as drugs and potential novel drug

The dark ages were characterised by a steep decline in discovery rate and development of novel bioactive medically significant drugs. The drop was a consequent of continuous re-discovery of similar molecules from the same ecological niches, usually soil (Belknap *et al.*, 2020). Given the notion and continuous quest for novel drug scaffolds, it is a priority to bio-prospect and mine largely unexploited reservoirs .

Over several decades natural products have been the starting point of discovering major chemotherapeutics and antimicrobials (Nguyen *et al.*, 2020). Microorganisms have been reported over the years to be the most prolific source of diverse novel chemical compounds with an equally wide array of scaffolds and bioactivities composing most currently valuable pharmaceutical products (Deshmukh *et al*., 2014). Fungi, actinomycetes and myxobacteria are the principal sources of natural products, particularly structurally diverse and bioactive secondary metabolites. Some of the secondary metabolites exhibit antibiotic, anticancer, antiparasitic and immunosuppressive properties (Juboi, 2017). Various metabolic engineering techniques have propelled the interest of screening natural products produced by microorganisms. Thus, enabling harnessing of the bioactivity, wide structural diversity, and subsequently utilised in the development of synthetic or semi-synthetic derivatives (Nguyen *et al.*, 2020). Furthermore, improvement in genetic and genomic analysis has further shown that the microorganisms possess much superior biosynthetic potential than previously known (Juboi, 2017).

Genome mining and ribosome engineering have been a revelation in drug discovery and is fast becoming an essential tool in evaluating the unprecedented biosynthetic ability of microorganisms (Belknap *et al.*, 2020)(Figure 2.7). Analytical methods have also evolved, for example, the hyphenated (LC-MS) liquid chromatograph coupled with mass spectrometry is an efficient, highly sensitive, precise method which can be employed for analysis of natural

product mainly compound identification, partly chemical structure elucidation and dereplication. Other analytical techniques which are used include high-performance liquid chromatography (HPLC), mass spectrometry, gas chromatography and nuclear magnetic resonance (NMR) spectroscopy (Juboi, 2017).

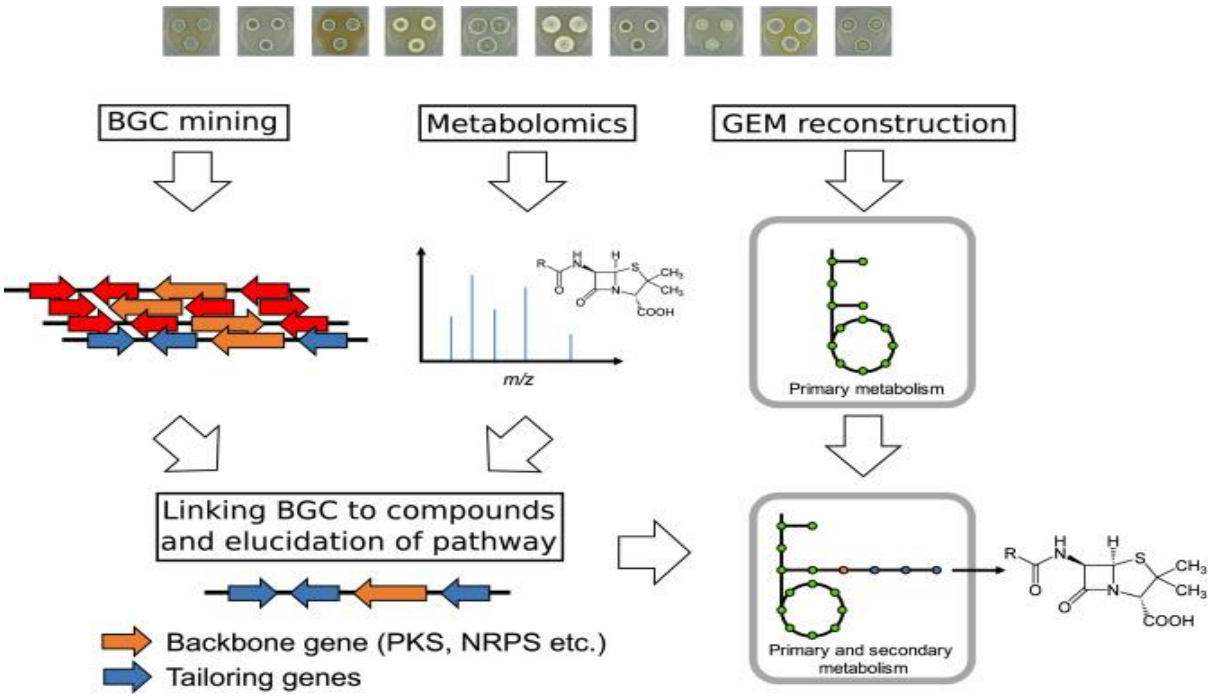

Figure 2.7: The combination of genome mining and metabolomics facilitates the discovery of novel bioactive secondary metabolites. Adapted from (Nielsen and Nielsen, 2017).

Molecular docking is a computer-aided approach widely used in structure-based rational drug design (Jiménez-Luna *et al.*, 2020). It involves an accurate assessment of the electrostatic and steric interaction between ligands (inhibitors, drug candidates or substrates) and target macromolecules (enzyme or receptor) (Singh, 2015). Virtual screening is used for the development of new leads in drug design and repurposing. For example, Itraconazole, Saquinavir, Raltegravir and Nelfanavir have been approved by the Food and Drug Administration (FDA) after the designing and repurposing. Safety and activity of potential drug molecules are essential in preclinical and clinical trials. Evaluation of lead compound toxicity using in vitro and in vivo is expensive and takes much time to perform. However, in silico

techniques are more straightforward and accelerate the assessment of potential drug leads. Thus, reducing the number in vitro and in vivo assays by selecting chemical collections with only desired pharmacokinetic properties (Daina and Zoete, 2019). A software quantitatively allocates scoring after accurately extracting data from the binding affinities of already bonded ligands. The lowest score presents the information on the highest most favourable ligand and receptor interests (Ullah *et al.*, 2019).

In drug discovery and development, the extent of oral bioavailability is essential. Principally, molecular properties of bioactive molecules are essential in determining oral bioavailability and influence the designing of new therapeutic agents (Daina *et al*., 2017). Clearance and metabolism of drugs are reduced when drugs are co-administered with drugs that inhibit drug-metabolizing enzymes. Polymorphism in enzymes that metabolize drugs such as cytochromes P-450 also reduces the metabolisms of the drugs, thus, lead to toxicity caused by extensive drug exposure. Lipinski rules have so far led to the successful development of drug candidates. These rules relate to lipophilicity (octanol-water partition), number hydrogen acceptors and donors and molecular weight (Veber *et al*., 2002)**.** Ultimately, the compound selected for medicinal development must exhibit potent bioactivity along with low toxicity. ADME (Absorption, Distribution, Metabolism and Excretion) online tool predicts the pharmacokinetic properties of the potential therapeutic compounds; thus, accelerates and minimizes the chances of pharmacokinetics related attrition in phase 1 clinical trials (Daina *et al*., 2017).

The *trpB* gene codes for tryptophan synthase subunit beta which catalsyes the last step of tryptophan biosynthetic pathway and the sythensis of tyrosine and phenylalanine. Notably this step only occurs in all prokaryotes, thus, is the enzyme can be used as a potential drug target (Abrahams *et al*., 2017). The peptidoglycan is essential for the synthesis of the bacterial cell wall, thus, critical for bacterial survival. UDP-N-acetylglucosamine 1-carboxyvinyltransfrase

is an enzyme which catalyzes the formation of peptidoglycan polymer (N-acetylmuramic acid and N-acetylglucosamine), the metabolism of nucleotide sugar and amino sugar. This enzyme is encoded by *murA* gene and is an important drug target (Dev *et al*., 2020). Lumazine synthase is an enzyme which catalyzes the biosynthesis of riboflavin in fungi and bacteria. This enzyme is an excellent drug target since fungi and bacteria cannot acquire riboflavin exogenously (Simhadri *et al.*, 2017).

Taxol is a billion-dollar cytotoxic compound which was first isolated from the stem bark of *Taxus brevifolia.* Isolation of Taxol from tree encountered drawbacks due to desiccation after removal of the bark from the tree. However, researchers also discovered that there are fungal species that could synthesise Taxol. The genes coding for the biosynthesis of Taxol were established in three out of 90 fungi endophytes from Taxus species. The genes (10-deacetylbaccatin-III-10-O- acetyltransferase, C-13 phenylpropanoid side chain-CoA acyltransferase) in fungal endophytes to be particular *Taxomyces andreane* exhibited high sequence similarity with those plant counterparts (Pirttil¨a and Frank, 2011). Bis-dethio-(bis-methyl-thio)-gliotoxin is an endophytic secondary metabolite extracted from crude extracts of *Penicillium sp.* BCC16054 and exhibited a MIC value of 48.8 ng/mL against *Mycobacterium tuberculosis,* suggesting that it can be a potential antitubercular drug (Shaaban *et al.*, 2013).

2.4 Prospecting enzymes

Ecological factors, along with the host, determine the range of enzymes which can be produced by different endophytes (Malfanova, 2013). Internal plant compartments are an inhospitable niche for aerobic microbes because of the rapid burst of reactive nitrogen and oxygen species which is typically termed the host induced stress response. Thus, endophytes to colonise such inhospitable niche they should possess detoxifying enzymes. The positive aspect revealed by

research is the discovery of genes coding for catalase, glutathione S-transferase, glutathione peroxidase and nitric oxide reductase in endophytic genomes in comparison to phytopathogens. These detoxifying enzymes enable the plant to protect the plant cells against oxidative damage. (Hardoim *et al.*, 2015). In a study carried out in India (Karnataka), endophytic fungal isolates from (*Tinospora cordifolia, Piper nigrum L, Piper longum L, Zingiber officinale Roscoe, Hedychium coronarium* and *Hedychium flavesce*) were examined for preliminary screening of enzyme production. Only 28% of the fungal isolates exhibited cellulase, while, 29% showed amylase activity, 18% exhibited pectinase activity, and 40% were positive for asparaginase (Uzma *et al*., 2016). These findings show that endophytes can produce essentials enzymes which can be utilised in industrial purposes.

2.5 Other application of endophytes

Endophytes can be used as bio-control agents, and research has shown great potential in this area (Porras-alfaro and Bayman, 2011). Endophytes form a protective barrier against colonisation of leaf surface by pathogens. Upon infection of the leaf surface by insects, alkaloids, volatile organic compounds and other compounds are released in a rapid defensive mechanism. If the pathogen invades into the plant, production of large volumes of reactive oxygen species (ROS) and synthesis of phenylpropanoids are triggered as well the activation of pathogen-associated molecular patterns (Nan *et al*., 2018)(Figure 2.7). This has been shown in bio-control research toward nematodes, where an endophytic bacterium *Rhizobium etli* strain G12 was demonstrated to induce systemic resistance toward *Meloidogyne incognita* a root-knot nematode (Martinuz *et al*., 2011). In another research carried out in Australia, the inoculation of *Beauveria bassiana* and *Lecanicillium lecanii* resulted in a decline in the reproduction and leaf consumption inflicted by the aphid *Aphis gossypii* and a reduction in the

growth of nymphs of the Australian plague locust *Chortoicetes terminifera* (Porras-alfaro and Bayman, 2011).

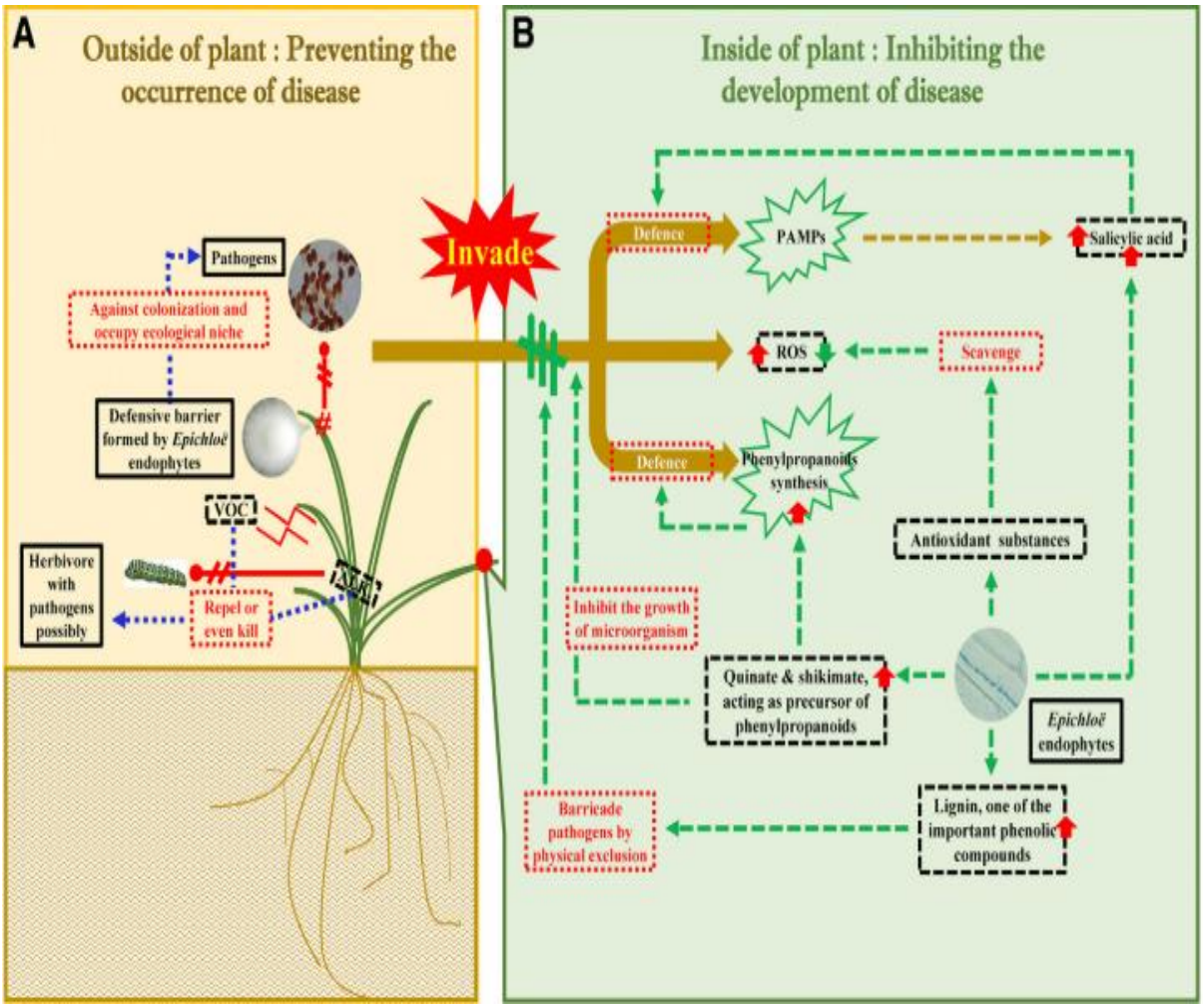

Figure 2.8: Interaction between the pathogens and Epichlo¨e endophytes. Adapted (Nan *et al*., 2018).

The induced resistance mediated by endophytes is non-specific and does not involve the toxic effects of the inducing agent (endophyte) as well as the absence of a dosage-response correlation (Goyena, 2019**).** Antibiotics, salicylic acid, siderophores, volatiles, N-acyl-homoserine lactones, flagella and lipopolysaccharides are some of the bacterial factors that trigger ISR induction (Hardoim *et al.*, 2015). In this regard, utilising symbiotic endophytes in breeding resistant cultivars present an environmentally and economically friendly technique,

subsequently reducing chemical exposure to the environment (Nan *et al*., 2018). Advantages of using endophytes as biocontrol agents include:

i. Biocontrol is a self-regulating method which does not require supervision as compared to use of insect and pesticides.
ii. It preserves the fitness of the ecosystems, thus, environmentally friendly.
iii. It is economically sustainable, whereas chemical usage requires personnel and constant purchase of the chemical agents.
iv. It presents a long-term solution for controlling harmful organisms.
v. It does not have side effects on human health
vi. The use of chemical possesses a severe threat after pathogens gain resistance, but with bio-control, there are no significant issues regarding the development of resistance (Dar *et al.*, 2019).

2.6 Antimicrobial susceptibility testing

Antimicrobial susceptibility testing (AST), is a method utilised to determine the effectiveness of antimicrobial therapy against a particular bacterial infection. Thus, assists medical personnel in the selection of drugs for the treatment of a particular infection and to reveal the fluctuation in trends in the local strains (Bagul *et al*., 2016). International agencies established the breakpoints in classifying the minimum inhibition concentration (MIC) of antibiotics in (AST) antimicrobial susceptibility testing. The decisions on whether an antimicrobial compound is susceptible or not is, this way, directly related to these breakpoints (Hudzicki, 2009)(Table 2.2). The Clinical and Laboratory Standards Institute (CLSI) established the limits of the universal guidelines used worldwide based on the mechanisms of drug resistance, pharmacokinetic-pharmacodynamic (PK-PD) and MIC distributions (Kassim *et al.*, 2016).

Table 2.2: Zones of inhibition ranges for Staphylococcus *spp*. (nearest whole mm). Adopted from (Hudzicki, 2009)

	Resistant	Intermediate	Susceptible
Cefazolin (30 µg)	≤ 14	15-17	≥ 18
Clindamycin (2 µg)	≤ 14	15-20	≥ 21
Erythromycin (15 µg)	≤ 13	14-22	≥ 23
Gentamicin (10 µg)	≤ 12	13-14	≥ 15
Oxacillin (1 µg)	≤ 10	11-12	≥ 13
Penicillin (10 µg)	≤ 28	--	≥ 29
Tobramycin (10 µg)	≤ 12	13-14	≥ 15
Vancomycin (30 µg)	--	--	≥ 15

2.6.1 Different mechanisms utilised by bacteria to resist antimicrobials

Microorganisms employ different mechanisms to resist antimicrobial agents. These methods include:

i. Efflux pump which removes accumulated antibiotics from the cell before reaching or binding it is intended target.

ii. Development of an impermeable barrier by Gram-negative bacteria, thus, prohibiting entry of antimicrobial drugs, e.g. Beta lactams.

iii. Genetic rearrangement/ altering, which consequently alters particular metabolic processes; thus, antimicrobial drugs cannot exert any effect.

iv. The bacteria synthesise enzymes (beta-lactamase produced by the bacteria hydrolyse beta-lactam antibiotics) which prevent the antibiotics from reaching the intended target by destroying them.

v. Mutation, for instance, methylation of the ribosomal RNA, consequently macrolide resistance development (Bagul, Technical and Society, 2016; *Meena et al., 2019*).

Activation of quorum sensing genes in microbes will result in virulence of the microorganism. *S. aureus* is a gram and coagulase-positive bacterium that is capable of causing infections to critical device-associated infections, sepsis and death. Explicitly *S. aureus* causes diseases by the synthesis of various toxins, and some strains are resistant to methicillin (MRSA). *S. epidermidis* is a coagulase-negative bacterium which forms biofilms which are significantly resistant to antimicrobials and host immune system activity (Rasooly *et al.*, 2019).

2.6.2 Agar well diffusion method

The Agar well diffusion method has been utilised for susceptibility testing of antifungal agents, e.g. itraconazole and fluconazole. The potency of the antimicrobial agents, pH of the agar medium, presence of thymine in agar medium, incubation conditions and density of the test strain inclusively affect the performance and findings of AST assay (Bagul *et al*., 2016)(Figure 2.7). Appropriate agar medium is prepared and after the agar has solidified, the bacterial (1-2 × 10^8) colony-forming units per millilitre CFU/ml suspension is promptly inoculated by swabbing using cotton swabs (Bakar *et al.*, 2020; Challaraj *et al*., 2020; Photolo *et al.*, 2020). A sterile cork borer then punches wells of approximately 6 millimetres in diameter. A volume of 25-50 µL of the antibiotic test solutions are then filled in the wells, and the plates are then incubated at 35 ± 2℃ for 18-24 hours. Calculation of the antibacterial agent activity occurs as follows: ZOI (Zone of inhibition.) = Total Diameter of growth inhibited zone minus diameter of the well . The agar well technique is a more convenient standardised diffusion variant used for testing aqueous suspensions of endophytic extracts than the disc diffusion variant in this research. This is because the disc surface (Whatman filter paper) is composed of numerous free

hydroxyl groups on each glucose residues; hence, the disc surface is hydrophilic. Cationic endophytic secondary metabolites will this way adsorb on the surface of the Whatman disc, hence, will not diffuse into the agar. The use of DMSO to reconstitute secondary metabolites also aids to the higher sensitivity of the agar well variant because compounds along with the carrier DMSO can diffuse with ease across the agar. In comparison, the lower sensitivity of the disc technique when testing natural products may also be attributed to the diffusion of compounds occurring through capillarity (Valgas *et al.*, 2007). Usually, the agar diffusion method is utilised for determining the MIC (minimum inhibition concentration) in solid media. This technique can accurately obtain the MIC by simple linear regression evaluation; thus, it is widely utilised in susceptibility assays (Bonev *et al*., 2008).

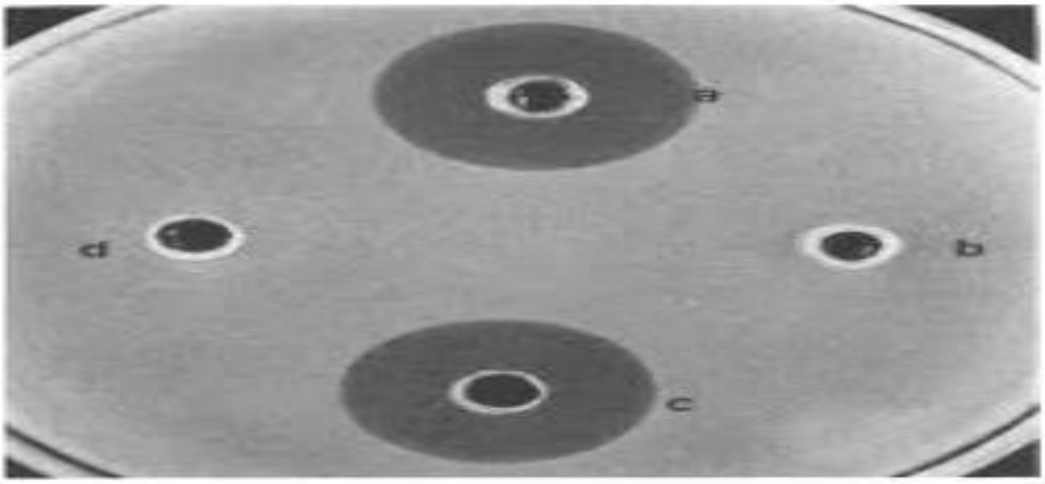

Figure 2. 9: Agar well diffusion method. Adapted from (Bagul, 2016).

This current research project seeks to identify and comprehensively evaluate the secondary metabolites produced by endophytes isolated from Zimbabwean medicinal plants. Findings from this current research project will try to address the need to discover environmentally friendly, low toxicity and immensely useful secondary metabolites. Thus, providing an alternative solution to alleviate the rising concerns of multidrug-resistant microorganisms, particularly in Zimbabwe.

CHAPTER 3

3. Materials and Methods

3.1 Sample collection

The study was conducted at the University of Zimbabwe which is located at latitude 17°47'01.3"S and longitude 31°02'54.9"E, at an altitude of 1483 m above sea level (masl). The site has a warm temperate climate with an average annual temperature range of 9 °C - 22 °C and an average annual rainfall of 831 mm received mainly during the summer months from November to March. The endophytic samples were isolated from Musekesa (*P. thonningii*), Mupane (*C. mopane*), Muzhozho (*V. amygdalina*), Mugan'acha (*L. discolour), P. angolensis,* Mutamba *(S. pungens*), Mukute (*S. guineense*) and Marula (*S. birrea*) and stored as liquid cultures. The samples were taken from trees that are common in Zimbabwe (Takarova, 2018).

3.2 Isolation and Maintenance of endophytes

Sterile plant segments from *P. thonningii, C. mopane, V. amygdalina, L. discolour, P. angolensis, S. pungens, S. guineense* and *S. birrea* were implanted on surface of potato dextrose agar (PDA) and nutrient agar in petri dishes. The petri dishes were incubated at room temperature in the dark and the growth of endophytic microoganisms were monitored. The grown endophytes were characterised according to morphology and spores. The endophytes were stored in liquid cultures under room temperature (Takarova, 2018). We collected the liquid endophytic cultures and cultivated them on Potato dextrose agar (PDA) (Biolab®) and nutrient agar (Biolab®). The Petri dishes were incubated under room temperature in the dark and were monitored daily to observe the growth of endophytic growth. The endophytes were allowed to grow for 4-7 weeks. The grown endophytes were macroscopically evaluated. The differentiated endophytes were isolated by streaking method onto PDA and MEA until pure

cultures were obtained. The 23 pure cultures obtained were numbered 1 to 23. For long term preservation, the agar blocks impregnated with endophytic colonies were immersed in 15% (v/v) glycerol and stored at -80 ℃.

3.3 Genomic DNA extraction

An aliquot 500 µl of the bacterial overnight culture was used for DNA extraction. The genomic DNA was extracted by adding 500 µl of lysis buffer into 2 ml tubes containing the fungal or bacterial samples. Each tube was mixed by inversion, and the mixture was incubated at room temperature for 10 minutes. The tubes containing the samples were then centrifuged at 10 000 revolutions per minute (rpm) for 1 minute. The supernatants were transferred into sterile 1.5 ml tubes and then centrifuged at 10 000 rpm for 1 minute. The supernatants were transferred to fresh sterile tubes, and equal volumes of isopropanol were added to each tube and the tubes mixed by inversion. The microfuge tubes were then centrifuged at 10 000 rpm for 2 minutes to pellet the genomic DNA. The pellets formed were washed with 300 µl of 70% ethanol and centrifuged at 10 000 rpm for 3 minutes, and the supernatants were poured off. The pellets were dried using the speed vac. The pellets were resuspended in 50 µl of T.E. buffer (10mM Tris-HCL, 0.1mM EDTA, pH 8.0). The integrity and size of the endophytic genomic DNA were evaluated on 0.8% agarose gel containing 2 µl Ethidium bromide (10 mg/ml) using electrophoresis at 150 volts and 400 Amps for 30 minutes. Ultraviolet light was used to visualize the agarose gel, and a picture was taken.

3.3.1 16S rRNA gene Amplification

For genotypic identification, the extracted total genomic DNA was used to amplify bacterial 16S rRNA gene regions using the universal forward primer (*27F*: AGATTTGATCCTGGCT) and universal reverse primer (*1492R*: CGGTACCTTGTTGTTAC). The PCR reaction was carried out in a 25 µl of a Master reaction mixture comprising of 5 µl of 5X PCR buffer, 2.5 µl of mM dNTPs, 1.5 µl of 25 mM $MgCL_2$, 1 µl of the forward primer and 1 µl reverse primer, 3 µl of Kirk-house *Taq* DNA polymerase, 10 µl of PCR water and 1 µl of DNA. The PCR amplification was carried out in an Applied Biosystems model 2720 thermal cycler using the following conditions: 1 initiation denaturation cycle at 94 ℃ for 3 minutes, 35 denaturation cycles at 94 ℃ for 30 seconds, 35 primer annealing cycles at 55 ℃ for 30 seconds, 35 extension cycles at 72 ℃ for 90 seconds, one elongation cycle at 72 ℃ for 5 minutes and the reaction is held indefinitely at 4 ℃. The PCR products were analysed on 1% agarose gel containing 2 µl Ethidium bromide (10 mg/ml) by electrophoresis at 150 volts and 400 Amps for 30 minutes. U.V light was used to visualize the agarose gel, and a picture was taken.

3.3.2 M13 RAPDs

Generic markers (RAPDs) were used differentiate between the endophytic compounds that have been identified as 16 S rRNA positive. The total extracted genomic DNA was used to amplify the RAPD using the M13 forward primer (5'-(TGTAAAACGACGGCCAGT)-3'). The PCR reaction was carried out in a 25 µl Master reaction mixture which consisted of 2.5 µl 10X BD PCR buffer, 2.5 µl dNTPs, 1 µl of M13 forward primer, 2.5 µl of $MgCl_2$, 0.25 µl of Firepol *Taq* DNA polymerase, 1 µl of DNA template, 15.25 µl of PCR water. The conditions used for the PCR amplification were as follows: 1 initiation denaturation cycle at 94 ℃ for 1 minutes, 40 denaturation cycles at 94 ℃ for 1 seconds, 40 primer annealing cycles at 38 ℃ for

1 minute, 35 extension cycles at 72 ℃ for 2 minutes, one elongation cycle at 72 ℃ for 10 minutes and the reaction is held indefinitely at 4 ℃. The PCR products were evaluated on 1% agarose gel containing 2 µl Ethidium bromide (10 mg/ml) by electrophoresis at 150 volts and 400 Amps for 30 minutes. U.V light was used to visualize the agarose gel, and a picture was taken. A dendrogram to compare the relatedness of the isolates was constructed by dendroUPGMA online tool (Garcia-Vallve *et al*., 1999).

3.4 Antagonist test

The *in vitro* antagonistic reaction of endophyte-endophyte was tested using the antagonistic assay modified (Takarova, 2018). PDA media was used for testing the antagonistic potential of endophytic isolates. The PDA media was autoclaved at 121 ℃ for 15 minutes at 15 psi pressure. After autoclaving the sterile molten PDA media was cooled to approximately 45 ℃ and then poured into a sterile petri dish to a final depth of 4 mm. The petri dish was divided into three segments, and on each segment, an endophytic plug was inoculated onto the PDA media. The culture was incubated at room temperature and observed daily for growth behaviour.

3.5 Production of secondary metabolites

The Secondary metabolites production was induced using fermentation broth in malt extract broth and Luria Bertani Broth (L.B) (Sigma-Aldrich®). The fermentation broth was prepared by inoculating 2 ml of an overnight liquid culture of bacterial endophyte into 20 ml Malt Extract Broth (MEB) (Sigma-Aldrich®). For fungal endophytes, the fermentation broth was prepared by inoculating MEB with 7-15 mm mycelium scrapped from PDA surface. The endophytic liquid cultures were then fermented at room temperature for 14 days.

3.5.1 Extraction of bioactive metabolites from bacterial and fungal cultures

The solvents were used as received from the supplier without further purification unless otherwise stated. Small scale extraction was performed after 14 days of fermentation of bacterial and fungal cultures. An aliquot (600 µl) of bacterial or fungal cultures was pipetted into 2 ml microfuge tubes. The tubes were centrifuged at 5 000 rpm for 5 minutes. The supernatant was transferred into a clean microfuge tube, an equal volume of the solvent (acetone or methanol or ethyl acetate) was added in each separate tube. The crude extract and solvents were centrifuged at 5 000 rpm for 5 minutes to separate the phases. The mass of an empty weigh boat was measured. The organic layer or aqueous phase, if no separation had occurred, was transferred into a weigh boat. The crude extracts in the weight boat were air-dried in a fume hood. The mass of the weigh boats with dried extracts was measured. The dried crude extracts of bacterial and fungal endophytes were dissolved in 2.5% dimethyl sulfoxide (DMSO) to formulate stock solution of crude fungal and bacterial extracts and the concentration was calculated in mg/ml / µl/ml.

3.6 Test-bacteria strains

The antibacterial efficacy of endophytic crude ethyl acetate, methanol and acetone extracts was assessed against *Escherichia coli* (American Type Culture Collection (ATCC) 35218) (Gram-negative bacteria) and *Staphylococcus aureus* (ATCC 25923) (Gram-positive bacteria). The microorganisms were obtained from the Department of Biochemistry, University of Zimbabwe (17°47'01.3"S 31°02'54.9"E). An aliquot of 500 µl of each stock solution of bacteria strains was inoculated into 5 ml L.B. broth under sterile conditions and incubated at 37 ℃. After 24 hours of incubation, the bacterial inoculum was diluted with sterile broth to 10^8 CFU/ml for antimicrobial.

3.7 Determination of antibacterial susceptibility

The endophytic crude (ethyl acetate, acetone and methanol) extracts were examined for antimicrobial efficacy against *Staphylococcus aureus* and *Escherichia coli* using the agar well diffusion method (Takarova, 2018). The sterilized L.B. molten agar was cooled to approximately 45 ℃ and subsequently inoculated with the test strains to make up a final concentration of 10^6 CFU/ml. The inoculated molten agar was dispensed into 90 mm diameter Petri dishes. Sterile tips with a diameter of 5 mm were utilized to punch wells into the solidified agar. A volume of 10 µl, 35 µl and 50 µl of reconstituted endophytic extracts was loaded into the agar well for antibacterial efficacy testing. The antibiotic ampicillin was used as positive controls, while 2.5% of the DMSO solution was used as a negative control. The assay plates were incubated at 37 ℃. The antibacterial activity was determined by measuring the zones of inhibition after 24 hours.

3.8 Chromatography assays

3.8.1 Qualitative analysis of endophytic extracts using TLC chromatography

The solvents were used as received from the supplier without further purification unless otherwise stated. Analytical thin-layer chromatography fingerprints of ethyl acetate, methanol and acetone extracts were carried out on aluminium sheets precoated with silica gel 60 (Sigma T-6770®), 10 µl of each extract was loaded as a band on the TLC analytical plates. The eluent solvent systems of diverse polarities which were used include., dichloromethane: ethyl acetate (20:80 DCM: E.A. polar). The eluted TLC plates were dried, and the separated chromatograms were visualized using ultraviolet light (254 and 365 nm wavelengths, U.V light lamp) and the bands were marked using a pencil. For optimal colour development, the TLC plates were

treated with vanillin sulphuric acid spray reagent (0.1 g vanillin, 28 mL methanol, 1 mL sulphuric acid) and then was heated in an oven at 110 ℃. The elution of the metabolites, along with selected solvents, was measured and the Rf value was calculated.

3.8.2 GC-MS analysis

Acetone extracts of endophytic samples 1, 3, 9 and 17 were selected for gc-mc analysing based on their antimicrobial efficacy. The method was modified from Zomorodian *et al.*, (2019). GC-MS system was equipped with a HS-5MS capillary column calibrated as follows; 30m × 250 µm inner diameter fused-silica capillary column × 0.25 µm stationary phase. Helium gas was used as a carrier gas, at a constant flow rate of 1 ml/min. The injector MS transfer line temperature was set at 250 ℃ while detector MS transfer line temperature was set at 290 ℃. An aliquot, (1 µl) of an endophytic sample was injected by a 10 µl syringe in a splitless mode into an Agilent 10991S-433UI GC system. The electron ionization mode was set at 10 eV. Column temperature was initially held at 60 ℃ for 5 minutes., and then gradually ramped at 6 ℃/min to 220 ℃, then kept for 10 minutes. Agilent Masshunter unknown Analysis Software was used in evaluating the mass spectra and chromatograms.

3.9 *In silico* molecular docking assay

The 3D protein structures of lumazine synthase (1I8D), Tryptophan synthase subunit beta (1ttq) and UDP-N-acetylglucosamine 1-carboxyvinyltransfrase (1uae) were downloaded from the Protein Databank RCSB (http://www.rcsb.org/p-db) in PDB format. Ampicillin was used as the standard compound. The ChemSpider web server (http://www.chemspider.com/) was used to download the 3D chemical structures of the selected endophytic compound in a Mol format file. The Mol format files of the compounds were converted into a PDB format by Open Babel

software. Water molecules were removed from in protein in preparation for docking. Auto Dock Tools package determined the configuration of the active sites of target proteins. The grid box dimensions were set at 40×40×40 and the exhaustive value used was 8. Auto dock Vina evaluated protein-ligand interactions. Discovery Studio (Version 5.0) predicted the feasibility of the molecular associations and binding affinity of the endophytic compounds and the target proteins (Singh, 2015).

3.10 Evaluation of biological activity

The (Prediction of Activity Spectra for Substances) PASSonline web server (http://www.pharmaexpert.ru/PASSonline) was used to determine the bio-activity of the endophytic compounds. The prediction of the compound bioactivity spectrum by PASSonline is expressed as the probable activity (Pa) and probable inactivity (Pi). The range for Pi and Pa is from 0.000 to 1.000. The results are were interpreted as follows: if Pa>0.7 it implied that the possibility to find the bio-activity of the compound is *in-vivo* and *in-vitro* is high; if 0.5<Pa>0.7, if Pa<0.5 the chance to obtain bioactivity from the compound is less, but rather, increased the chances of obtaining a novel compound.

3.11Evaluation of drug-like properties

The evaluation of drug likeness, pharmacokinetics and pharmacological chemistry friendliness of the selected endophytic compounds was performed by SwissADME online tool (http://www.swissadme.ch/). Lipinski's Rule of Five was used as the criteria for evaluating the drug-likeness of the selected endophytic compounds. The criteria was: molecular mass should be less than 500 Da, hydrogen bonds donors and acceptors should be less than 5 and 10,

respectively, the lipophilicity should be less than 5 and the molar refractivity should be between 40-130 (Simhadri *et al.*, 2017).

CHAPTER 4

4. Results

4.1 Molecular characterisation

Genomic DNA of endophytic samples that exhibited potent antimicrobial activity was succefully extracted. Good quality genomic DNA was shown by approximately 10 000 bp bands in lane 1 to 9 (Figure 4.1). Amplification of the 16 S rRNA gene was performed to evaluate if the endophytes are bacteria. Endophytic samples 1, 3, 9, 10, 12, 15, 18, 17 and 19 found to be bacteria as illustrated by the 1500 bp amplicons on a 1 % ethidium bromide-stained TAE agarose gel (Figure 4.2). The band in lane 2 is faint which might be due to small quantities of template genomic DNA. RAPDs analysis using M13 forward primer showed that the endophytic bacteria are different as illustrated by the distribution of bands (Figure 4.3) and the dendrogram (APPENDIX V). Samples 12 and 3 are closely related and originate from the same ancestral bacteria. Also, sample 12 and 3 are distantly related to all samples as illustrated by the length of the branch. Sample 17 is distantly related to sample 1,3, 9, 10, 15, 18 and 19. sample 1 and 18 have the same ancestral origin, while sample 10 and 19 have the same ancestral origin.

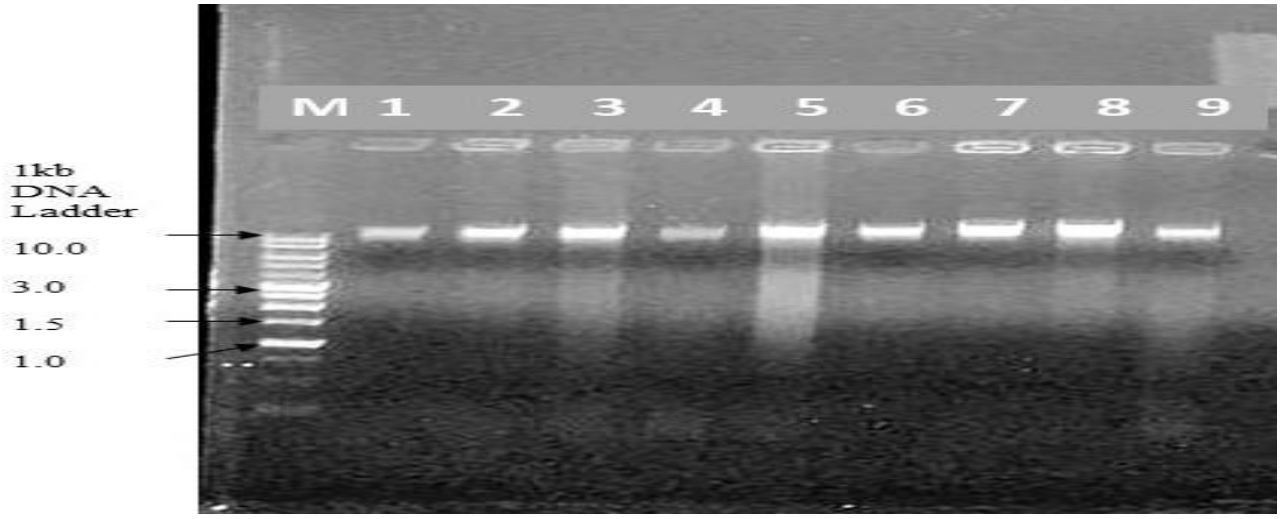

Figure 4.1: Ethidium bromide-stained 0.8 % TAE agarose gel showing genomic DNA of endophytes visualized using UV light. Lane M, Molecular weight marker (1 kb DNA ladder). Lane 1 to 9, sample 1, 3, 9, 10, 12, 15, 18, 17 and 19. Note 10.0 represents 10 000 bp.

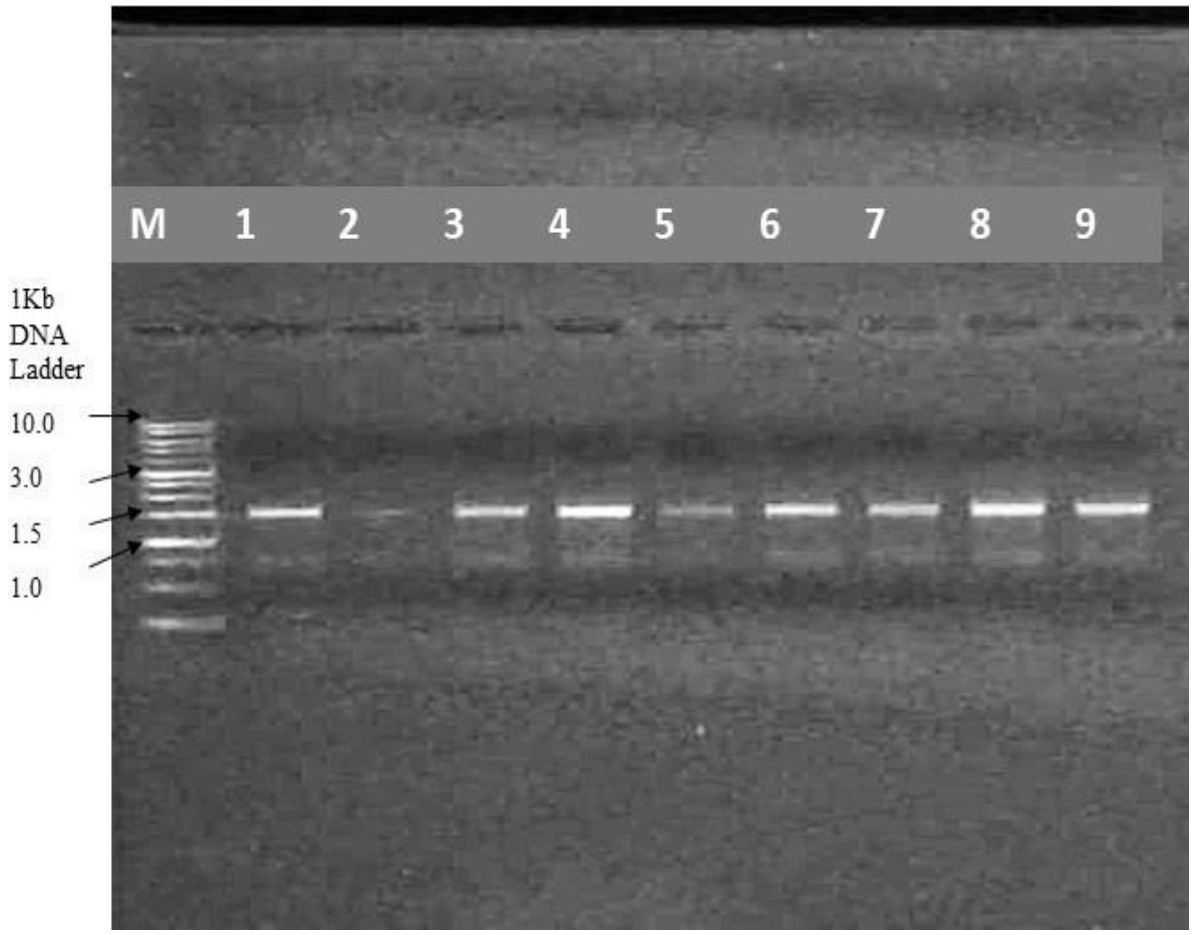

Figure 4.2: Ethidium bromide-stained 1 % TAE agarose gel showing polymerase chain reaction products from endophytic samples obtained by using 27F and 1492R primers to amplify approximately 1500 bp of 16 S rRNA gene. Lane M; Molecular weight marker (1 kb DNA ladder). Lane 1 to 9; 1, 3, 9, 10, 12, 15, 18, 17 and 19. Lane 2 the band is faint. Note 10.0 represents 10 000 bp.

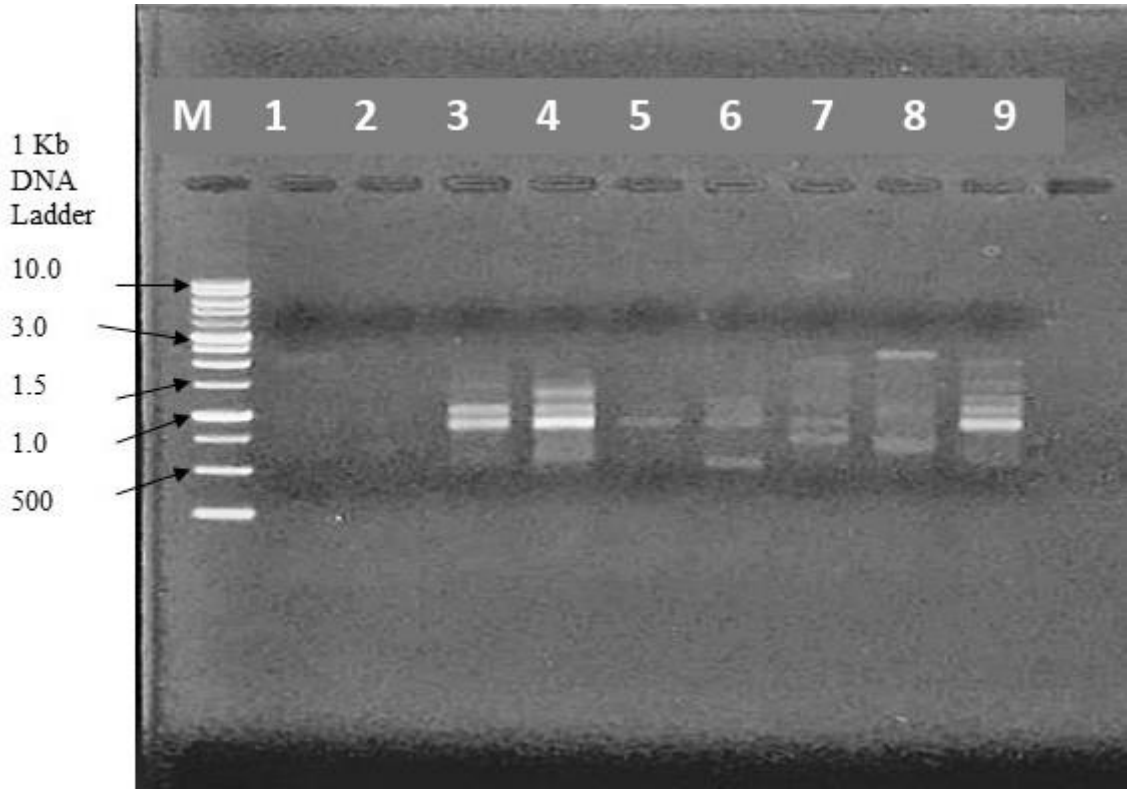

Figure 4.3: Ethidium bromide-stained 1 % TAE agarose gel showing M13 RAPDs amplicons visualized using the UV light. Lane M represent the molecular weight marker while 1 to 9 represent sample 1, 3, 9, 10, 12, 15, 18, 17 and 19. Note 10.0 represents 10 000 bp, 500 represents 500 bp.

4.2 Antagonist assay

the endophytic cultures were isolated until pure isolates were obtained. The pure isolates were cultivated on PDA and nutrient agar. The pure isolates were then tested for antagonist assay. The in vitro antagonist assay demonstrates the interaction between endophyte-endophyte from different tree sources and also establishes if the endophytes isolated secrete extracellular bioactive secondary metabolites in defence response. The assay also establishes if the endophytes require co-cultivation for the secretion of more unique extracellular bioactive secondary metabolites. Endophytic isolates 3, 22 and 6 aggressively proliferated towards the other endophytic isolates. The proliferation stopped before physical contact with the biomass of endophytic isolates 1, 5, 8, 14, 15 and 12 signified by a zone of inhibition. (Figure 4.4 a-h) The endophytic isolate 5 exhibited the largest zone of inhibition (Figure 4.4 d). The colour of the biomass of 6 changed from yellowish to slightly reddish when it approached other endophytic isolates biomass signifying interspecies communication (Figure 4.4 b).

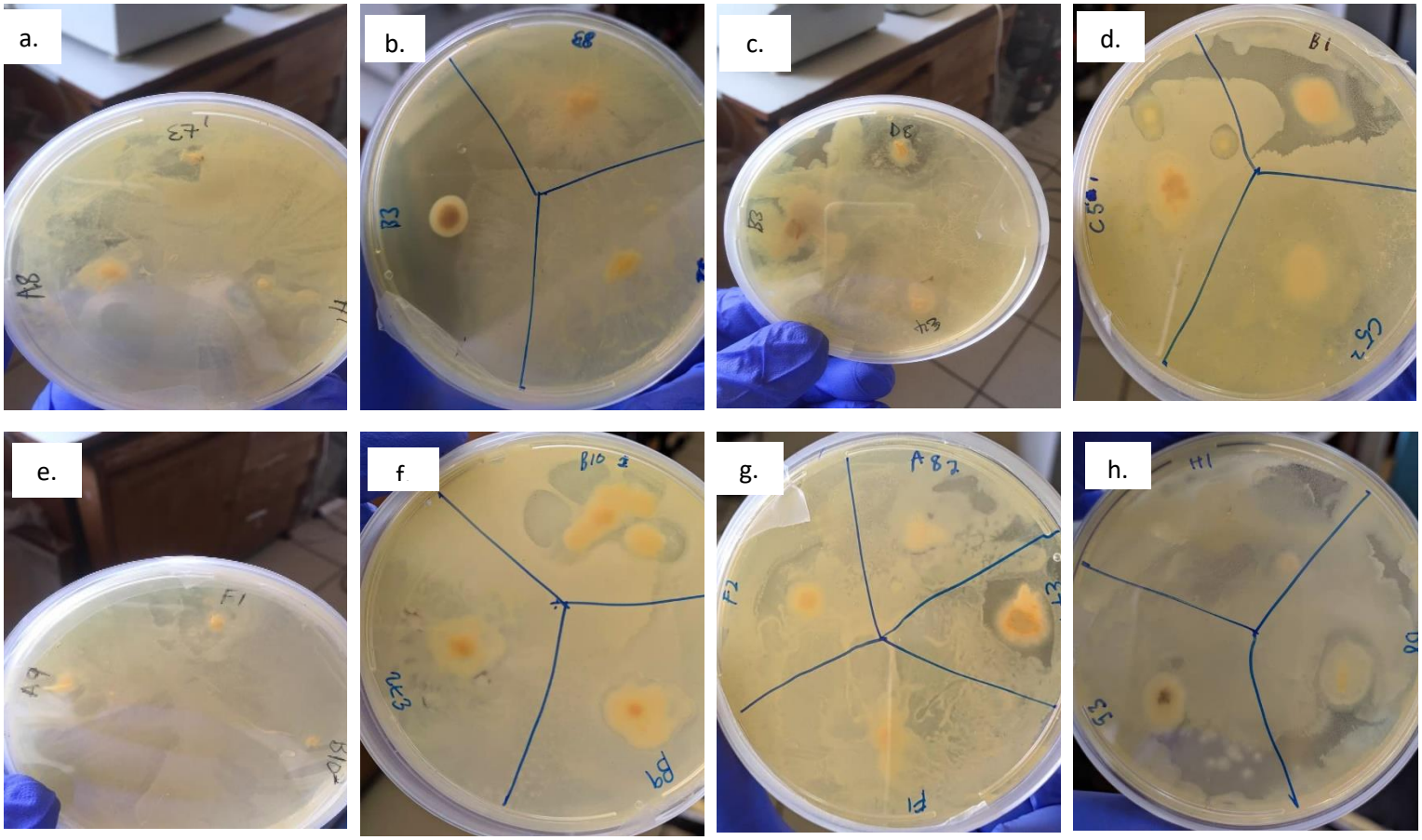

Figure 4.4: Interaction of different endophytic isolates observed antagonistic culture assay. (a-h) zones of inhibition exhibited by endophytic isolates. Sample number 1, 3, 5, 6, 8, 14, 15, 12 and 22 represent endophytic isolate A8, A9, B1, B3, $B10^{1}$, $E7^{1}$, $E7^{2}$, D8 and H1 respectively.

4.2 Antimicrobial properties of endophytic crude extracts

Evaluation of endophytic bioactive secondary metabolites as targets for discovery of novel drugs and as an alternative route of combating AMR, we investigated the antimicrobial efficacy of endophytic extracts against two bacterial species which are *S. aureus* (Gram-positive bacteria) and *E. coli* (Gram-negative bacteria) (Table 4.1, Table 4.2, Table 4.3). Three different volumes were used in an attempt to evaluate the relatedness of dosage, solubility and antimicrobial efficacy of the endophytic compounds. An aliquot of 50 µl from 100 µl of endophytic extracts (APPENDIX I-IV) showed incredible antimicrobial efficacy. Broadly, the zones of inhibition diameter ranged from 0-35 mm (Table 4.1, Table 4.2, Table 4.3). The extracts from endophytic samples 1, 3, 4 and 20 showed the strong antimicrobial potency against both *S. aureus* and *E. coli*. The endophytic extracts of samples 4, 6, 7, 8, 15, 16, 18, 19 and 23 exhibited moderate antimicrobial activity against *E. coli* only, while extracts of endophytic samples 14, 16 and 22 showed antimicrobial activity against *S. aureus* only. The extracts of endophytic samples 5, 6, 12,15, 19 and 23 exhibited moderate antimicrobial potency against *E. coli*, while 2,12, 14, 15, 22 and 23 showed moderate antimicrobial potency against *S. aureus* (Table 4.1, Table 4.2, Table 4.3).

The clarity of the zones of inhibition elucidates the minimal concentrations of the endophytic crude extracts which exhibit potency against *S. aureus* and *E. coli.* The results from the agar well diffusion assay for antimicrobial effect shows that utilizing acetone as the extracting solvent presents higher efficacy against *S. aureus* and *E. coli*. Notably, endophytic crude extracts from sample 1, 3, 9, 17, 18 and 19 which were extracted by acetone showed relatively the highest antimicrobial potency against *S. aureus* (Gram-positive bacteria) and *E. coli* (Table 4.2). Endophytic extract from sample 1 obtained from ethyl acetate as the extractant exhibited

strong potency against *S. aureus* and *E. coli* while extracts from sample 8 and 23 showed potent activity against *E. coli* only (Table 4.1).

Acetone and ethyl acetate crude extract from sample 1 exhibited the highest antimicrobial potency against *S. aureus* and *E. coli, respectively*. The acetone extracts of endophytic sample 1 and 3 solvent exhibited the highest potency against both test organisms *S. aureus* and *E. coli*. The endophytic sample 1 showed 35 mm and 29 mm zones of inhibition against *S. aureus* and *E. coli*, respectively. While, endophytic sample 3 exhibited 23 mm and 34 mm zones of inhibition against *S. aureus* and *E. coli*, respectively (Table 4.2). When methanol we used as the extracting solvent, endophytic samples 3, 4 and 20 exhibited strong potency against *E. coli* and *S. aureus* (Table 4.3). The effects of the negative control Dimethyl sulfoxide (DMSO) 2.5 % and positive control Ampicillin 10 µg/ml we observed. The findings revealed different zones of growth inhibition in positive controls. The positive control zones of inhibition for *S. aureus* and *E. coli* were 20 and 17, respectively. There was no zone of inhibition observed by DMSO as a negative control (Table 4.4). We selected endophytic samples 1, 3, 9 and 17 which showed strong antimicrobial potency against either *S. aureus* or *E. coli* for TLC, GC/MS spectrometry assays.

Table 4.1: Qualitative assessment of endophytic crude extracts' antimicrobial efficacy expressed in the diameter of the zone of inhibition (based on the translucency of zones of inhibition).

Sample. no	Endophyte isolate	Origin	Solvent used for extraction	Zone of inhibition (mm)					
				E. coli ATCC 35218			S. *aureus* ATCC 25923		
				10µl	**35 µl**	**50 µl**	**10 µl**	**35 µl**	**50 µl**
1	A8[1]	*P. thonningii*	Ethyl acetate	14	17	25	6	12	20
2	A8[2]	*P. thonningii*	Ethyl acetate	7	7	13	0	8	10
3	A9[1]	*P. thonningii*	Ethyl acetate	0	2	11	0	2	10
4	A9[2]	*P. thonningii*	Ethyl acetate	0	0	0	0	3	8
5	B1	*C. mopane*	Ethyl acetate	0	0	5	0	3	5
6	B3	*C. mopane*	Ethyl acetate	0	5	7	0	7	10
7	B6	*C. mopane*	Ethyl acetate	0	1	3	0	0	0
8	B10[1]	*C. mopane*	Ethyl acetate	7	15	25	0	0	0
9	B10[2]	*C. mopane*	Ethyl acetate	0	0	0	0	0	0
10	C5[1]	*V. amygdalina*	Ethyl acetate	0	0	0	0	0	0
11	C5[2]	*V. amygdalina*	Ethyl acetate	0	0	0	0	0	0
12	D8	*L. discolour*	Ethyl acetate	2	10	16	0	0	13
13	E4	*P. angolensis*	Ethyl acetate	0	0	9	0	7	12
14	E7[1]	*P. angolensis*	Ethyl acetate	0	0	0	0	0	9
15	E7[2]	*P. angolensis*	Ethyl acetate	3	5	15	0	0	0
16	E8[1]	*P. angolensis*	Ethyl acetate	0	8	11	6	13	15
17	E8[2]	*P. angolensis*	Ethyl acetate	0	3	7	0	11	14
18	F1	*S. pungens*	Ethyl acetate	0	6	6	0	0	0
19	F2	*S. pungens*	Ethyl acetate	3	9	0	0	0	0
20	G1	*S. birrea*	Ethyl acetate	0	0	0	0	5	8
21	G3	*S. birrea*	Ethyl acetate	0	0	0	0	0	0
22	H1	*S. guineense*	Ethyl acetate	0	0	0	0	10	10
23	H3	*S. guineense*	Ethyl acetate	18	23	25	0	0	0

Strong crude extract's antibacterial potency (25-35 mm)

Moderate crude extract's antibacterial potency (15-24 mm)

Low susceptibility of either *E. coli* or *S. aureus* to the respective endophytic crude extract (10-0 mm)

No inhibition of *E. coli* and *S. aureus* (0 mm)

Table 4.2: Qualitative assessment of endophytic crude extracts' antimicrobial efficacy expressed in the diameter of the zone of inhibition (based on the translucency of zones of inhibition).

Sample. no	Endophyte isolate	Origin	Solvent used for extraction	Zone of inhibition (mm)					
				E. coli ATCC 35218			S. *aureus* ATCC 25923		
				10 µl	**35 µl**	**50 µl**	**10 µl**	**35 µl**	**50 µl**
1	A8[1]	*P. thonningii*	Acetone	9	24	29	13	27	35
2	A8[2]	*P. thonningii*	Acetone	0	6	8	6	15	20
3	A9[1]	*P. thonningii*	Acetone	15	25	34	12	17	23
4	A9[2]	*P. thonningii*	Acetone	0	9	21	0	0	5
5	B1	*C. mopane*	Acetone	0	7	18	0	0	10
6	B3	*C. mopane*	Acetone	7	14	20	0	0	0
7	B6	*C. mopane*	Acetone	14	15	25	0	0	0
8	B10[1]	*C. mopane*	Acetone	0	0	8	0	10	12
9	B10[2]	*C. mopane*	Acetone	0	10	17	20	26	30
10	C5[1]	*V. amygdalina*	Acetone	3	12	12	15	23	31
11	C5[2]	*V. amygdalina*	Acetone	2	8	15	0	0	0
12	D8	*L. discolour*	Acetone	11	17	22	6	13	21
13	E4	*P. angolensis*	Acetone	0	2	11	0	0	0
14	E7[1]	*P. angolensis*	Acetone	0	0	5	0	10	21
15	E7[2]	*P. angolensis*	Acetone	0	11	18	5	19	22
16	E8[1]	*P. angolensis*	Acetone	0	10	15	0	0	0
17	E8[2]	*P. angolensis*	Acetone	6	24	27	13	13	15
18	F1	*S. pungens*	Acetone	10	20	27	0	10	15
19	F2	*S. pungens*	Acetone	6	14	25	4	7	15
20	G1	*S. birrea*	Acetone	0	7	14	3	9	10
21	G3	*S. birrea*	Acetone	0	0	7	0	0	10
22	H1	*S. guineense*	Acetone	0	0	0	14	18	22
23	H3	*S. guineense*	Acetone	14	14	17	5	12	17

Strong crude extract's antibacterial potency (25-35 mm)

Moderate crude extract's antibacterial potency (15-24 mm).

Low susceptibility of either *E. coli* or *S. aureus* to the respective endophytic crude extract (10-0 mm)

No inhibition of *E. coli* and *S. aureus* (0 mm)

Table 4.3: Qualitative assessment of endophytic crude extracts' antimicrobial efficacy (based on the translucency of zones of inhibition and expressed in the diameter of the zone of inhibition).

Sample. no	Endophyte isolate	Origin	Solvent used for extraction	Zone of inhibition (mm)					
				E. coli ATCC 35218			S. *aureus* ATCC 25923		
				10 µl	**35 µl**	**50 µl**	**10 µl**	**35 µl**	**50 µl**
1	A8[1]	*P. thonningii*	Methanol	4	12	21	0	8	15
2	A8[2]	*P. thonningii*	Methanol	0	0	0	0	0	0
3	A9[1]	*P. thonningii*	Methanol	5	16	20	9	18	25
4	A9[2]	*P. thonningii*	Methanol	8	14	22	4	17	26
5	B1	*C. mopane*	Methanol	6	16	20	7	13	20
6	B3	*C. mopane*	Methanol	2	9	15	0	0	0
7	B6	*C. mopane*	Methanol	0	8	15	0	6	15
8	B10[1]	*C. mopane*	Methanol	8	13	15	0	0	0
9	B10[2]	*C. mopane*	Methanol	0	5	10	0	3	12
10	C5[1]	*V. amygdalina*	Methanol	0	0	0	0	0	0
11	C5[2]	*V. amygdalina*	Methanol	0	0	0	0	0	0
12	D8	*L. discolour*	Methanol	0	0	0	0	0	0
13	E4	*P. angolensis*	Methanol	0	0	0	0	0	0
14	E7[1]	*P. angolensis*	Methanol	0	0	0	0	0	0
15	E7[2]	*P. angolensis*	Methanol	8	16	20	13	15	20
16	E8[1]	*P. angolensis*	Methanol	0	5	7	0	3	7
17	E8[2]	*P. angolensis*	Methanol	0	0	0	0	10	14
18	F1	*S. pungens*	Methanol	0	0	0	0	0	0
19	F2	*S. pungens*	Methanol	10	20	23	0	0	0
20	G1	*S. birrea*	Methanol	6	14	23	9	20	25
21	G3	*S. birrea*	Methanol	0	0	0	0	0	0
22	H1	*S. guineense*	Methanol	0	6	9	0	0	0
23	H3	*S. guineense*	Methanol	0	0	8	0	2	8

Strong crude extract's antibacterial potency (25-35 mm)

Moderate crude extract's antibacterial potency (15-24 mm)

Low susceptibility of either *E. coli* or *S. aureus* to the respective endophytic crude extract (10-0 mm)

No inhibition of *E. coli* and *S. aureus* (0 mm)

Table 4.4: Determination of negative (2.5% DMSO) and positive control (Ampicillin 10 µg/ml) on test bacteria.

Bacteria	Positive control (Ampicillin 10 µg/ml) ZOI (mm)	Negative control 2.5% DMSO ZOI (mm)
E. coli	17	0
S. aureus	20	0

4.3 Characterization of endophytic extracts

The screening of the endophytic ethyl acetate extracts in this study using thin-layer chromatography showed different chemical components as depicted by the different colours (a, b, c, d, e). The solvent systems separated the compounds, DCM/EA 20:80 dichloromethane: ethyl-acetate. Most of the separated compounds may be non-polar compounds. The retention factor (Rf) of the chromatograms was obtained by dividing the distance travelled by the compound by the solvent distance. The profile of ethyl acetate samples 2, 5, 6, 7 and 11 after derivatization with vanillin sulphuric acid methanol spray reagent contained a yellow pigment observed at (Rf value) (Figure 4.5 a and Figure 4.5 f). According to the charring profile of all the metabolites after derivatizing with vanillin sulphuric acid methanol spray reagent indicated the presence of terpenoids (blueish purple) Rf value 6.5, flavonoids (yellow) Rf value 0.06, reddish (stilbenes) Rf value 0.31 (Figure 4.5 a and Figure 4.5 f).

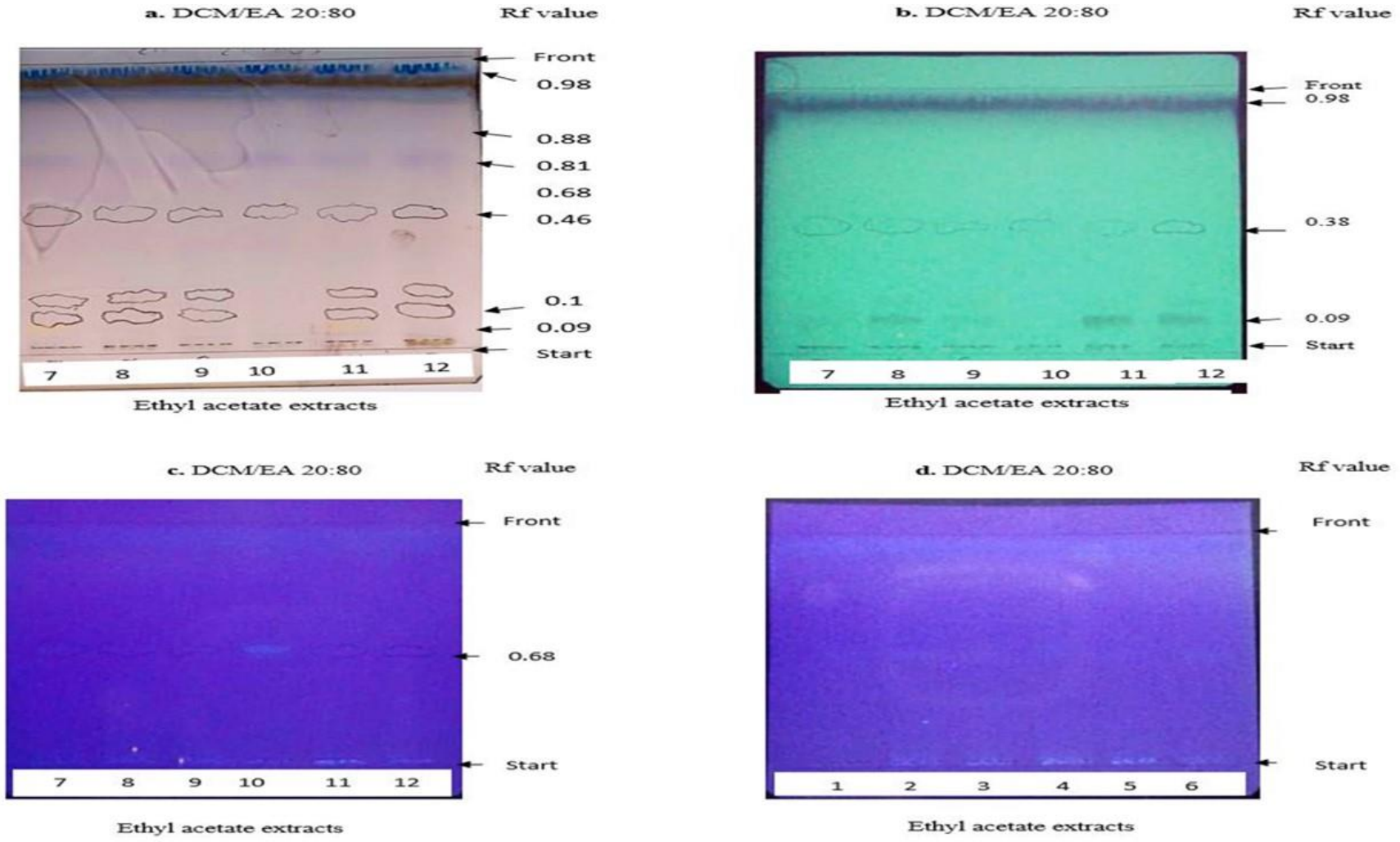

Figure 4.5: Thin layer chromatogram of the endophytic ethyl acetate extracts. a) after derivatization with Vanillin-Sulphuric acid methanol reagent; b) UV 254 nm. The pencil circles are compounds bands visualized at 254/365 nm UV wavelength. (c, d) Thin layer chromatogram of the endophytic ethyl acetate extracts visualized at UV 365 nm.

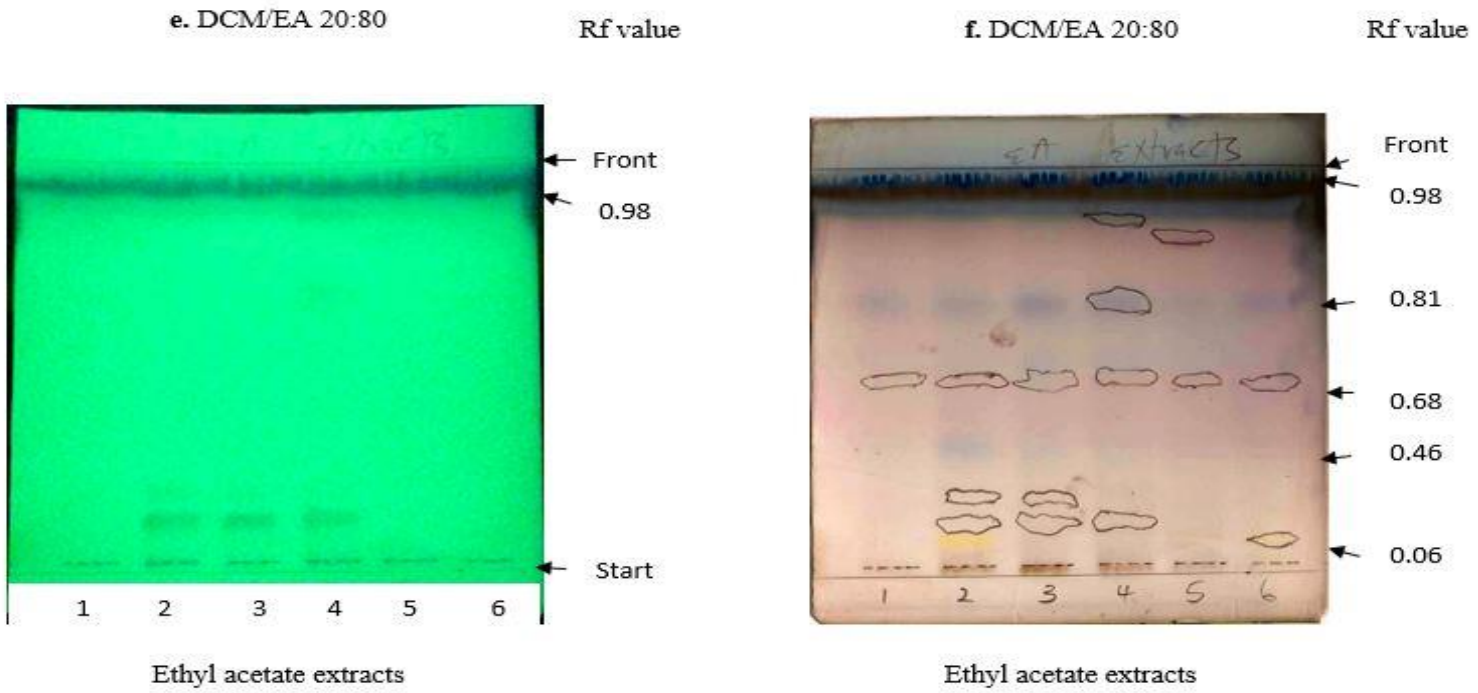

Figure 4.5 continued (e, f) Thin layer chromatogram of the endophytic ethyl acetate extracts. e) UV 254 nm; f) after spraying with Vanillin-Sulphuric acid methanol reagent. The pencil circles are compounds bands visualized at 254/365 nm UV wavelength.

4.3.1 GC-MS analysis of acetone extracts

The large zones of inhibition (antimicrobial efficacy) from acetone endophytic extracts from samples 1, 3, 9 and 17 prompted us to evaluate the chemical constituents present in the extracts that are responsible for the antimicrobial properties. GC-MS was used to chemical evaluation of the endophytic extracts. Match score of the Agilent Mass hunter Unknown Analysis Software was set at 90 % and was then used in identifying the unknown constituents based on the spectra of the compounds. The GC profile of the constituents showed that the extracts contain a wide array of compounds ranging from polar to non-polar. The bioactivity, molecular weight, molecular formula, area and retention time of the endophytic compounds from acetone extracts of sample 1, 3, 9 and 17 are shown in (Table 4.5). The nature of endophytic bioactive constituents identified by the GC-MS profile include alkaloids, indolizine derivatives, quinone, furan derivatives, organic acids, fused uracils, fused uracils, aroma compounds and phenolic compounds and pyrazolo(3,4-d)pyrimidine derivatives. The complex peaks of the endophytic samples are shown acquisition/ retention time (x-axis) and counts (y-axis) (Figure 4.6) Octadecane, eicosane and hexadecane were present in all the endophytic acetone extracts. Most of the endophytic compounds were ranged from very soluble to moderately soluble and satisfied the Lipinski's rule. (+)1-(4-Methylacridine-9-yl)-3-((tetrahyrofuran-2-yl) methyl) thiourea satisfied Lipinski's rule for drug-likeness, had a bioavailability of 0.55 and could penetrate through the brain-blood barrier, thus, was predicted as a lead compound for therapeutic purposes. However, it was produced in small quantities. The constituents with the largest area under the curve were selected for molecular docking assay. The constituents selected for molecular docking were 5H,10H-Dipyrrolo[1,2-a:1',2'-d]pyrazine-5,10-dione, octahydro-, (5aS,10aS)- (area under the curve 100936317), 2-Piperidinone (area under the curve 344080639), Octadecane (area under the curve 61655978), 2-(1H-Imidazol-2-yl)acetic acid (3644570) and 3-Amino-2,2,4-trimethylhexane (106840849) (Figure 4.5)

Table 4.5: Constituents of acetone extract of endophytic samples.

Constituent of sample 1	Retention time	Area	MW g/mol	MF	Water solubility	BBB permeation	Drug-likeness (Lipinski's)	Synthetic accessibility	Bioavailability
1-Tetradecene	23.607	7163804	196.37	$C_{14}H_{28}$	Moderately soluble		Yes	2.38	0.55
9-Eicosene, (E)-	34.091	1366114	280.53	$C_{20}H_{40}$	Poorly soluble	No	Yes	3.72	0.55
4-Methylstilbene	29.765	36920	194.27	$C_{15}H_{14}$	Moderately soluble	Yes	Yes	1.92	0.55
Xanthene	30.784	203011	182.22	$C_{13}H_{10}O$	Moderately soluble	Yes	Yes	2.35	0.55
2-(1-Fluorovinyl)-5-nitropyridine	26.679	3272623		$C_7H_5FN_2O_2$	Poorly soluble	No	Yes	2.72	0.55
Eicosane	39.747	2192073	282.55	$C_{20}H_{42}$	Poorly soluble	No	Yes	2.72	0.55
1,2-Benzenedicarboxylic acid, bis(2-methylpropyl) ester	28.702	898674	278.34	$C_{16}H_{22}O_4$	Moderately soluble	Yes	Yes	2.36	0.55
4-Hexen-1-ol, 4-methyl-	27.512	4867236	114.19	$C_7H_{14}O$	Very soluble	Yes	Yes	1.93	0.55
5-(t-Butyl)-2(5H)-thiophenone	26.292	7139592	156.25	$C_8H_{12}OS$	soluble	Yes	Yes	2.73	0.55

Table 4.5 (Continued)

Constituents of sample 1	Retention time	Area	MW (g/mol)	MF	Water solubility	BBB permeation	Drug-likeness (Lipinski's)	Synthetic accessibility	Bioavailability
Pyrrolo[1,2-a]pyrazine-1,4-dione, hexahydro-3-(phenylmethyl)-	39.312	42807186	244.29	$C_{14}H_{16}N_2O_2$	Soluble	No	Yes	2.46	0.55
Deferoxamine	38.565	58029161	560.68	$C_{25}H_{48}N_6O_8$	Very soluble	No	No	4.10	0.17
Hexadecane	23.749	34766126	226.44	$C_{16}H_{34}$	Poorly soluble	No	Yes	2.26	0.55
.alpha.-(Methoxycarbonyl)-1,3-dioxolan-2-ylideneacetic acid	21.878	13275059	188.13	$C_7H_8O_6$	Very soluble	No	Yes	2.88	0.56
4-Heptanone, 2,6-dimethyl-	9.228	9758968	142.24	$C_9H_{18}O$	soluble	Yes	Yes	1.32	0.55
Tetradecane	19.652	26615161	198.39	$C_{14}H_30$	Moderately soluble	No	Yes	2.04	0.55
Pyrrolo[1,2-a]pyrazine-1,4-dione, hexahydro-	27.111	59763297	154.17	$C_7H_{10}N_2O_2$	Soluble	No	Yes; 0 violation	1.77	0.55
2,2-Dimethoxy-5,5-di-n-propyl-1,3,4-.deta.(3)-oxadiazoline	8.063	3676252	216.28	$C_{10}H_{20}N_2O_3$	Soluble	No	Yes; 0 violation	2.90	0.55
5-Hexen-2-amine, N-methyl-, (.+-.)-	7.079	1812668	113.20	$C_7H_{15}N$	Very soluble	Yes	Yes; 0 violation	1.02	0.55

Table 4.5 (Continued)

Constituent of sample 1	Retention time	Area	MW g/mol	MF	Water solubility	BBB permeation	Drug-likeness (Lipinski's)	Synthetic accessibility	Bioavailability
Dodecane	14.948	8010158	170.33	$C_{12}H_{26}$	Moderately soluble	No	Yes; 1 violation: MLOGP>4.15	1.83	0.55
2H-Pyrrol-2-one, 1,5-dihydro-4-methoxy-	18.562	23993745	113.11	$C_5H_7NO_2$	Very soluble	No	Yes	2.26	0.56
Undecane	12.249	7136161	156.31	$C_{11}H_{24}$	Soluble	No	Yes; 1 violation: MLOGP>4.15	1.72	0.55
3-Acetyl-1,3-dimethyltriazene	7.351	6116261	115.13	$C_4H_9N_3O$	Very soluble	No	Yes; 0 violation	2.47	0.55
Benzeneethanamine	12.538	72771092	121.18	$C_8H_{11}N$	Very soluble	Yes	Yes; 0 violation	1.00	0.55
Decane	9.229	12253665	142.28	$C_{10}H_{22}$	Soluble	yes	Yes; 1 violation: MLOGP>4.15	1.62	0.55
Pyridine, 2,3,4,5-tetrahydro-	4.487	13208702	83.13	C_5H_9N	Very soluble	No	Yes; 0 violation	2.50	0.55
Sesquiterpene Lactone	20.965	84777	236.35	$C_{15}H_{24}O_2$	Soluble	Yes	Yes; 0 violation	1.89	0.55

Table 4.5 (Continued)

Constituent of sample 9	Retention time	Area	MW g/mol	MF	Water solubility	BBB permeation	Drug-likeness (Lipinski's)	Synthetic accessibility	Bioavailability
Pyridine, 2,3,4,5-tetrahydro-	4.672	12567496	83.13	C_5H_9N	Very soluble	No	Yes; 0 violation	2.50	0.55
2-Pyrrolidinone	11.993	23239473	85.10	C_4H_7NO	Highly soluble	No	Yes; 0 violation	1.00	0.55
Heptane, 3,4-dimethyl-	9.230	24366239	128.26	C_9H_{20}	soluble	yes	Yes; 1 violation: MLOGP>4.15	2.24	0.55
Undecane	12.253	12564597	156.31	$C_{11}H_{24}$	soluble	No	Yes; 1 violation: MLOGP>4.15	1.72	0.55
Butanedioic acid, dimethyl ester	10.451	1311164	146.14	$C_6H_{10}O_4$	Very soluble	No	Yes; 0 violation	1.65	0.55
Pyrrolo[1,2-a]pyrazine-1,4-dione, hexahydro-	27.053	54239803	154.17	$C_7H_{10}N_2O_2$	Very soluble	No	Yes; 0 violation	1.77	0.55
Tetradecane	19.654	25937460	198.39	$C_{14}H_{30}$	Moderately soluble	No	Yes; 1 violation: MLOGP>4.15	2.04	0.55
2-Butanone, 1,1-dichloro-3,3-dimethyl-	9.230	14379473	169.05	$C_6H_{10}Cl_2O$	soluble	yes	Yes; 0 violation	1.73	0.55
Hexadecane	23.751	31709817	226.44	$C_{16}H_{34}$	Moderately soluble	No	Yes; 1 violation: MLOGP>4.15	2.26	0.55

Table 4.5 (Continued)

Constituent of sample 9	Retention time	Area	MW g/mol	MF	Water solubility	BBB permeation	Drug-likeness (Lipinski's)	Synthetic accessibility	Bioavailability
Pyrrolo[1,2-a]pyrazine-1,4-dione, hexahydro-3-(phenylmethyl)-	37.958	29606934	244.29	$C_{14}H_{16}N_2O_2$	soluble	No	Yes; 0 violation	2.46	0.55
Octadecane	27.419	23153653	254.49	$C_{18}H_{38}$	Poorly soluble	No	Yes; 1 violation: MLOGP>4.15	2.49	0.55
(S)-(-)-2-Acetylaminopropan-1-ol	22.306	12848727	117.15	$C_5H_{11}NO_2$	Highly soluble	No	Yes; 0 violation	1.19	0.55
2,4(1H,3H)-Pyrimidinedione	24.851	17200797	112.09	$C_4H_4N_2O_2$	Very soluble	No	Yes; 0 violation	1.35	0.55
2-[1'-(Diisopropylaminoethyl)cyclopentyl]cyclopentanone	26.702	3025630	279.46	$C_{18}H_{33}NO$	Moderately soluble	Yes	Yes; 0 violation	3.02	0.55
5H,10H-Dipyrrolo[1,2-a:1',2'-d]pyrazine-5,10-dione, octahydro-, (5aS,10aS)-	29.980	100936317	194.23	$C_{10}H_{14}N_2O_2$	soluble	Yes	Yes; 0 violation	1.99	0.55
Cyclopropanemethanamine, .alpha.-(1,1-dimethylethyl)-N,N-diethyl-	25.144	1036504	183.33	$C_{12}H_{25}N$	soluble	Yes	Yes; 0 violation	2.02	0.55
4-Hexen-1-ol, 4-methyl-	27.425	3226367	114.19	$C_7H_{14}O$	Very soluble	Yes	Yes; 0 violation	1.93	0.55
Pyrrolo[1,2-a]pyrazine-1,4-dione, hexahydro-3-(phenylmethyl)-	37.958	29606934	244.29	$C_{14}H_{16}N_2O_2$	soluble	No	Yes; 0 violation	2.46	0.55
anti-O,O'-dibenzene	29.873	1802333	156.22	$C_{12}H_{12}$	Moderately soluble	Yes	Yes; 1 violation: MLOGP>4.15	1.00	0.55

Table 4.5 (Continued)

Constituent of sample 3	Retention time	Area	MW g/mol	MF	Water solubility	BBB permeation	Drug-likeness (Lipinski's)	Synthetic accessibility	Bioavailability
N-ETHYLPYRROLIDINE	4.326	6467814	99.17	$C_6H_{13}N$	Very soluble	No	Yes; 0 violation	1.00	0.55
2-Pyrrolidinone	11.933	13403793	85.10	C_4H_7NO	Very soluble	No	Yes; 0 violation	2.51	0.55
Benzeneethanamine	12.806	82788841	121.18	$C_8H_{11}N$	Very soluble	Yes	Yes; 0 violation	1.00	0.55
Ornithine	18.156	42794565	132.16	$C_5H_{12}N_2O_2$	Very soluble	No	Yes; 0 violation	1.78	0.55
1,2,4-Trioxolane, 3-(4-chlorophenyl)-5-(4-methoxyphenyl)-, cis-	20.188	182601739	292.71	$C_{15}H_{13}ClO_4$	Moderately soluble	Yes	Yes; 0 violation	2.33	0.55
5-(4-Fluorophenyl)tetrazole	20.181	232115610	164.14	$C_7H_5FN_4$	soluble	Yes	Yes; 0 violation	1.76	0.56
2-Piperidinone	15.032	344080639	99.13	C_5H_9NO	Very soluble	No	Yes; 0 violation	1.10	0.55
4a,8b-trans-9-methylperhydro-4,5,8a,9a-tetraazafluorene	26.021	47147574	196.29	$C_{10}H_{20}N_4$	Very soluble	No	Yes; 0 violation	2.76	0.55
Pyrrolo[1,2-a]pyrazine-1,4-dione, hexahydro-	27.142	24726626	154.17	$C_7H_{10}N_2O_2$	Very soluble	No	Yes; 0 violation	1.77	0.55

Table 4.5 (Continued)

Constituent of sample 3	Retention time	Area	MW g/mol	MF	Water solubility	BBB permeation	Drug-likeness (Lipinski's)	Synthetic accessibility	Bioavailability
Pyrrolo[1,2-a]pyrazine-1,4-dione, hexahydro-	27.142	24726626	154.17	$C_7H_{10}N_2O_2$	Very soluble	No	Yes; 0 violation	1.77	0.55
Eicosane	34.210	9266646	282.55	$C_{20}H_{42}$	Poorly soluble	No	Yes; 1 violation: MLOGP>4.15	2.72	0.55
Octadecane	27.421	29809138	254.49	$C_{18}H_{38}$	Poorly soluble	No	Yes; 1 violation: MLOGP>4.15	2.49	0.55
Hexadecane	23.753	27948387	226.44	$C_{16}H_{34}$	Moderately soluble	No	Yes; 1 violation: MLOGP>4.15	2.26	0.55
1-Nonadecene	34.095	1960233	266.51	$C_{19}H_{38}$	Poorly soluble	No	Yes; 1 violation: MLOGP>4.15	2.93	0.55
Pentadecane	16.931	878488	212.41	$C_{15}H_{32}$	Moderately soluble	No	Yes; 1 violation: MLOGP>4.15	2.15	0.55
Octadecane	17.131	303841	254.49	$C_{18}H_{38}$	Poorly soluble	No	Yes; 1 violation: MLOGP>4.15	2.49	0.55
3H-furazano[3,4-d]pyrimidine-5,7-quinone	25.385	2345330	154.08	$C_4H_2N_4O_3$	Very soluble	No	Yes; 0 violation	3.44	0.55

Table 4.5 (continued)

Constituent of sample 17	Retention time	Area	MW g/mol	MF	Water solubility	BBB permeation	Drug-likeness (Lipinski's)	Synthetic accessibility	Bioavailability
Osmium, [methyl 2-(1,1-dimethylethyl)-4,5-dihydroxy-3-oxazolidinecarboxylato(2-)-O4,O5]dioxobis(pyridine)-, [OC-6-44-[2R-(2.alpha.,4.beta.,5.beta.)]]-	3.302	505718		$C_{19}H_{25}N_3O_7Os$	Not found	Not found	Not found	Not found	Not found
2,3-Butanediol, [R-(R*,R*)]-	3.984	43737272	90.12	$C_4H_{10}O_2$	Highly soluble	No	Yes; 0 violation	1.48	0.55
(1S,2R,4S)-N-[2'-(N',N'-Dimethylamino)ethyl]-2-hydroxy-7,7-dimethylbicyclo[2.2.1]hept-1-ylmethanesulfonamide	3.582	931465	304.45	$C_{14}H_{28}N_2O_3S$	soluble	Yes	Yes; 0 violation	3.69	0.55
Benzeneethanamine	12.495	47450016	121.18	$C_8H_{11}N$	Very soluble	Yes	Yes; 0 violation	1.00	0.55
Decane	9.236	10355884	142.28	$C_{10}H_{22}$	Soluble	Yes	Yes; 1 violation: MLOGP>4.15	1.62	0.55
2H-Pyrrol-2-one, 1,5-dihydro-4-methoxy-	18.582	14623773	113.11	$C_5H_7NO_2$	Very soluble	No	Yes	2.26	0.56
Tetradecane	19.659	36638241	198.39	$C_{14}H_{30}$	Moderately soluble	No	Yes; 1 violation: MLOGP>4.15	2.04	0.55
Octadecane	27.426	61655978	254.49	$C_{18}H_{38}$	Poorly soluble	No	Yes; 1 violation: MLOGP>4.15	2.49	0.55
1-(Ethoxycarbonyl)-2-(1'-deuteriooctylidene)cyclopropyl Methyl Ketone	12.210	18723010		$C_{16}H_{25}DO_3$	Not found	Not found	Not found	Not found	Not found

Table 4.5 (continued)

Constituent of sample 17	Retention time	Area	MW g/mol	MF	Water solubility	BBB permeation	Drug-likeness (Lipinski's)	Synthetic accessibility	Bioavailability
3-Isobutylhexahydropyrrolo[1,2-A]pyrazine-1,4-dione	29.906	35826317	210.27	$C_{11}H_{18}N_2O_2$	Very soluble	No	Yes; 0 violation	2.44	0.55
Hexadecane	23.757	62750709	226.44	$C_{16}H_{34}$	Moderately soluble	No	Yes; 1 violation: MLOGP>4.15	2.26	0.55
Pyrrolo[1,2-a]pyrazine-1,4-dione, hexahydro-3-(phenylmethyl)-	39.315	40832556	244.29	$C_{14}H_{16}N_2O_2$	Soluble	No	Yes; 0 violation	2.46	0.55
Eicosane	30.752	37785278	282.55	$C_{20}H_{42}$	Poorly soluble	No	Yes; 1 violation: MLOGP>4.15	2.72	0.55
2-(1H-Imidazol-2-yl)acetic acid	22.845	3644570	126.11	$C_5H_6N_2O_2$	Very soluble	No	Yes; 0 violation	1.53	0.56
(1S,2R,4S)-N-[2'-(Morpholin-4-yl)ethyl]-2-hydroxy-7,7-dimethylbicyclo[2.2.1]hept-1-ylmethanesulfonamide	22.967	13281098	346.49	$C_{16}H_{30}N_2O_4S$	soluble	No	Yes; 0 violation	3.03	0.55
Docosane	34.218	18298132	310.60	$C_{22}H_{46}$	Poorly soluble	No	Yes; 1 violation: MLOGP>4.15	2.96	0.55
3-Octadecene, (E)-	30.655	7397657	252.48	$C_{18}H_{36}$	Poorly soluble	No	Yes; 1 violation: MLOGP>4.15	3.49	0.55
1H-Pyrrolo[1,2-a]indole, 2,3-dihydro-	23.642	8090400	157.21	$C_{11}H_{11}N$	soluble	Yes	Yes; 0 violation	1.66	0.55

Table 4.5 (Continued)

Constituent of sample 17	Retention time	Area	MW g/mol	MF	Water solubility	BBB permeation	Drug-likeness (Lipinski's)	Synthetic accessibility	Bioavailability
3-Amino-2,2,4-trimethylhexane	25.097	106840849	143	$C_9H_{21}N$	Soluble	Yes	Yes; 0 violation	1.32	0.55
3-exo-methyl- and 3-endo-methyl-cis-3,3a,4,5,6,6a-hexahydro-4,5,6-methenocyclopentapyrazoles	30.599	2757645	134.18	$C_8H_{10}N_2$	Soluble	No	Yes; 0 violation	1.60	0.55
1-Benzylidene-2,4-cyclopentadiene	35.782	1039781	154.21	$C_{12}H_{10}$	Very soluble	Yes	Yes; 1 violation: MLOGP>4.15	1.00	0.55
Acetic acid, butyl ester	4.123	4269600	116.16	$C_6H_{12}O_2$	Very soluble	Yes	Yes	1.10	0.55
Butanedioic acid, dimethyl ester	10.444	1311164	146.14	$C_6H_{10}O_4$	Very soluble	No	Yes	1.65	0.55
alpha.-(Methoxycarbonyl)-1,3-dioxolan-2-ylideneacetic acid	21.878	13275059	188.13	$C_7H_8O_6$	Very soluble	No	Yes	2.91	0.55

Molecular weight-MW; Molecular formula-MF; Drug-likeness according to Lipinski's rule of five, synthetic accessibility- (1 very easy, 10 very difficult), Bioavailability-(0-1), Blood brain barrier-BBB; MLOGP-partition coefficient

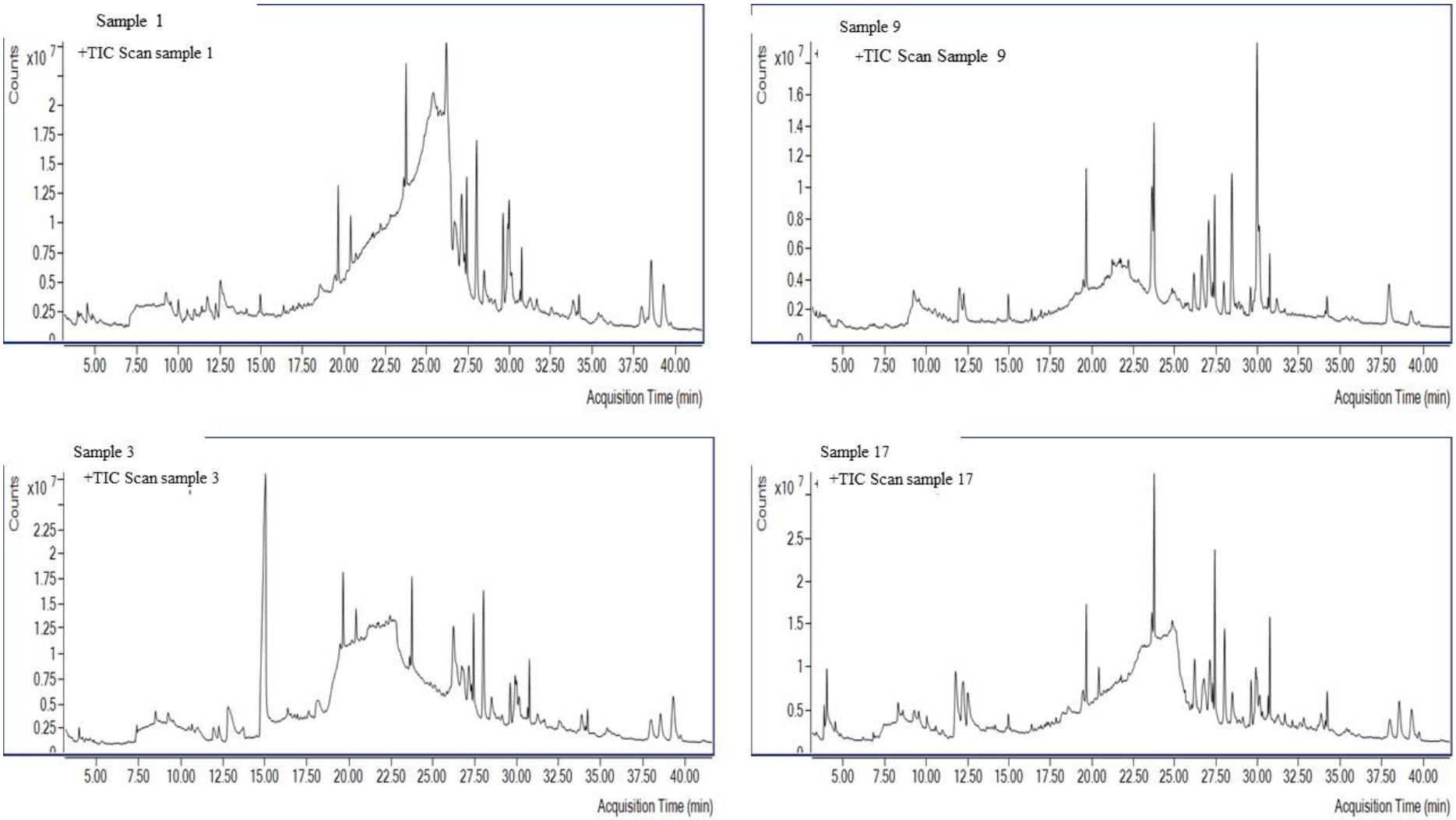

Figure 4.6 : The representative GC-MS spectrum of endophytic acetone extract of sample 1, 3, 9 and 17.

4.4 Prediction of bioactivity spectrum of selected endophytic compounds

Table 4.6: Predicted bioactivity spectrum of 3-Amino-2,2,4-trimethylhexane. Pa>90

Pa	Pi	Bioactivity spectrum
0,953	0,001	Exoribonuclease II inhibitor
0,949	0,004	CDP-glycerol glycerophosphotransferase inhibitor
0,939	0,003	Phobic disorders treatment
0,934	0,002	Polyamine-transporting ATPase inhibitor
0,933	0,003	Acylcarnitine hydrolase inhibitor
0,924	0,002	Venombin AB inhibitor
0,911	0,004	G-protein-coupled receptor kinase inhibitor
0,911	0,004	Beta-adrenergic receptor kinase inhibitor
0,911	0,004	5 Hydroxytryptamine release stimulant
0,910	0,004	Glucose oxidase inhibitor
0,908	0,006	Mucositis treatment
0,905	0,004	Superoxide dismutase inhibitor
0,903	0,004	Pro-opiomelanocortin converting enzyme inhibitor

Table 4.7: Bioactivity spectrum of octadecane. Pa>90.

Pa	Pi	Bioactivity spectrum
0,954	0,002	Sugar-phosphatase inhibitor
0,950	0,002	Saccharopepsin inhibitor
0,950	0,002	Chymosin inhibitor
0,950	0,002	Acrocylindropepsin inhibitor
0,942	0,002	Acylcarnitine hydrolase inhibitor
0,941	0,002	Alkylacetylglycerophosphatase inhibitor
0,940	0,002	Carboxypeptidase Taq inhibitor
0,935	0,002	Cutinase inhibitor
0,936	0,003	Polyporopepsin inhibitor
0,935	0,003	Alkenylglycerophosphocholine hydrolase inhibitor
0,934	0,002	Acetylesterase inhibitor
0,934	0,003	Ubiquinol-cytochrome-c reductase inhibitor
0,931	0,001	Glucan 1,4-alpha-maltotriohydrolase inhibitor
0,930	0,002	Pullulanase inhibitor
0,927	0,002	Gluconate 5-dehydrogenase inhibitor
0,924	0,004	Phobic disorders treatment
0,918	0,004	5 Hydroxytryptamine release stimulant
0,913	0,002	Exoribonuclease II inhibitor
0,910	0,002	Xylan endo-1,3-beta-xylosidase inhibitor

Table 4.8: Bioactivity spectrum of 2-(1H-Imidazol-2-yl)acetic acid. Pa>70

Pa	Pi	Bioactivity spectrum
0,925	0,003	Mannotetraose 2-alpha-N-acetylglucosaminyltransferase inhibitor
0,861	0,003	Pterin deaminase inhibitor
0,826	0,006	Fucosterol-epoxide lyase inhibitor
0,831	0,013	Antieczematic
0,806	0,007	Carboxypeptidase Taq inhibitor
0,790	0,007	Pseudolysin inhibitor
0,797	0,022	CYP2J substrate
0,788	0,013	Nicotinic alpha6beta3beta4alpha5 receptor antagonist
0,769	0,006	Glutamine-phenylpyruvate transaminase inhibitor
0,759	0,005	Thioredoxin inhibitor
0,758	0,004	Insulin promoter
0,776	0,026	Chymosin inhibitor
0,776	0,026	Acrocylindropepsin inhibitor
0,776	0,026	Saccharopepsin inhibitor
0,766	0,019	Pro-opiomelanocortin converting enzyme inhibitor
0,739	0,010	Creatininase inhibitor
0,705	0,015	Pullulanase inhibitor
0,743	0,057	Phobic disorders treatment

Table 4. 9 Bioactivity spectrum of 2-Piperidinone. Pa> 70

Pa	Pi	Bioactivity spectrum
0,890	0,003	Glucan endo-1,6-beta-glucosidase inhibitor
0,857	0,005	Pullulanase inhibitor
0,845	0,005	Nicotinic alpha6beta3beta4alpha5 receptor antagonist
0,842	0,005	Nicotinic alpha2beta2 receptor antagonist
0,828	0,003	Glucan 1,4-alpha-maltotriohydrolase inhibitor
0,820	0,003	(S)-6-hydroxynicotine oxidase inhibitor
0,820	0,005	Ribulose-phosphate 3-epimerase inhibitor
0,819	0,005	Creatininase inhibitor
0,836	0,024	Aspulvinone dimethylallyltransferase inhibitor
0,822	0,026	Phobic disorders treatment
0,817	0,032	Membrane integrity agonist
0,794	0,017	Sugar-phosphatase inhibitor
0,778	0,003	Glucan 1,4-alpha-maltotetraohydrolase inhibitor
0,781	0,011	Alkylacetylglycerophosphatase inhibitor
0,775	0,005	L-glutamate oxidase inhibitor
0,758	0,005	Xylan endo-1,3-beta-xylosidase inhibitor
0,749	0,005	Cardiovascular analeptic
0,755	0,012	Carboxypeptidase Taq inhibitor

Table 4. 10: Bioactivity spectrum of 5H,10H-Dipyrrolo[1,2-a:1',2'-d]pyrazine-5,10-dione, octahydro-, (5aS,10aS)-.Pa>70.

Pa	Pi	Bioactivity spectrum
0,892	0,004	Nicotinic alpha2beta2 receptor antagonist
0,818	0,027	Phobic disorders treatment
0,796	0,008	Ribulose-phosphate 3-epimerase inhibitor
0,788	0,021	Antieczematic
0,769	0,004	(R)-6-hydroxynicotine oxidase inhibitor
0,770	0,011	Glucan endo-1,6-beta-glucosidase inhibitor
0,762	0,005	Antihypoxic
0,756	0,010	UDP-N-acetylglucosamine 4-epimerase inhibitor
0,743	0,004	Glucan 1,4-alpha-maltotetraohydrolase inhibitor
0,760	0,025	Nootropic
0,752	0,020	Membrane permeability inhibitor
0,733	0,003	Na+-transporting two-sector ATPase inhibitor
0,732	0,003	Polarisation stimulant
0,731	0,008	Methylamine-glutamate N-methyltransferase inhibitor
0,729	0,007	Glucan 1,4-alpha-maltotriohydrolase inhibitor
0,742	0,029	Antineurotic
0,713	0,006	Cardiovascular analeptic
0,714	0,010	Gluconate 5-dehydrogenase inhibitor

Generally, the endophytic compounds were predicted to possess medicinal properties which include anti-microbial, anti-fungal, anti-viral, anti-diabetic, anti-tumour, anti-cancer, treatment of anxiety, anti-protozoal, anti-asthmatic, anti-eczematic, antiseborrheic, anaesthetic general and antiallergic (Table 4.6, Table 4.7, Table 4.8, Table 4.9, Table 4.10). Precisely, 5H,10H-Dipyrrolo[1,2-a:1',2'-d]pyrazine-5,10-dione, octahydro-, (5aS,10aS)- was predicted to have higher chances of bioactivity spectrum as a membrane permeability inhibitor, Na+-transporting two-sector ATPase inhibitor, UDP-N-acetylglucosamine 4-epimerase inhibitor, glucan 1,4-

alpha-maltotetraohydrolase inhibitor and Glucan endo-1,6-beta-glucosidase inhibitor (Table 4.10). Inhibition of these enzymes is fatal to microorganisms. Also, 2-Piperidinone was predicted to have higher chances of inhibiting pullulanase, glucan endo-1,6-beta-glucosidase, glucan 1,4-alpha-maltotetraohydrolase and sugar-phosphatase (Table 4.9). 3-Amino-2,2,4-trimethylhexane had highest probability of inhibiting exoribonuclease II (Table 4.6) whilst 2-(1H-Imidazol-2-yl)acetic acid has the highest probability of inhibiting mannotetraose 2-alpha-N-acetylglucosaminyltransferase (Table 4.8). Octadecane was predicted to have high chances of inhibiting sugar-phosphatase, saccharopepsin and acrocylindropepsin.

4.5 Molecular Docking

To evaluate the binding affinities of the selected endophytic compounds and to establish if the selected compounds are highly specific and inhibit the selected macromolecular targets, molecular docking study was performed. The bacterial target proteins, namely lumazine synthase, Tryptophan synthase and UDP-N-acetylglucosamine 1-carboxyvinyltransfrase were docked with 3-Amino-2,2,4-trimethylhexane, Octadecane, 2-(1H-Imidazol-2-yl)acetic acid, 2-Piperidinone and 5H,10H-Dipyrrolo[1,2-a:1',2'-d]pyrazine-5,10-dione, octahydro-, (5aS,10aS)- (Figure 4.7, Figure 4.8, Figure 4.9, Figure 4.10, Figure 4.11). Ampicillin, a commercial antibiotic drug was used as the reference drug in the docking study. The binding affinities are shown in (Table 4.11, Table 4.12, Table 4.13) The endophytic compounds exhibited binding affinity which ranged from -3.7 to -6.4 kcal/mol. Endophytic compound 5H,10H-Dipyrrolo[1,2-a:1',2'-d]pyrazine-5,10-dione, octahydro-, (5aS,10aS)- showed relatively stronger binding affinities on all protein targets than other compounds. The strongest binding affinity -6.4 kcal/mol observed on the interaction of 5H,10H-Dipyrrolo[1,2-a:1',2'-d]pyrazine-5,10-dione, octahydro-, (5aS,10aS)- with Thr:50, His:102, Cys:48 and Ile:162 residues of lumazine synthase (Table 4.11). Followed by -6.1 kcal/mol observed on the

interaction of 5H,10H-Dipyrrolo[1,2-a:1',2'-d]pyrazine-5,10-dione, octahydro-, (5aS,10aS)- with Val:163; Gly:164; His:125; Arg:91; Pro:121 and Leu:124 residues of UDP-N-acetylglucosamine 1-carboxyvinyltransfrase (Table 4.13). Conventional hydrogen bonds, carbon hydrogen bonds, alkyl, π-anion, π-sigma, π-alkyl interactions were observed at the active site of the target protein as result of the interaction of amino acids residues and selected endophytic compounds (Figure 4.12, Figure 4.13, Figure 4.14, Figure 4.15, Figure 4.16, Figure 4.17). An unfavourable donor-donor interaction was formed between Asn:23 residue of the active site of UDP-N-acetylglucosamine 1-carboxyvinyltransfrase with 2-(1H-Imidazol-2-yl)acetic acid (Figure 4.14).

Table 4. 11: Binding affinity of target macromolecule (lumazine synthase) with endophytic compounds. Ampicillin was used as a standard commercial drug.

Protein +ligand	Binding affinity with Audock Vina (kcal/mol)	RMSD l.b	RMSD u.b	Interacting residues
Ampicillin + lumazine synthase	-7.7	0.000	0.000	Gly A:95; Thr A:3; Gln A:7; Met A:32; Arg A:86
3-Amino-2,2,4-trimethylhexane + lumazine synthase	-4.0	0.000	0.000	Arg A: 168; Ile A:145; Val A:6; Ile A:5; Thr C:50; Ser A:146
Octadecane + lumazine synthase	-3.9	0.000	0.000	Leu A:98; Leu B:98; Ala A:190; Phe C:90; Gln A:187; Pro A:186; Met A:1
2-(1H-Imidazol-2-yl)acetic acid + lumazine synthase	-4.8	0.000	0.000	Lys A:137; His A:160; Thr A:148; Gly A:150
2-Piperidinone + lumazine synthase	-4.5	0.000	0.000	Lys B:89; Asp B:92; Ile B:5; Glu B:93
5H,10H-Dipyrrolo[1,2-a:1',2'-d]pyrazine-5,10-dione, octahydro-, (5aS,10aS)- + lumazine synthase	-6.4	0.000	0.000	Thr C:50; His C:102; Cys C:48; Ile A:162

RMSD:root mean square deviation; l.b: lower bound; u.b: upper bound; Phe: Phenylalanine; Leu: Leucine; Ser: Serine; Cys: Cysteine; Trp: Tryptophan; Arg: Arginine; Ala: Alanine; Gly: Glycine; Thr: Threonine; Glu: Glutamate; Met: Methionine; Gln: Glutamine; His: Histidine; Ile: Isoleucine; Lys: Lysine; Val: Valine; Pro: Proline

Table 4.12: Binding affinity of target macromolecule (Tryptophan synthase subunit beta) with endophytic compound.

Protein +ligand	Binding affinity with Audock Vina (kcal/mol)	RMSD l.b.	RMSD u.b	Interacting residues
Ampicillin + Tryptophan synthase subunit beta	-7.6	0.000	0.000	Ala B:85; Glu B:350; Lys B:87; Gly B:303; Gly B:189; Cys B:230
3-Amino-2,2,4-trimethylhexane + Tryptophan synthase subunit beta	-4.6	0.000	0.000	Leu B:166; Phe B:306; Cys B:170; Gly B:234; Gly B:233; Thr B:190; Ser B:235
Octadecane + Tryptophan synthase subunit beta	-5.2	0.000	0.000	Leu B:166; His B:86; Ala B:85; Phe B:306
2-(1H-Imidazol-2-yl)acetic acid + Tryptophan synthase subunit beta	-4.0	0.000	0.000	Leu B:166
2-Piperidinone + Tryptophan synthase subunit beta	-3.9	0.000	0.000	Pro B:285; Phe B:12; Ala B: 314; Ser B:318
5H,10H-Dipyrrolo[1,2-a:1',2'-d]pyrazine-5,10-dione, octahydro-, (5aS,10aS)- + Tryptophan synthase subunit beta	-5.6	0.000	0.000	Pro A:78; Leu A:105; Arg A: 117; Phe A:82

RMSD:root mean square deviation; l.b: lower bound; u.b: upper bound; Phe: Phenylalanine; Leu: Leucine; Ser: Serine; Cys: Cysteine; Trp: Tryptophan; Arg: Arginine; Ala: Alanine; Gly: Glycine; Thr: Threonine; Glu: Glutamate; Met: Methionine; Gln: Glutamine; His: Histidine; Ile: Isoleucine; Lys: Lysine; Val: Valine; Pro: Proline

Table 4.13: Binding affinity of target macromolecule (UDP-N-acetylglucosamine 1-carboxyvinyltransfrase) with endophytic compound.

Protein +ligand	Binding affinity with Audock Vina (kcal/mol)	RMSD l.b.	RMSD u.b	Interacting residues
Ampicillin + UDP-N-acetylglucosamine 1-carboxyvinyltransfrase	-8.8	0.000	0.000	His A:125; Ser A:162; Arg A:91; Gly A:164; Val A:163; Asp A:305; Phe A:328
3-Amino-2,2,4-trimethylhexane + UDP-N-acetylglucosamine 1-carboxyvinyltransfrase	-3.7	0.000	0.000	Val A:163; Arg A:120; Arg A:91; Gly A:164; Trp A:95
Octadecane + UDP-N-acetylglucosamine 1-carboxyvinyltransfrase	-4.9	0.000	0.000	Arg A:91; Val A:163; Trp A:95; Phe A:328; Thr A:304; Pro A:298
2-(1H-Imidazol-2-yl)acetic acid + UDP-N-acetylglucosamine 1-carboxyvinyltransfrase	-4.8	0.000	0.000	Lys A:22; Arg A:397; Cys A:115; Arg A: 120; Asn A:23
2-Piperidinone + UDP-N-acetylglucosamine 1-carboxyvinyltransfrase	-4.0	0.000	0.000	Arg A:91; Arg A:120; Val A:163
5H,10H-Dipyrrolo[1,2-a:1',2'-d]pyrazine-5,10-dione, octahydro-, (5aS,10aS)- + UDP-N-acetylglucosamine 1-carboxyvinyltransfrase	-6.1	0.000	0.000	Leu A:124; Pro A:121; Arg A:91; His A: 125; Val A:163

RMSD:root mean square deviation; l.b: lower bound; u.b: upper bound; Phe: Phenylalanine; Leu: Leucine; Ser: Serine; Cys: Cysteine; Trp: Tryptophan; Arg: Arginine; Ala: Alanine; Gly: Glycine; Thr: Threonine; Glu: Glutamate; Met: Methionine; Gln: Glutamine; His: Histidine; Ile: Isoleucine; Lys: Lysine; Val: Valine; Pro: Proline

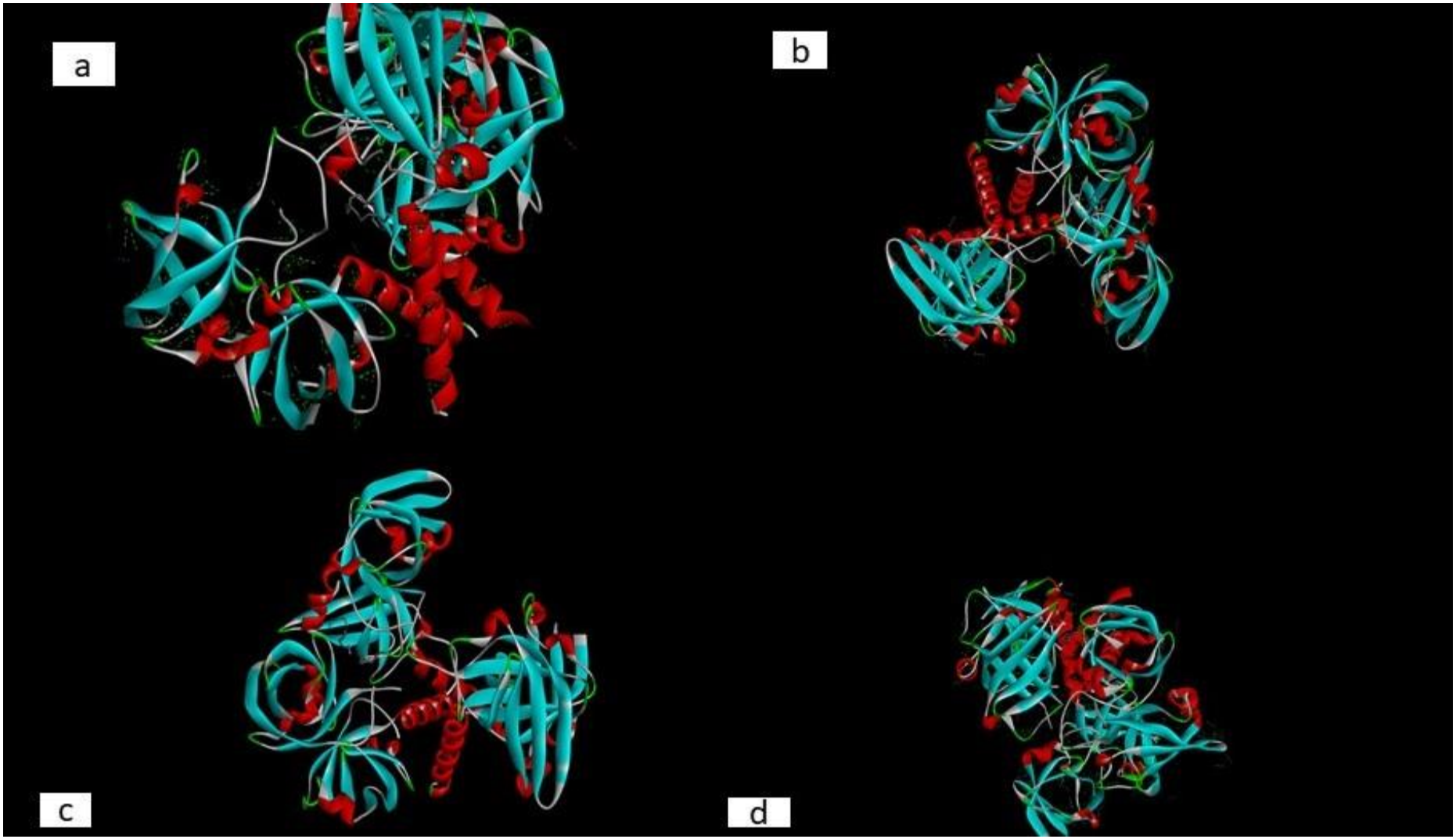

Figure 4.7: Docking poses of lumazine synthase protein with endophytic compounds. a). lumazine synthase with Octadecane b). lumazine synthase with ampicillin c). lumazine synthase with 3-Amino-2,2,4-trimethylhexane d). lumazine synthase with 2-(1H-Imidazol-2-yl)acetic acid.

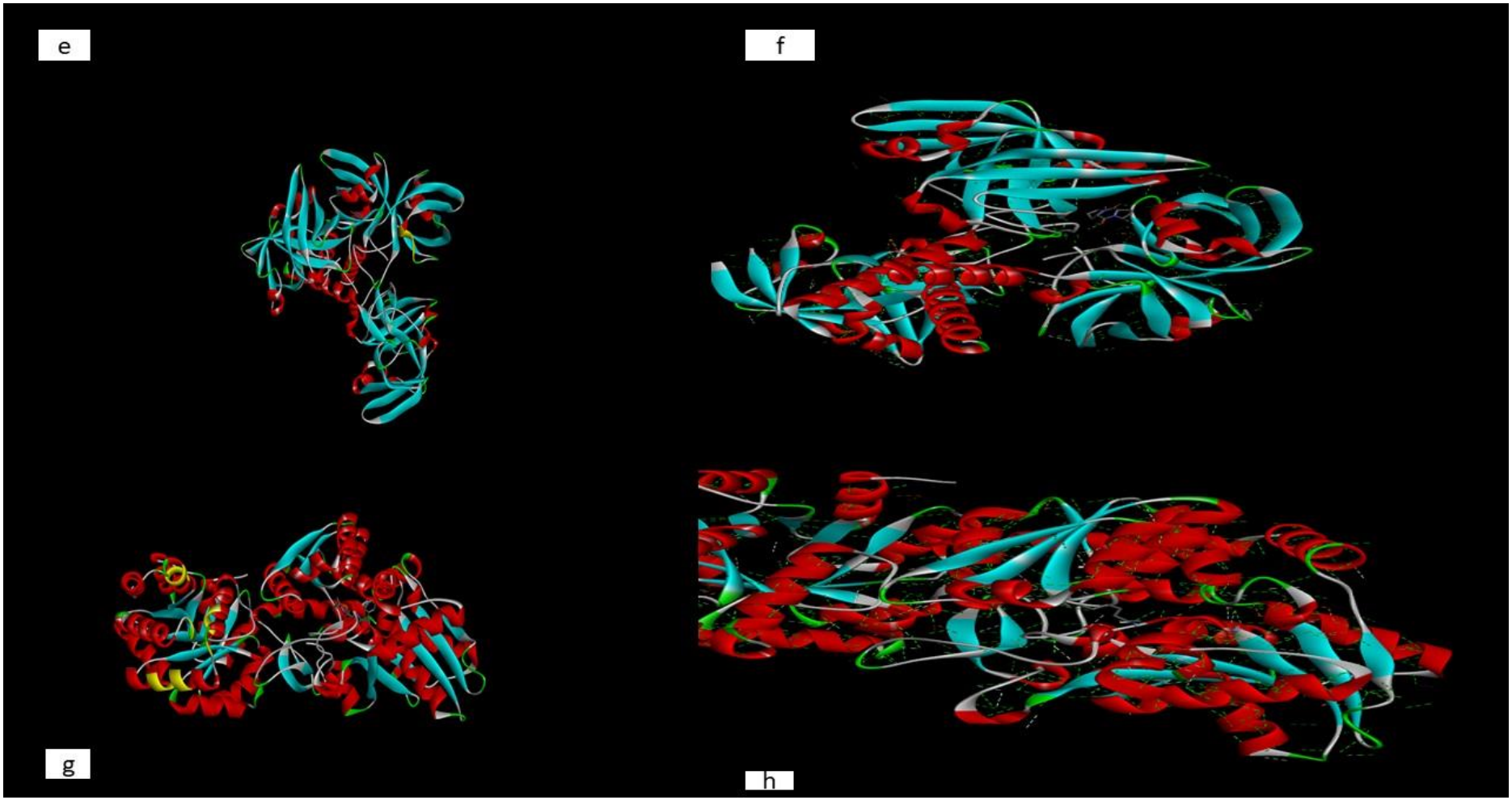

Figure 4.8: Docking poses of target proteins with endophytic compounds. e). lumazine synthase with 2-Piperidinone f). lumazine synthase with 5H,10H-Dipyrrolo[1,2-a:1',2'-d]pyrazine-5,10-dione, octahydro-, (5aS,10aS)- g). Tryptophan synthase subunit beta with ampicillin h). Tryptophan synthase subunit beta with 3-Amino-2,2,4-trimethylhexane.

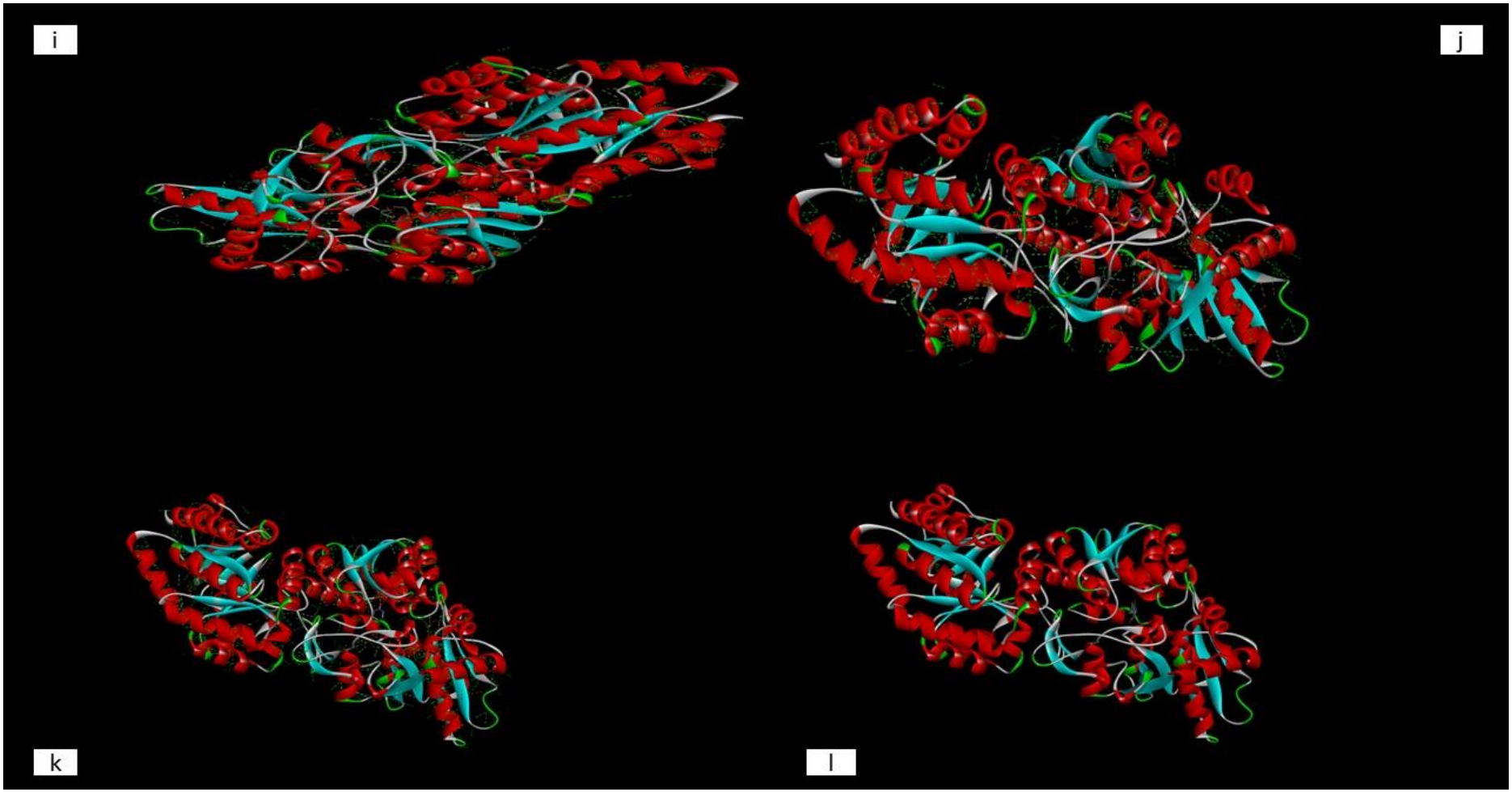

Figure 4.9: Docking poses of target protein with endophytic compounds. i). Tryptophan synthase subunit beta with Octadecane j). Tryptophan synthase subunit beta with 2-(1H-Imidazol-2-yl)acetic acid k). Tryptophan synthase subunit beta with 2-Piperidinone l). Tryptophan synthase subunit beta with 5H,10H-Dipyrrolo[1,2-a:1',2'-d]pyrazine-5,10-dione, octahydro-, (5aS,10aS)- .

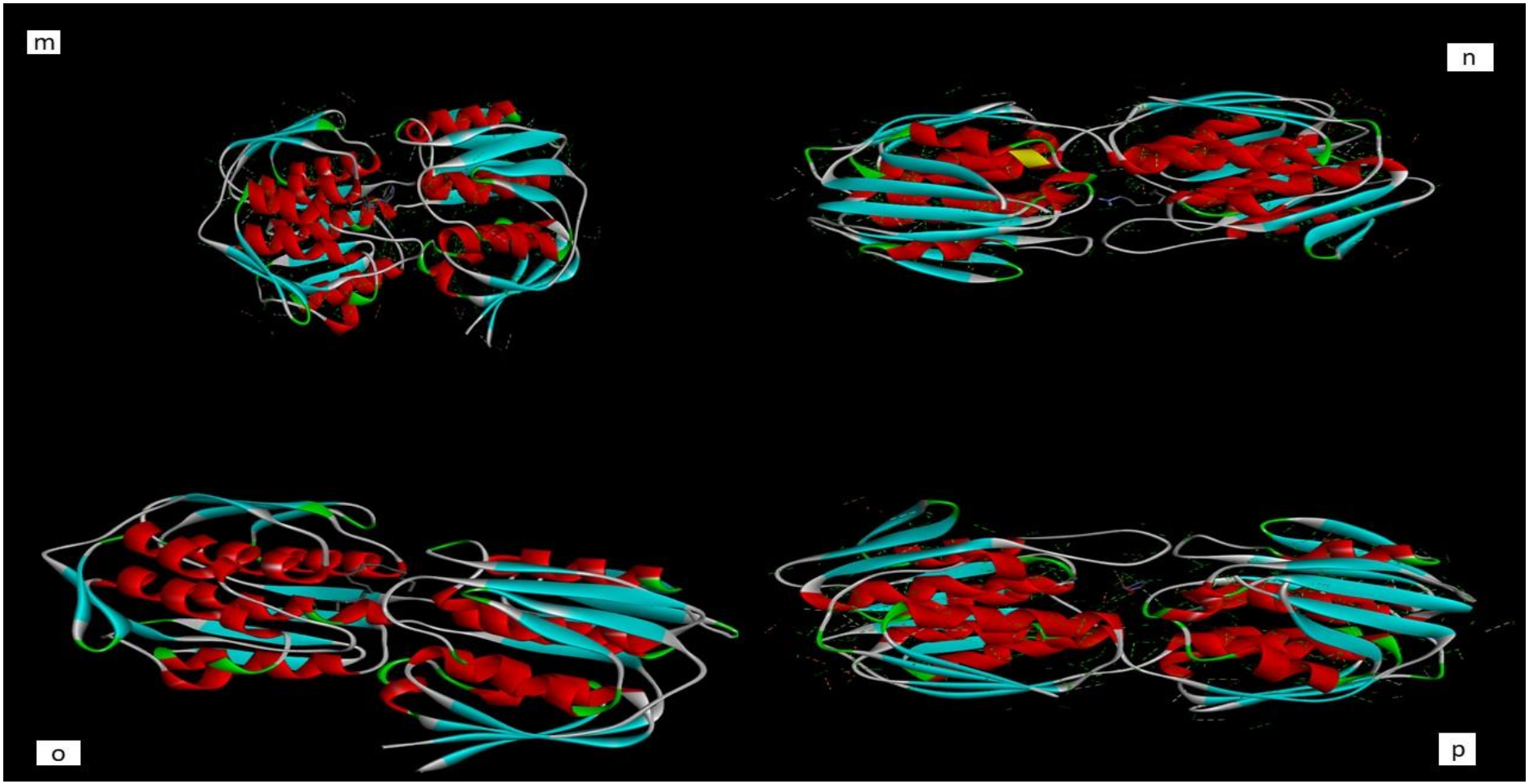

Figure 4.10: Docking poses of target protein with endophytic compounds. m). UDP-N-acetylglucosamine 1-carboxyvinyltransfrase with ampicillin n). UDP-N-acetylglucosamine 1-carboxyvinyltransfrase with 3-Amino-2,2,4-trimethylhexane o). UDP-N-acetylglucosamine 1-carboxyvinyltransfrase with Octadecane p). UDP-N-acetylglucosamine 1-carboxyvinyltransfrase with 2-(1H-Imidazol-2-yl)acetic acid.

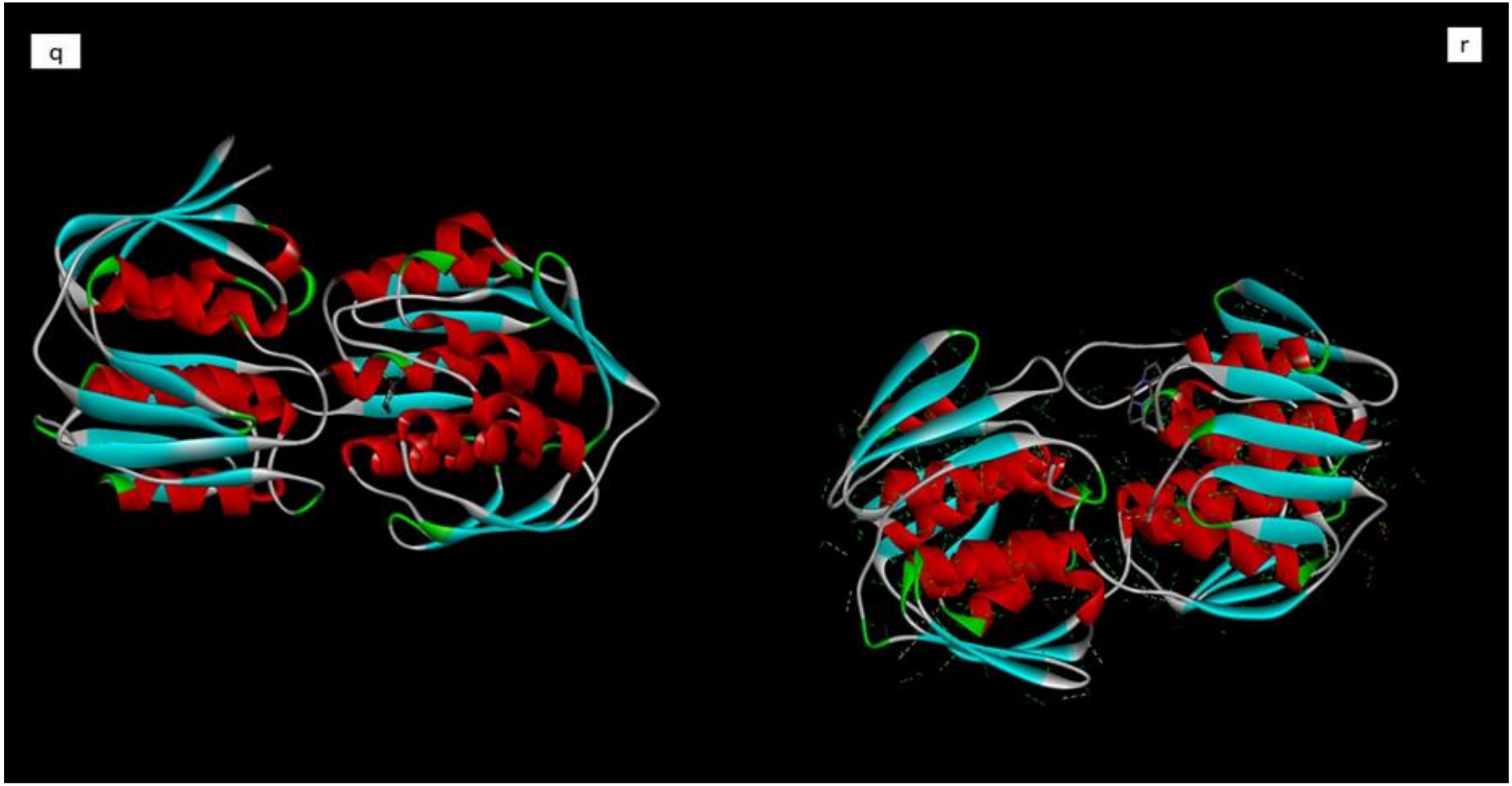

Figure 4.11: Docking poses of target protein with endophytic compounds. q). UDP-N-acetylglucosamine 1-carboxyvinyltransfrase with 2-Piperidinone r). UDP-N-acetylglucosamine 1-carboxyvinyltransfrase with 5H,10H-Dipyrrolo[1,2-a:1',2'-d]pyrazine-5,10-dione, octahydro-, (5aS,10aS)-.

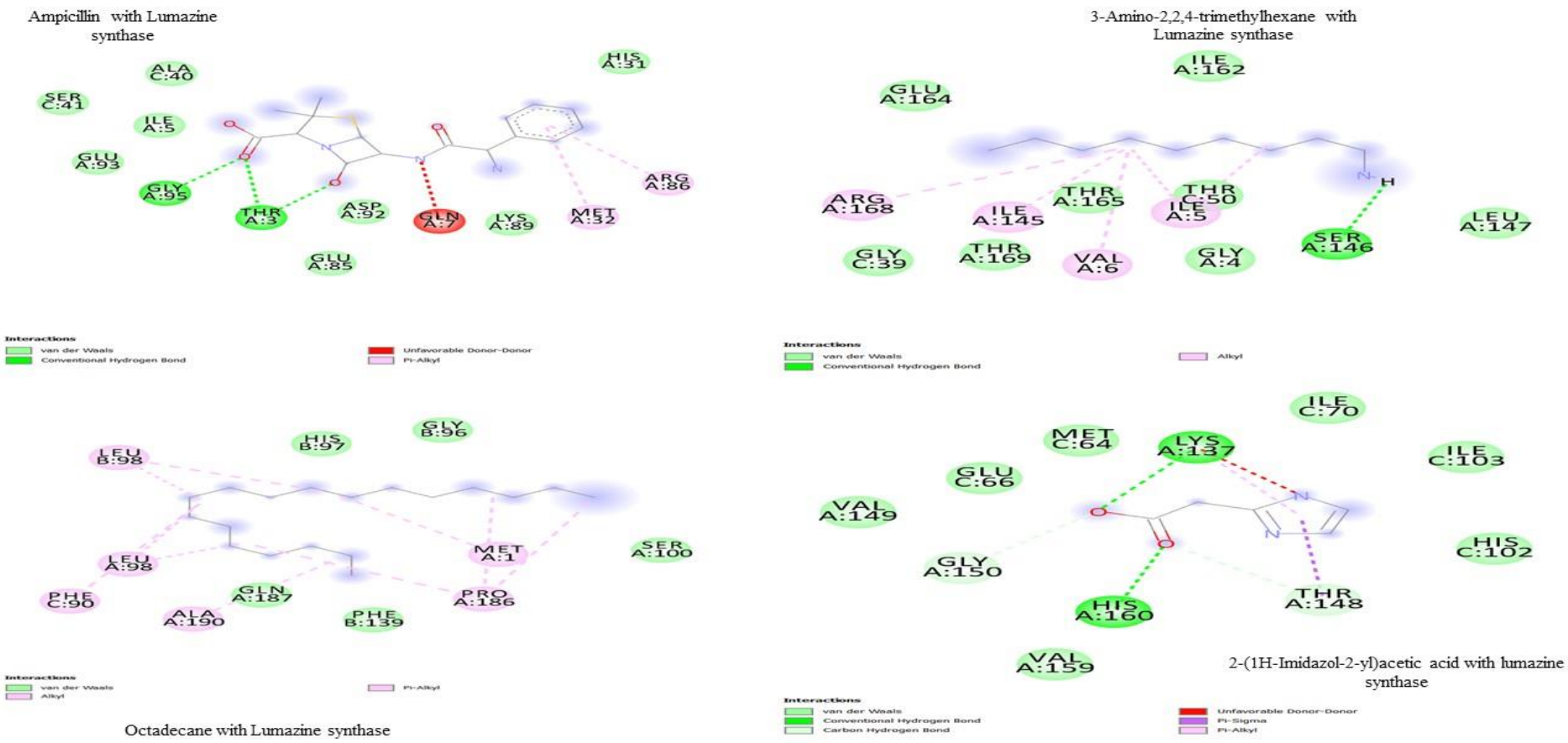

Figure 4.12: Interaction of endophytic compounds with residues of lumazine synthase. Ampicillin was the standard commercial drug used.

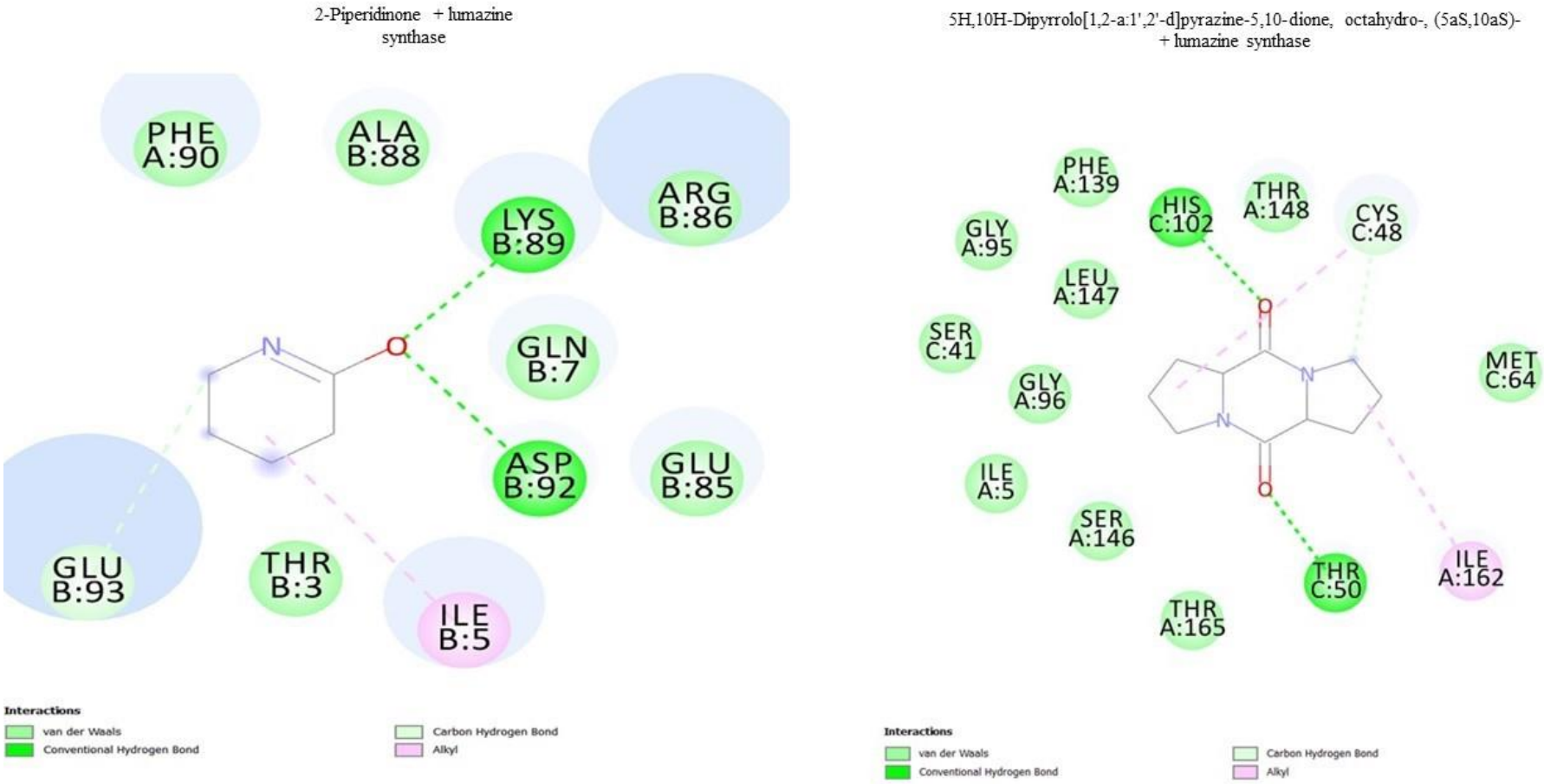

Figure 4.13: Interaction of endophytic compounds with residues of lumazine synthase.

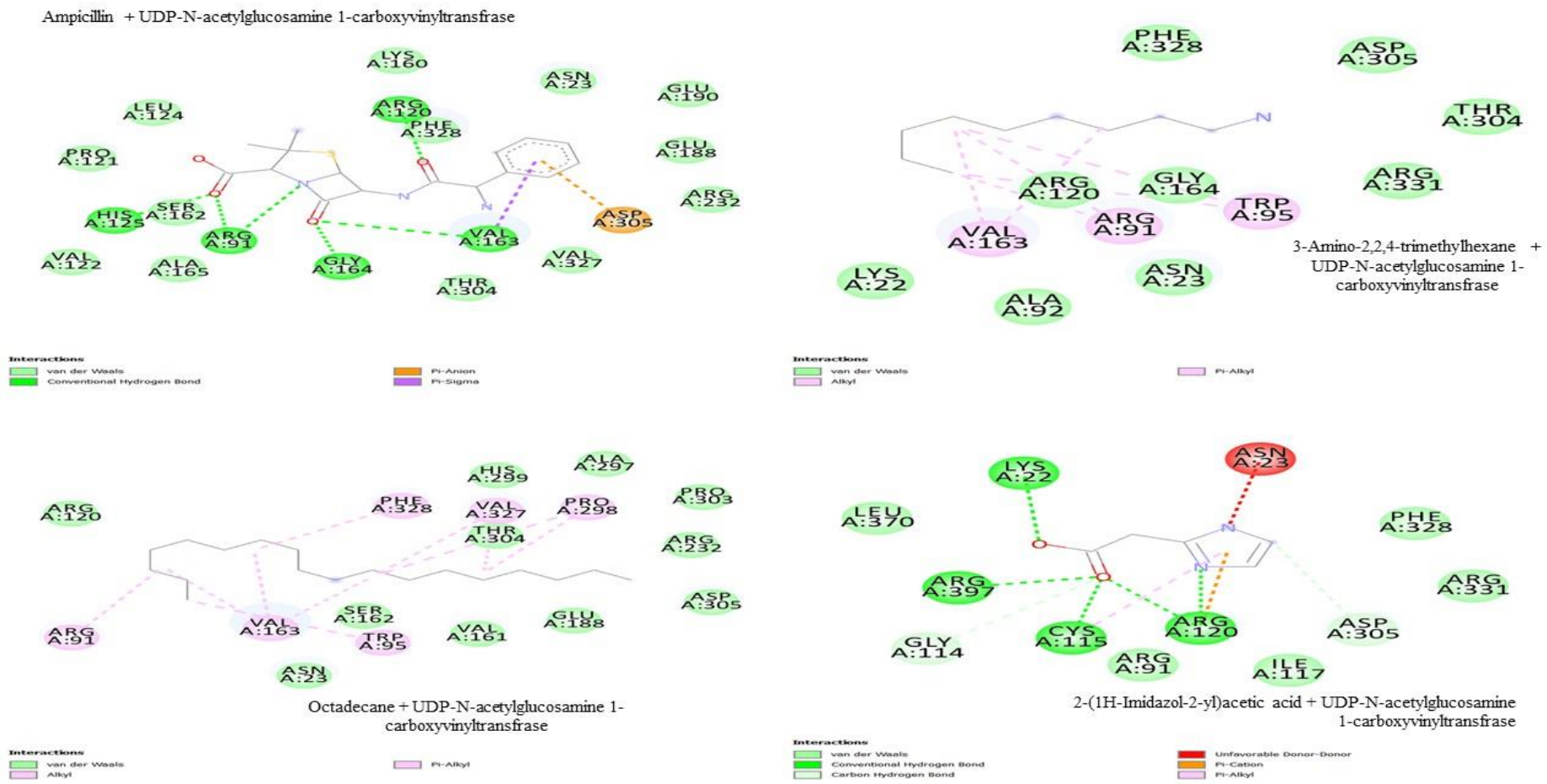

Figure 4.14: Interaction of endophytic compounds with residues of UDP-N-acetylglucosamine 1-carboxyvinyltransfrase. Ampillicin was used as standard commercial drug.

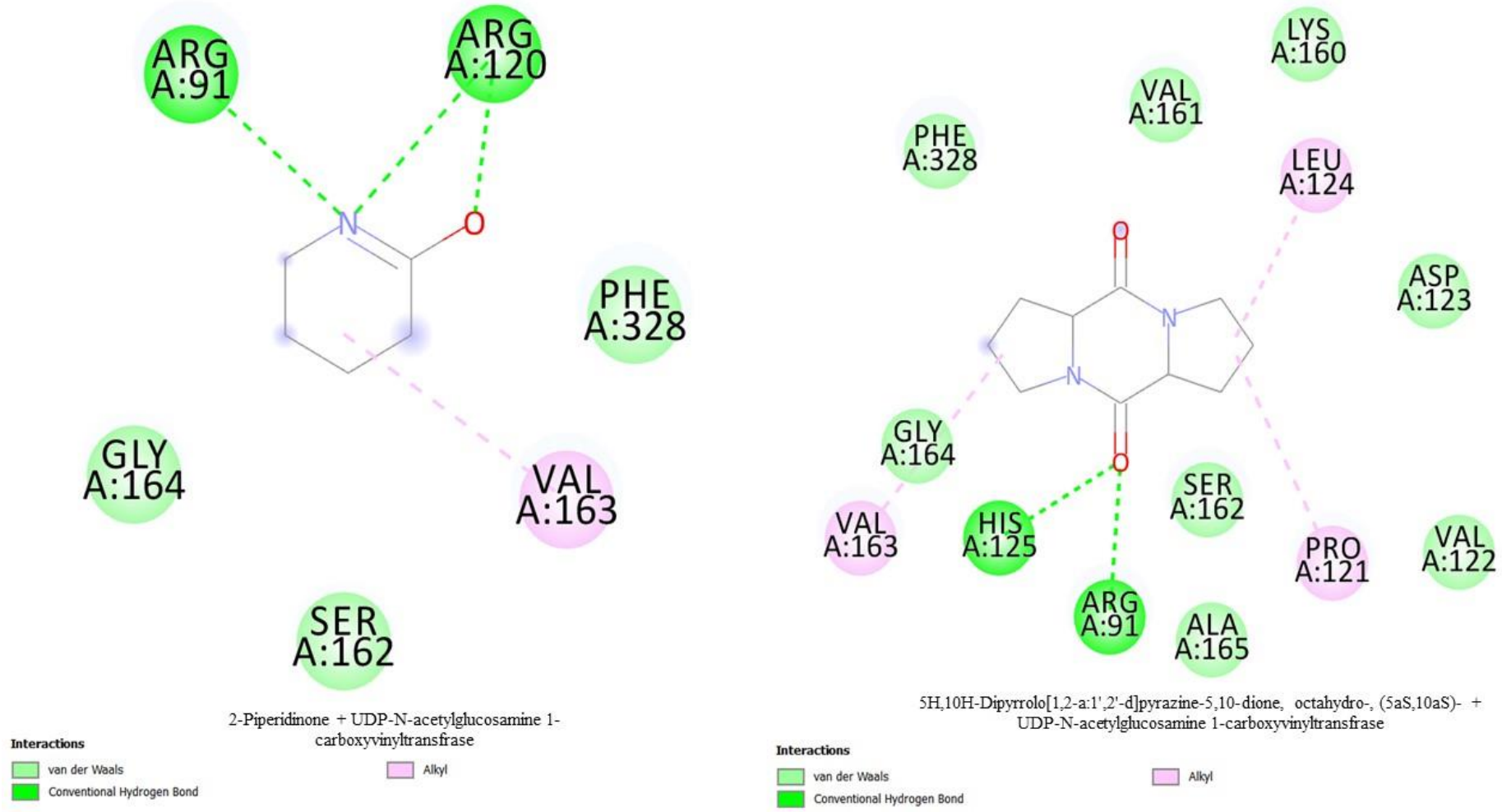

Figure 4.15: Interaction of endophytic compounds with residues of UDP-N-acetylglucosamine 1-carboxyvinyltransfrase.

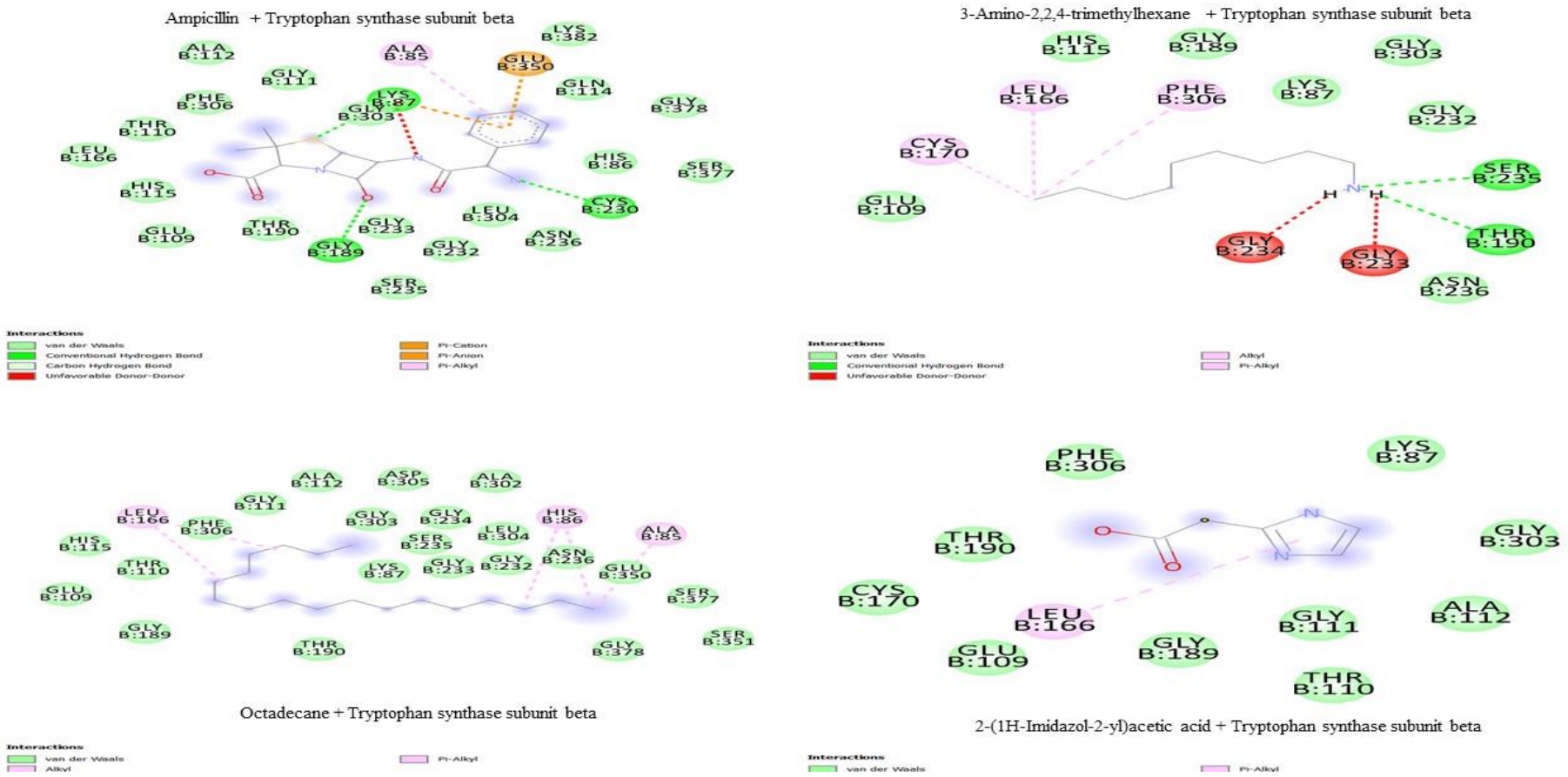

Figure 4.16: Interaction of endophytic compounds with residues of tryptophan synthase subunit beta. Ampillicin was used as standard commercial drug.

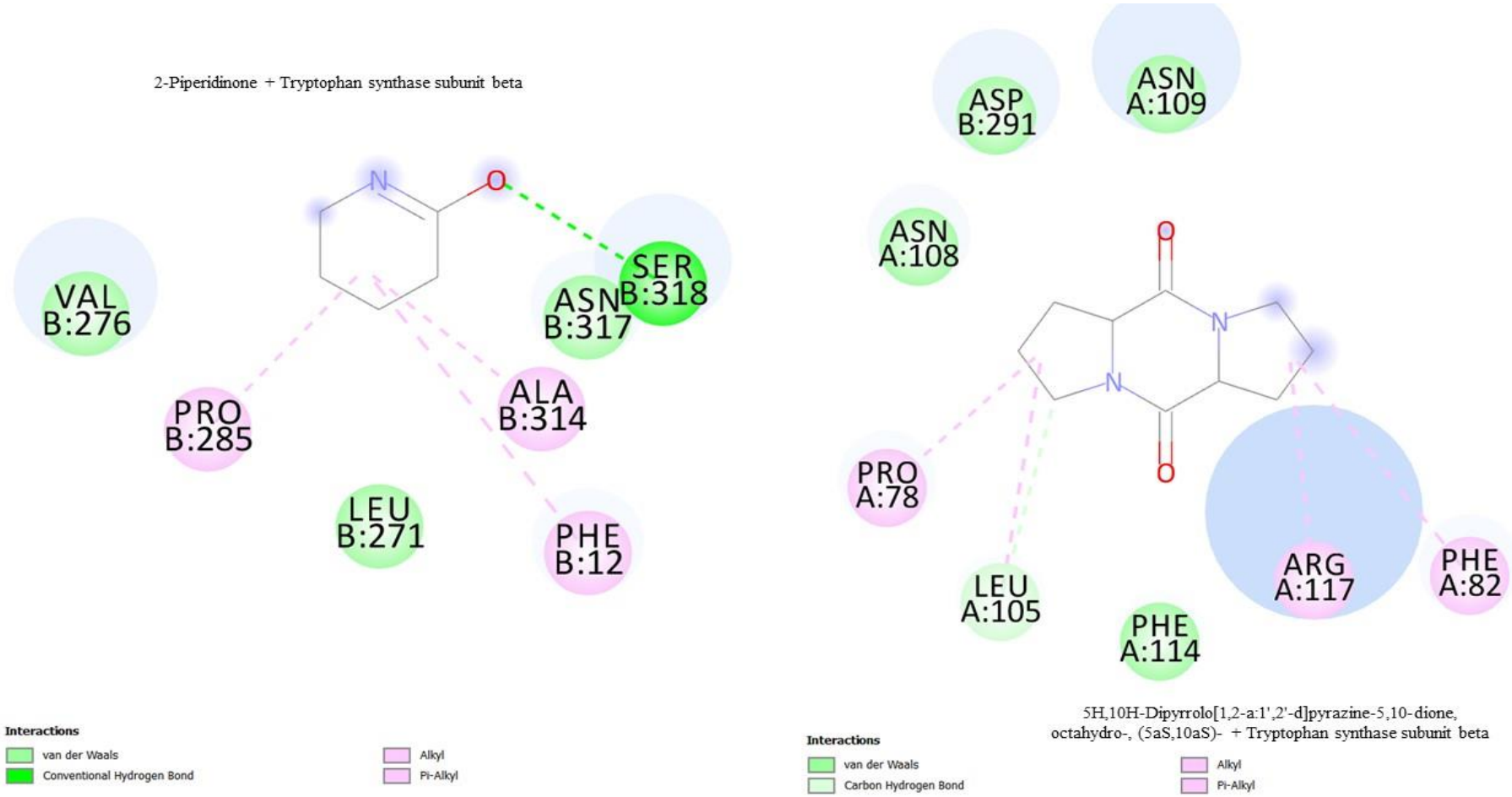

Figure 4.17: Interaction of endophytic compounds with residues of tryptophan synthase subunit beta.

CHAPTER 5

5. DISCUSSION

5.1 Molecular characterization endophytes

Endophytic cultures were isolated by streaking to obtain 23 pure isolates. The 23 pure cultures were assayed for the potential to extracellularly secret compounds which have antimicrobial activity. Nine endophytic samples were chosen based on the potency of the antimicrobial efficacy of the respective acetone, methanol and ethyl acetate extracts. In this study, we isolated genomic DNA of endophytes (Figure 4.1) and amplified the 16 S rRNA gene. Approximately, a 1500 bp amplicon was identified for all 9 of the endophytes that produced potent bioactive metabolites, thus, providing a positive identity that the 9 endophytic samples are bacteria (Figure 4.2).

Generic markers were used to differentiate the relatedness of the endophytic bacteria. RAPDs (random amplified polymorphic DNA) assay using M13 forward primer was performed and the distribution of the bands illustrated that the endophytic bacteria are not the same (Figure 4.3). Sample 2 and 3 are closely related and likely originated from the same ancestral bacteria. Also, sample 2 and 3 are distantly related to all the bacterial endophytes. Sample 1 and 18 are closely related, while sample 10 and 19 are closely related. Sample 17 is distantly related to sample 1, 3, 9, 10, 12, 15 and 18 (APPENDIX V). The diversity of the bacterial endophytes is because the endophytes were isolated from different hosts (trees). Also, distribution of endophytic community is tissue specific, implying that a single branch can harbour different types of endophytes. Noteworthy, only the RAPD sequences are easily detected because not all amplified sequences are polymorphic.

Our findings are consistent with other reports that have demonstrated that endophytic bacteria are prolific producers of important bioactive secondary metabolites (Eyre *et al.*, 2019; Nguyen

et al., 2019; Photolo *et al.*, 2020). The 16 S rRNA gene is highly conserved within all bacteria genome and is a housekeeping genetic marker which is commonly used for identification of bacteria (Zin *et al.*, 2020). External factors determine the composition of microbiomes inside plants. These major factors include weather, nutrient availability, plant species, location, soil composition and water (Eyre *et al.*, 2019)**.**

5.2 Antagonistic activity

The preliminary antagonistic screening of endophyte-endophyte in this study indicated the ability of endophytes to secrete bioactive secondary metabolites with antimicrobial properties as illustrated by the clear zones of inhibition (Figure 4.4). Endophytic samples 14 and 5 remarkably repelled other endophytes in the antagonistic screening assay. In contrast, *E. coli* and *S. aureus* exhibited moderate susceptibility to the extracts of endophytic sample 14 (0-21mm zone of inhibition) and sample 5 (0-20 mm inhibition). Undoubtedly, the interaction of endophytic samples in the same Petri dish as samples 14 and 5 present evidence that microbial interaction promotes production of more unique ligands that inhibit or accelerates particular functions of the cells.

These findings are consistent with numerous literature which illustrate that endophytes are legitimate sources of bioactive secondary metabolites (Manganyi *et al.*, 2019; Yasser *et al.*, 2019; Naama-amar *et al.*, 2020; Pelo *et al*., 2020). The co-cultivation approach promotes interspecies interaction and has been effectively utilized in the activation of silent biosynthetic gene clusters (BGCs); thus, stimulates and improves the production of bioactive secondary metabolites. Co-cultivation of *Acremoniun pilosum F47* and *Pleosporales sp. F46* by (Wang *et al.*, 2020) resulted in the discovery of new zinniol analogues (pleoniols A-C). Numerous studies have illustrated that the interaction of microorganisms is critical in the activation of the

production of metabolites by fungi and bacteria (McLean *et al.*, 2019; Nguyen *et al.*, 2019; Belknap *et al.*, 2020).

Notably, the availability of nutrition and interaction of microorganisms influence the global regulatory systems in microorganisms. Global regulators are known to indirectly or directly determine the expression of (BGCs) biosynthetic gene clusters by controlling the expression levels of cluster situated regulators (CSRs) (Belknap *et al.*, 2020; Nguyen *et al.*, 2020). The concentration of many valuable secondary metabolites is controlled by the tight cross-regulation of the transcription and translation of other BGCs in the genome by some CSRs (Kusari *et al.*, 2012). It is therefore imperative to observe and understand how the endophytic isolates empirically react to other microbes outside the plant environment.

5.3 Antimicrobial efficacy of endophytic extracts

In this research, we tested antimicrobial activity using endophytic ethyl acetate, methanol and acetone crude extracts. We used agar well diffusion technique, and we observed variations in the zones of inhibition (Table 4.1, Table 4.2, Table 4.3) between the crude extracts from endophytes isolated from *P. thonningii, C. mopane, V. amygdalina, L. discolour, P. angolensis, S. pungens, S. guineense* and *S. birrea*. Relative *in vitro* examination of the endophytic crude extracts showed that acetone extracts were substantially more potent than methanol and ethyl acetate extracts against the test microbes *S. aureus* and *E. coli*. This finding supports the notion that acetone is the best solvent for extracting a wide range of phyto-related (endophytic) compounds with different polarities (Famuyide *et al.*, 2019b, 2019a). The endophytic acetone crude extracts of sample 1 showed the potent antimicrobial efficacy 35 mm and 29 mm zones of inhibition towards *S. aureus* and *E. coli*, respectively. While acetone crude extracts of sample 3 exhibited 23 mm and 34 mm zones of inhibition against *S. aureus* and *E. coli*,

respectively. Zones of inhibition which are more than 13 mm and 17 mm for ampicillin against *S. aureus* and *E. coli*, respectively, the bacterial is considered to be susceptible to the antimicrobial agent.

In our research, the antimicrobial efficacy varied, but most of the extracts expressed strong, broad range potency. However, acetone crude extracts of sample 9 showed a significant difference in zones of inhibition 30 mm and 17 mm against *S. aureus* and *E. coli*, respectively. While acetone crude extracts of sample 11 exhibited 31 mm and 12 mm zones of inhibition against *S. aureus* and *E. coli,* respectively. It is noteworthy that the variation in the antimicrobial efficacy by the endophytic extracts from the same tree source in this study confirms that distinct, unprecedented and usually very complicated chemical configurations which result from the addition of different side-chain groups are secreted as secondary metabolites by endophytes. Some antimicrobial compounds exhibit stronger potency against Gram-positive bacteria than towards Gram-negative bacteria, while some antibiotics have broad-spectrum activity against both Gram-negative bacteria and Gram-positive bacteria. Thus, the antimicrobial efficacy of different bioactive metabolites is not equal in regards to bioactivity range (Torres *et al.*, 2019).

The antimicrobial results (Table 4.1, Table 4.2, Table 4.3) obtained from this research corroborate with earlier reports (Eze *et al.*, 2019; Wang *et al.*, 2019; Yasser *et al.*, 2019; Manganyi *et al.*, 2019; Nuankeaw *et al.*, 2020) that illustrate that endophytes are reservoirs of secondary metabolites with excellent antimicrobial potency. The distinction in the potency of endophytic (ethyl acetate, methanol and acetone) crude extracts from different endophytic tree sources consistent with previous studies that have illustrated the diversity in bioactive metabolites produced by different strains and genera of endophytes, hence, different antimicrobial properties (Wang *et al.*, 2007; Eze *et al.*, 2019; Hardoim, 2019; Hinterdobler and Schinnerl, 2019; Ma *et al.*, 2019; Wu *et al.*, 2019; Yuan *et al.*, 2019**)**. A vast gene pool, building

blocks and modification steps drive variations in enzymatic mechanisms which are responsible for the diverse structures of the metabolite classes (Berdy, 2005).

5.4 Characterization of metabolites secreted by endophytes

The qualitative TLC profiling of the endophytic (ethyl acetate, acetone and methanol) extracts in this research was based on the quenching intensity/colour of the extracts, and it remarkably showed the presence of numerous compounds. The charring profile of the compounds after derivatization with vanillin sulphuric acid methanol spray reagent showed the presence of terpenoids (blueish purple), flavonoids (yellow), stilbenes (red) (Figure 4.5 f). Flavonoids appear (yellow, pinkish or orange) whereas stilbenes appear (bright red to dark pink colour) whilst terpenoids produce a bluish-purple colour after spraying with vanillin (Taganna *et al.*, 2011). The numerous endophytic compounds gave different Rf values in dichloromethane: ethyl acetate solvent system (Figure 4.5 a-f). The Rf values determined the polarity of the endophytic chemicals, and this also aids in the selection of an appropriate solvent system for separation of pure compounds by column chromatography (Tijjani, 2018).

Endophytic secondary metabolites such as diterpenes, cardiac glycosides, tannins, alkaloids, flavonoids, saponins and phenols have been qualitatively screened in numerous studies. TLC, column chromatography, HPLC and GC-MS produce a more detailed evaluation of the endophytic biotope constituents (Figueiredo *et al.*, 2009; Eze *et al.*, 2019; Ma *et al.*, 2019; Manganyi *et al.*, 2019; Mohamed *et al*., 2020; Naama-amar *et al.*, 2020; Nuankeaw *et al.*, 2020). Thin-layer chromatography is the most straightforward and cheapest technique that is utilized in separation, estimation and identification of a mixture of single compounds in numerous extracts (Tijjani, 2018). Endophytes produce a unique wide consortium of molecular scaffolds of bioactive secondary metabolites. However, there is a need to have a clear and

precise knowledge of the nature of bioactive metabolites secreted by endophytes (Brader *et al.*, 2014). This compelled us to perform a GC-MS analysis on endophytic samples 1, 3, 9 and 17 to precisely identify the compounds present and make deductions on the ones that may be responsible for antimicrobial activity. Bioactive compounds are essential in drug discovery because they can be used as templates for synthetic modifications or can be used in their natural form (Aboody and Mickymaray, 2020).

5.5 GC-MS analysis of endophytic compounds

In this study, the GC-MS profile showed the presence of phyto-related compounds in acetone extracts of endophytic samples 1, 3, 9, and 17. Medicinally essential bioactive constituents were present in all extracts of all endophytic samples. The chromatogram predicted the presence of a wide variety of compounds which have antimicrobial, anti-fungal, anti-viral, anti-diabetic, anti-tumour, anti-cancer, anxiolytic, anti-protozoal, anti-asthmatic, anti-eczematic, antiseborrheic, anaesthetic general and antiallergic activities. Sulfonamide derivatives, indolizine derivatives, quinone derivatives, furan derivatives, organic acids, pyrazolo(3,4-d)pyrimidine derivatives, fused uracils, aroma compounds and phenolic compounds were identified in the GC-MS profile.

Hexadecane is an essential constituent that was found in all the endophytic acetone extracts in this study (Table 4.5). Hexadecane has been reported to possess antimicrobial activity in previous studies where it was found to be part of the bioactive constituents from ethyl acetate extract of *Phomopsis sp* (Paniculata, 2015). Eicosane is another important phyto related compound that was identified in this research (Table 4.5). Eicosane extracted from organic extracts and essential oil from *Cestrum nocturnum* was reported to possess antimicrobial activity and is also a principal constituent of *Aloe vera* (Paniculata, 2015)**.** Furan derivatives

and sulfonamide derivatives were observed in GC-MS profile in all endophytic samples (1, 3, 9 and 17) (Table 4.5).

Bioactivity prediction by PASSonline webserver of some endophytic acetone extracts showed that the endophytic compounds have a wide bioactivity spectrum. For instance, a furan derivative (+)1-(4-Methylacridine-9-yl)-3-((tetrahyrofuran-2-yl) methyl) thiourea was predicted to exhibit antiviral and antibacterial bioactivity. Precisely, (+)1-(4-Methylacridine-9-yl)-3-((tetrahyrofuran-2-yl) methyl) was predicted to inhibit the formation of the cell wall by inhibiting the enzymes (Undecaprenyldiphospho-muramoylpentapeptide beta-N-acetylglucosaminyltransferase and Mannotetraose 2-alpha-N-acetylglucosaminyltransferase inhibitor) responsible for catalysing the essential steps in the formation of the bacterial cell wall. Also, (+)1-(4-Methylacridine-9-yl)-3-((tetrahyrofuran-2-yl) methyl) thiourea inhibits deoxyribonuclease X and thymidylate 5'-phosphatase. SwissAMDE tool predicted that (+)1-(4-Methylacridine-9-yl)-3-((tetrahyrofuran-2-yl) methyl) satisfied the pharmacokinetic criteria of a lead compound for therapeutic purposes, for example, Lipinski's rule of five, water solubility and lipophilicity. However, the compound was produced in small quantities, thus, was not considered for molecular docking assay. Our research is consistent with other reports (Supuran, 2011; Simhadri *et al.*, 2017) which demonstrated that furan, sulfonamide derivatives possess potent antimicrobial and antifungal activity.

Derivatives of natural alkaloid products are prominently used as medicinal drugs and agricultural products because they exhibit potent antibacterial (Sparafloxacin and Ciprofloxacin), anticancer (Irinotecan, Gefitinib, Camptothecin and Topotecan), antiviral (Saquinavir), antimalarial (Chloroquine, Quinine, Mefloquine and Quinidine), antipysochotic (Brepiprazole and Aripiprazole), anthelmintic (Oxamniquine), insecticidal, cardioprotective (Vesnarinone), anti-inflammatory and antifungal. Camptothecin potently and inhibits

topoisomerase 1, an enzyme responsible for DNA replication explicitly. Hence, cell death as a result of cell cycle arrest in S-phase (Shang *et al.*, 2018).

Xanthine derivatives have been reported from plants and natural sources. In this study, xanthene was present in small quantities in the crude endophytic acetone extracts (Table 4.5). This finding is consistent with a study which has demonstrated that xanthine derivatives are produced in small quantities from natural sources, hence, extensive extraction is uneconomical. Xanthine derivatives are commonly used in the treatment of respiratory diseases, neurostimulation, cardiovascular diseases and treatment of gastric distress (Singh *et al.*, 2018)**.**

Pyrazolo(3,4-d)pyrimidine derivatives are purine analogues which have been demonstrated to exhibit antiviral, antimicrobial, anticancer, xanthine oxidase inhibitor, anti-inflammatory and antimetabolites. In this study pyrazolo(3,4-d)pyrimidine derivatives were observed in all endophytic acetone samples. Interestingly, 5H,10H-Dipyrrolo[1,2-a:1',2'-d]pyrazine-5,10-dione, octahydro-, (5aS,10aS)- was observed in relatively large quantities in this study. The presence of the above-identified endophytic compounds in endophytic acetone extracts of samples 1,3,9 and 17 may be responsible for the potent antimicrobial efficacy as shown by a broad zone of inhibition (Table 4.2). Also, the bioactive compounds are predicted to exhibit multiple bioactivity functions; thus, they may be responsible for therapeutic properties exhibited by medicinal plants *P. thonningii*, *C. mopane* and *P. angolensis*. The findings from the complex GC-MS profile validate the suggested synergistic effect of the bioactive endophytic secondary metabolites which is shown remarkably by the broad-spectrum activity and broad zones of inhibition exhibited by extracts, for example, sample 1 (35 mm and 29 mm) against *S. aureus* and *E. coli* respectively (Table 4.2). Bioactive secondary metabolites have been demonstrated to inhibit the growth and proliferation of microbes through various modes of action for different targets, for example, inhibiting cell wall, RNA and protein synthesis or inhibiting DNA replication (Torres *et al.*, 2019). Thus, the biosynthetic ability of endophytes

to produce numerous therapeutically important compounds with a higher affinity for multiple macromolecular bacterial targets may help in combating microbial resistance.

The concentration of endophytic compounds shown by area under the curve from the GC-MS profile (Table 4.5) provides an insight into the biosynthetic skill of the endophytic bacteria under laboratory conditions. The endophytic compounds which had the largest peak area under the curve were chosen for *in silico* molecular docking assay. The major constituents in all four endophytic extracts chosen for molecular docking include 3-Amino-2,2,4-trimethylhexane (area under the curve 106840849), octadecane (area under the curve 61655978), 2-(1H-Imidazol-2-yl)acetic acid (area 3644570), 2-Piperidinone (area under the 344080639) and 5H,10H-Dipyrrolo[1,2-a:1',2'-d]pyrazine-5,10-dione, octahydro-, (5aS,10aS)- (area under the curve 100936317). On that account, fermentation conditions can be altered to overexpress the synthesis of a protein responsible for the production of lead therapeutic compounds. However, this goal can only be achieved by knowledge of metabolic regulation of the endophytic cell. The knowledge can be acquired by whole genomic sequencing of an endophytic isolate to evaluate the conserved genes responsible for the synthesis of the metabolites. Thus, enabling removal of rate-limiting allosteric and transcription steps by promoter engineering, genetically inhibiting the pathways that compete with the pathway of the desired product and promoting the transport of the desired constituent out of the cell (Primrose and Twyman, 2006).

The quality of potential therapeutic candidates is increasing due to the evaluation of physicochemical properties of the selected potential drug scaffolds as a result reducing the failures related to pharmacokinetics in phase 1 clinical trials. Oral dosing is the highly preferred drug administration method because of the patient's comfort and compliance (Daina and Zoete, 2016). Traditional medicine concoction is also usually administered orally (Ngarivhume *et al.*, 2015), thus, the solubility of medicinally important compounds is universally essential.

The water solubility of endophytic constituents predicted by the SwissADME tool ranged from soluble to very soluble, with eicosane, 2-(1-Fluorovinyl)-5-nitropyridine, octadecane, hexadecane exhibiting poor water solubility. The solubility of the selected endophytic compounds 3-Amino-2,2,4-trimethylhexane, octadecane, 2-(1H-Imidazol-2-yl)acetic acid (area 3644570), 2-Piperidinone and 5H,10H-Dipyrrolo[1,2-a:1',2'-d]pyrazine-5,10-dione, octahydro-, (5aS,10aS)- was predicted to be soluble, poorly soluble, soluble, very soluble and soluble, respectively (Table 4.5). Solubility of the endophytic compounds is determined by their molecular structures. These finding correlate with studies which show that traditional medicinal concoctions were prepared by socking the plant parts in either in hot or cold water to extract the therapeutically essential compounds (Ngarivhume *et al.*, 2015). The solubility of a lead molecule in drug development determines the adsorption of the drug and makes the formulation and handling procedure easier. Also, a highly soluble drug is ideal for parenteral use because a small volume of a pharmaceutical dosage can be delivered sufficiently to elicit a response (Daina *et al*., 2017).

The above selected compounds satisfied Lipinski's rule of five; thus, can be used as potential scaffolds for medicinal drugs because they can be easily accessed synthetically and are exceptionally bioavailable. Exceptional bioavailability of the selected endophytic compounds implies that the *in-vitro* antimicrobial activity can be translated into a potent antimicrobial drug. These findings are also supported by the bioactivity spectrum predicted by (Prediction of Activity Spectra for Substances) PASSonline tool. The interpretation of findings from PASSonline tool is that if the predicted bioactivity spectrum is above 0.7, the chances of obtaining the bioactivity *in-vitro* and *in-vivo* are higher.

Amino-2,2,4-trimethylhexane was predicted to possess antiviral, antimicrobial, preneoplastic conditions treatment, phobic disorder treatment, antifungal, muco-membranous protector, cytoprotectant. Precisely, amino-2,2,4-trimethylhexane was predicted to inhibit

exoribonuclease II, yeast ribonuclease and DNA 3-methyladenine enzymes which are critical for the survival of microorganisms. It also has higher chances of inhibiting pullulanase; thus, can deprive microbes of acquiring extracellular fermentable sugars. Amino-2,2,4-trimethylhexane was predicted to function in phobic disorder treatment and 5 hydroxytryptamine release stimulants (Table 4.6). PASSonline has also been predicted that amino-2,2,4-trimethylhexane is a complement factor D inhibitor, which is fascinating because complement factor inhibitors are reported to be under clinical trials for the treatment of glomerular diseases and renal treatment (Zipfel *et al.*, 2019). Also, Amino-2,2,4-trimethylhexane was predicted to inhibit superoxide dismutase. Preclinical NSCLC mouse trials have shown that inhibition of superoxide dismutase 1 suppresses tumour growth and induces cell apoptosis (Glasauer *et al.*, 2014).

Endophytic compound 5H,10H-Dipyrrolo[1,2-a:1',2'-d]pyrazine-5,10-dione, octahydro-, (5aS,10aS)- was predicted to inhibit membrane permeability, glucan 1,4-alpha-maltotriohydrolase, glucan 1,4-alpha-maltotetraohydrolase and gluconate 5-dehydrogenase (Table 4.10).The enzymes are important for the survival of microorganisms. Also, it was predicted to function as phobic disorders treatment and nicotinic alpha4beta4 receptor agonist.

5H,10H-Dipyrrolo[1,2-a:1',2'-d]pyrazine-5,10-dione, octahydro-, (5aS,10aS)- was predicted to inhibit Na+-transporting two-sector ATPase which is an essential enzyme which compose the bacterial type III secretion system (T3SS). T3SS are responsible for the virulence of pathogenic bacteria because they translocate bacterial effectors proteins, thus, enabling successful invasion of host cells and ultimately colonize and replicate in the host (Coburn *et al.*, 2007). Inhibition Na+-transporting two-sector ATPase will results in protection of host cells from infection by pathogenic bacteria.

Also, endophytic compound 5H,10H-Dipyrrolo[1,2-a:1',2'-d]pyrazine-5,10-dione, octahydro-, (5aS,10aS)- was predicted to inhibit glucan endo-1,6-beta-glucosidase. Glucan endo-1,6-beta-

glucosidase is enzyme found in *Trichoderma* genus soilborne, wood decaying and an opportunistic pathogen to immunocompromised humans (Druzhinina and Kubicek, 2005). The enzyme catalysis the hydrolysis of (α-1-6) bonds in (α-1-6) β-D-glucans which is an essential step in the carbohydrate metabolic process of *Trichoderma* genus. These findings support the notion that endophytes protect the host plant from invasion by pathogenic microbial strains. These findings are also consistent with reports which have demonstrated that pyrazolo(3,4-d)pyrimidine derivatives are used as antidepressant drugs, for treatment of Alzheimer's disease and exhibit potent antimicrobial efficacy (El-Kalyoubi and Agili, 2016).

Endophytic compound 2-Piperidinone was predicted to inhibit glucan 1,4-alpha-maltotetraohydrolase (Table 4.9), a bacterial enzyme responsible the hydrolysis of 1,4-α-D glycosidic linkages. Inhibition of bacterial glucan 1,4-alpha-maltotetraohydrolase may be fatal because of failure to access reduced sugars. These predicted bioactivity spectrum by PASSonline tool of endophytic compounds are consistent with the knowledge that native African societies have used traditional therapeutic plants for the treatment of kidney diseases, liver diseases, viral and bacterial infections, blood circulation problems, proctitis, gastrointestinal, respiratory and urinal-genital problems (Ojewole, 2004; Fotio *et al.*, 2009; Ojewole *et al.*, 2010; Gouwakinnou *et al.*, 2011; Gaertin *et al.*, 2020).

Inhibition of lumazine synthase, tryptophan synthase and UDP-N-acetylglucosamine 1-carboxyvinyltransfrase can be the help in combating antimicrobial resistance in microorganisms because the enzymes catalyse essential steps required for survival of the bacteria. Thus, lumazine synthase, tryptophan synthase and UDP-N-acetylglucosamine 1-carboxyvinyltransfrase were selected as bacterial protein targets to evaluate the molecular interactions of the endophytic compounds and the enzymes.

5.6 Molecular docking

The understanding of energetics and geometrical features of the interactions between biological macromolecules and ligand is essential in the success of rational drug discovery. Multiple non-covalent interactions are mainly formed when low molecular weight ligands bind to side chains of protein binding pocket residues, thus, forming a specific protein-ligand complex. The interactions include hydrophobic association, hydrogen bonds, van der Waals interactions, cation-π interactions, salt bridges, π-π aromatic stacking, electrostatic interactions and halogen bonds (Brylinski, 2018). In this study, conventional hydrogen bonds, carbon-hydrogen bonds, alkyl interactions, π-anion, π-sigma, π-alkyl interactions were observed due to the interaction of residues at the active sites of target proteins and endophytic compounds. Bioactive compounds effectively and specifically bind to macromolecular targets, consequently modulating molecular recognition and gene regulation (Erbaş, 2018). This prompted us to evaluate the degree of binding affinities exhibited by endophytic compounds to pocket residues of target bacterial proteins.

Ampicillin drug was used as a standard drug for comparison of the binding affinities of the selected endophytic compounds. Formation and stability of a protein-ligand complex are determined by the negative energy of a free system. Thus, the larger the negative enthalpy change the more spontaneous the formation of a protein-ligand complex and the more stable the protein-ligand complex (Du *et al.*, 2016). In this study, 5H,10H-Dipyrrolo[1,2-a:1',2'-d]pyrazine-5,10-dione, octahydro-, (5aS,10aS)- exhibited the highest specificity and binding affinities on all the selected drug targets (lumazine synthase, tryptophan synthase and UDP-N-acetylglucosamine 1-carboxyvinyltransfrase), with the highest binding affinity on lumazine synthase -6.4 kcal/mol (Table 4.11).

A comparison of binding affinities between 5H,10H-Dipyrrolo[1,2-a:1',2'-d]pyrazine-5,10-dione, octahydro-, (5aS,10aS)- and standard ampicillin with lumazine synthase shows that 5H,10H-Dipyrrolo[1,2-a:1',2'-d]pyrazine-5,10-dione, octahydro-, (5aS,10aS)- has approximately -1.3 kcal/mol weaker binding affinity (Table 4.11). In a recent docking study, lumazine synthase was used as a drug target for phytochemical compounds (methyl-2-pentene and 2,6-octadienal, 3, 7-dimethyl). The binding affinities of methyl-2-pentene and 2,6-octadienal, 3, 7-dimethyl against lumazine synthase were -4.2 and -5.8 kcal/mol, respectively (Simhadri *et al.*, 2017)**.**

Our study correlates with these findings because binding affinities of our selected endophytic compounds ranged from -3.9 to -6.4 kcal/mol for lumazine synthase. Noteworthy, 5H,10H-Dipyrrolo[1,2-a:1',2'-d]pyrazine-5,10-dione, octahydro-, (5aS,10aS)- binding affinity with lumazine synthase is -1.7kcal/mol slightly weaker than the reference clotrimazole used in a study by (Simhadri *et al.*, 2017). A ligand which exhibits high specificity and affinity to a protein even in low concentration cannot be displaced by a high concentration of a weaker interacting ligand. These results suggest that 5H,10H-Dipyrrolo[1,2-a:1',2'-d]pyrazine-5,10-dione, octahydro-, (5aS,10aS)- is a potent inhibitor of lumazine synthase.

Interestingly, the affinity and specificity of 5H,10H-Dipyrrolo[1,2-a:1',2'-d]pyrazine-5,10-dione, octahydro-, (5aS,10aS)- to lumazine synthase is due to two conventional hydrogen bonds (His:102 and Thr:50), carbon hydrogen bond(Cys:48) and alkyl interactions (Ile:162 and Cys:48) formed by the ligand-protein complex (Figure 4. 13). Precisely, the hydrogen bonds are responsible for the stabilization of 5H,10H-Dipyrrolo[1,2-a:1',2'-d]pyrazine-5,10-dione, octahydro-, (5aS,10aS)- and lumazine synthase complex.

The observed binding affinity of 5H,10H-Dipyrrolo[1,2-a:1',2'-d]pyrazine-5,10-dione, octahydro-, (5aS,10aS)- with UDP-N-acetylglucosamine 1-carboxyvinyltransfrase was -6.1

kcal/mol. The stability and specificity of 5H,10H-Dipyrrolo[1,2-a:1',2'-d]pyrazine-5,10-dione, octahydro-, (5aS,10aS)- and UDP-N-acetylglucosamine 1-carboxyvinyltransfrase complex is due to two conventional hydrogen bonds formed by the interaction of His:125 and Arg:91 residues with the atoms of 5H,10H-Dipyrrolo[1,2-a:1',2'-d]pyrazine-5,10-dione, octahydro-, (5aS,10aS)-. Also, alkyl interactions were observed between 5H,10H-Dipyrrolo[1,2-a:1',2'-d]pyrazine-5,10-dione, octahydro-, (5aS,10aS)- molecule and Val:163, Pro:121 and Leu:124 residues of UDP-N-acetylglucosamine 1-carboxyvinyltransfrase (Figure 4.15). Our finding are consistent with a study which has demonstrated that Pyrazolo[3,4-d]pyrimidine derivatives exhibit potent antimicrobial activity (El-Kalyoubi and Agili, 2016).

Endophytic compounds, 2-(1H-Imidazol-2-yl)acetic acid and octadecane also demonstrated exceptional affinity on all three protein targets. However, 2-(1H-Imidazol-2-yl)acetic acid formed an unfavourable donor-donor interaction with Asn:23 residue of the active site of UDP-N-acetylglucosamine 1-carboxyvinyltransfrase. Octadecane was predicted to be a poorly soluble molecule, thus, cannot be considered as a lead molecule. In the quest for potential potent antimicrobial compounds which will help in combating antimicrobial resistance, we have identified 5H,10H-Dipyrrolo[1,2-a:1',2'-d]pyrazine-5,10-dione, octahydro-, (5aS,10aS)- as lead antimicrobial drug scaffold.

In this study, ampicillin interacted with Gly:95, Thr:3, Gln:7, Met:32 and Arg:86 residues of lumazine synthase while 5H,10H-Dipyrrolo[1,2-a:1',2'-d]pyrazine-5,10-dione, octahydro-, (5aS,10aS)- interacted with Thr:50, His:102, Cys:48 and Ile:162 residues of lumazine synthase. Since ampicillin and 5H,10H-Dipyrrolo[1,2-a:1',2'-d]pyrazine-5,10-dione, octahydro-, (5aS,10aS)- interact with different pocket residues of lumazine synthase, combining them in a concoction can yield a potent combination which can potentially help suppress the development of tolerance, persistence or resistance to antibiotics by pathogens. Efficacy of plant-related/ endophytic bioactive compounds is known to increase when combined with

amphipathic compounds, thus, act synergistically. For instance, the *S. aureus* pump *NorA MDR* was inhibited by a combination of phyto-related compound berberine and 50-methoxyhydnocarpin. 50-methoxyhydnocarpin enhances the inhibitory activity of berberine (Matar *et al*., 2020). The use of a combination of bioactive metabolites and antibiotics can be the dawn for serendipitous antimicrobial combination therapies (Torres *et al.*, 2019).

Endophytic compound 5H,10H-Dipyrrolo[1,2-a:1',2'-d]pyrazine-5,10-dione, octahydro-, (5aS,10aS)- is a major constituent as illustrated by the GC-MS profile (Table 4.5). This is promising as it can be easily obtained through fermentation process. Thus, the ability of endophytes to synthesize and secret potent bioactive compounds extracellularly satisfy the need to produce novel therapeutically important drugs by fermentation. Also, endophytes as credible sources of therapeutically essential drugs help in preserving the traditional medicinal plants which have extensively depleted due to over-harvesting

5.7. Conclusion

The GC-MS profile showed the presence of bioactive endophytic compounds that possess vast therapeutic potential. The bioactive compounds identified in this research may be responsible for the pharmacological properties of the host medicinal plants *P. thonningii, C. mopane* and *P. angolensis*. The endophytes from the *P. thonningii*, *C. mopane*, *P. angolensis*, *V. amygdalina, S. pungens, S. birrea* and *S. guineense* are easily cultured under laboratory conditions for the synthesis of bioactive secondary metabolites through fermentation. Thus, it will protect and preserve medicinal plants from excessive harvesting, which consequently affects environmental biodiversity. Results from this study also confirmed that metabolite profiling is a faster approach which accelerates the discovery of therapeutic lead drug scaffolds. The computational tools used in this study provided an in-depth understanding of the protein-

ligand interactions and the pharmacokinetic properties of endophytic compounds. Molecular characterisation of the endophytes enabled us to identify 10 prolific bacterial endophytes. RAPDs evaluation has shown that the endophytic bacteria are not the same microorganisms. However, there is need to sequence the 16 S rRNA gene so as to have the exact identity of the bacterial endophytes. Ultimately, this research is useful to the pharmaceutical industry in relation to the production of drugs from bioactive natural compounds extracted from endophytes.

Reference

Aboody, M.S. Al, Mickymaray, S., 2020. Anti-fungal efficacy and mechanisms of flavonoids. Antibiotics 9. https://doi.org/10.3390/antibiotics9020045

Abubakar, M., Majinda, R., 2016. GC-MS Analysis and Preliminary Antimicrobial Activity of Albizia adianthifolia (Schumach) and Pterocarpus angolensis (DC). Medicines 3, 3. https://doi.org/10.3390/medicines3010003

Adebola, M.O., Bello, T.S., Oyelade, A.E., Aremu, M.B., Egubagi, M.J., Umar, S.M., 2020. Fungicidal Activities of Methanolic Plant Extracts on Mycelia Growth of Fusarium oxysporum Associated With Sweet Orange (Citrus sinensis (Linnaeus) Osbeck) 32, 1–8.

Adeniyi, S.A., Orjiekwe, C.L., Ehiagbonare, J.E., Arimah, B.D., 2010. Preliminary phytochemical analysis and insecticidal activity of ethanolic extracts of four tropical plants (Vernonia amygdalina, Sida acuta, Ocimum gratissimum and Telfaria occidentalis) against beans weevil (Acanthscelides obtectus). Int. J. Phys. Sci. 5, 753–792.

Abrahams, K.A., Cox, J.A.G., Fütterer, K., Rullas, J., Ortega-Muro, F., Loman, N.J., Moynihan, P.J., Pérez-Herrán, E., Jiménez, E., Esquivias, J., Barros, D., Ballell, L., Alemparte, C., Besra, G.S., 2017. Inhibiting mycobacterial tryptophan synthase by targeting the inter-subunit interface. Sci. Rep. 7, 1–15. https://doi.org/10.1038/s41598-017-09642-y

Afab, K., Shaheen, F., Mohammad, F.V., Noorwala, M., Ahmad, V.U., 1996. Saponins Used in Traditional and Modern Medicine. Advences Exp. Med. Biol. 404, 429–442. https://doi.org/10.1007/978-1-4899-1367-8

Afolayan, M., Srivedavyasasri, R., Asekun, O.T., Familoni, O.B., Orishadipe, A., Zulfiqar, F.,

Ibrahim, M.A., Ross, S.A., 2018. Phytochemical study of Piliostigma thonningii, a medicinal plant grown in Nigeria. Med. Chem. Res. 27, 2325–2330. https://doi.org/10.1007/s00044-018-2238-1

Agrawal, D.C., Tsay, H., Wu, Y., 2017. Medicinal Plants and Fungi : Recent Advances in Research and Development.

Alara, O.R., Abdurahman, N.H., Ukaegbu, C.I., Kabbashi, N.A., 2019. Extraction and characterization of bioactive compounds in Vernonia amygdalina leaf ethanolic extract comparing Soxhlet and microwave-assisted extraction techniques . J. Taibah Univ. Sci. 13, 414–422. https://doi.org/10.1080/16583655.2019.1582460

Alaribe, F.N., Motaung, K.S.C.M., 2019. Medicinal Plants in Tissue Engineering and Regenerative Medicine in the African Continent. Tissue Eng. - Part A 25, 827–829. https://doi.org/10.1089/ten.tea.2019.0060

Almubayedh, H., Ahmad, R., 2020. Ethnopharmacology, phytochemistry, biological activities, and therapeutic applications of Cedrela serrata Royle: A mini review. J. Ethnopharmacol. 246, 112206. https://doi.org/10.1016/j.jep.2019.112206

Annunziato, G., 2019. Strategies to overcome antimicrobial resistance (AMR) making use of non-essential target inhibitors: A review. Int. J. Mol. Sci. 20. https://doi.org/10.3390/ijms20235844

Ashour, A.S., El Aziz, M.M.A., Gomha Melad, A.S., 2019. A review on saponins from medicinal plants: chemistry, isolation, and determination. J. Nanomedicine Res. 7, 282–288. https://doi.org/10.15406/jnmr.2019.07.00199

Avedissian, S.N., Liu, J., Rhodes, N.J., Lee, A., Pais, G.M., Hauser, A.R., Scheetz, M.H., 2019. A review of the clinical pharmacokinetics of polymyxin b. Antibiotics 8, 1–11.

https://doi.org/10.3390/antibiotics8010031

Bagul, U., Technical, S., Society, E., 2016. Antibiotic susceptibility testing: a review on current practices.

Bakar, B.A., Razarinah, W., Abdul, W., Osman, C.P., 2020. Antimicrobial Activity of Curry Leaves (Murayya koenigii) on Selected Foodborne Pathogens. Sci. Lett. 14, 7–13. https://doi.org/10.1234/jmpc.v14i1.7778

Belknap, K.C., Park, C.J., Barth, B.M., Andam, C.P., 2020. Genome mining of biosynthetic and chemotherapeutic gene clusters in Streptomyces bacteria. Sci. Rep. 10, 2003. https://doi.org/10.1038/s41598-020-58904-9

Bell, T.H., Hockett, K.L., Alcal, R.I., Barbercheck, M., Beattie, G.A., Bruns, M.A., Carlson, J.E., Chung, T., Collins, A., Emmett, B., Esker, P., Garrett, K.A., Glenna, L., Gugino, B.K., 2019. Manipulating Wild and Tamed Phytobiomes : Challenges and Opportunities 3, 3–21. https://doi.org/10.1094/PBIOMES-01-19-0006-W

Berdy, J., 2005. Bioactive Microbial Metabolites. J. Antibiot. 58, 1–26.

Bonev, B., Hooper, J., Parisot, J., 2008. Principles of assessing bacterial susceptibility to antibiotics using the agar diffusion method. J. Antimicrob. Chemother. 61, 1295–1301. https://doi.org/10.1093/jac/dkn090

Brader, G., Compant, S., Mitter, B., Trognitz, F., Sessitsch, A., 2014. Metabolic potential of endophytic bacteria. Curr. Opin. Biotechnol. 27, 30–37. https://doi.org/10.1016/j.copbio.2013.09.012

Brylinski, M., 2018. Aromatic interactions at the ligand-protein interface: Implications for the development of docking scoring functions. Chem Biol Drug Des. 91, 380–390. https://doi.org/10.1111/cbdd.13084.

Calzetta, L., Pistocchini, E., Leo, A., Roncada, P., Ritondo, B.L., Palma, E., di Cave, D., Britti, D., 2020. Anthelminthic medicinal plants in veterinary ethnopharmacology: A network meta-analysis following the PRISMA-P and PROSPERO recommendations. Heliyon 6, e03256. https://doi.org/10.1016/j.heliyon.2020.e03256

Chaachouay, N., Benkhnigue, O., Fadli, M., El Ibaoui, H., Zidane, L., 2019. Ethnobotanical and ethnopharmacological studies of medicinal and aromatic plants used in the treatment of metabolic diseases in the Moroccan Rif. Heliyon 5, e02191. https://doi.org/10.1016/j.heliyon.2019.e02191

Chadha, N., Mishra, M., Rajpal, K., Bajaj, R., Choudhary, D.K., Varma, A., 2015. An ecological role of fungal endophytes to ameliorate plants under biotic stress. Arch. Microbiol. 197, 869–881. https://doi.org/10.1007/s00203-015-1130-3

Challaraj Emmanuel, E.S., Biji, V., Krishna, G.N., 2020. A characteristic study on the effect of ginger and nutmeg extracts on Pseudomonas and E.coli biofilms. Int. J. Res. Pharm. Sci. 11, 386–396. https://doi.org/10.26452/ijrps.v11i1.1832

Chen, C.H., Lu, T.K., 2020. Development and challenges of antimicrobial peptides for therapeutic applications. Antibiotics 9. https://doi.org/10.3390/antibiotics9010024

Chinnasamy, P., Arumugam, R., 2018. In silico prediction of anticarcinogenic bioactivities of traditional anti-inflammatory plants used by tribal healers in Sathyamangalam wildlife Sanctuary, India . Egypt. J. Basic Appl. Sci. 5, 265–279. https://doi.org/10.1016/j.ejbas.2018.10.002

Clift, C., 2019. Review of Progress on Antimicrobial Resistance: Background and Analysis. Cent. Glob. Heal. Secur. 54. https://doi.org/10.13140/RG.2.2.22042.80323

Coburn, B., Sekirov, I., Finlay, B.B., 2007. Type III secretion systems and disease. Clin.

Microbiol. Rev. 20, 535–549. https://doi.org/10.1128/CMR.00013-07

Cui, Q., Du, R., Liu, M., Rong, L., 2020. Lignans and their derivatives from plants as antivirals. Molecules 25, 1–17. https://doi.org/10.3390/molecules25010183

Daina, A., Michielin, O., Zoete, V., 2017. SwissADME: A free web tool to evaluate pharmacokinetics, drug-likeness and medicinal chemistry friendliness of small molecules. Sci. Rep. 7, 1–13. https://doi.org/10.1038/srep42717

Daina, A., Zoete, V., 2019. Application of the swissdrugdesign online resources in virtual screening. Int. J. Mol. Sci. 20. https://doi.org/10.3390/ijms20184612

Daina, A., Zoete, V., 2016. A BOILED-Egg To Predict Gastrointestinal Absorption and Brain Penetration of Small Molecules. ChemMedChem 1117–1121. https://doi.org/10.1002/cmdc.201600182

Dar, Z.A., Rifat, B., Bhat, J.I.A., Bhatti, A.A., Haq, S., Amin, A., Dar, S.A., 2019. Potential Role of Endophytes for Sustainable Environment 78–95. https://doi.org/10.4018/978-1-5225-7387-6.ch005

Dasofunjo, K., Asuk, A.A., Ezugwu, H.C., Nwodo, O.F.C., Olatunji, T.L., 2013. Aphrodisiac effect of ethanol extract of Piliostigma thonningii leaf on male albino wistar rats. J. Appl. Pharm. Sci. 3, 130–135. https://doi.org/10.7324/JAPS.2013.31023

Deshmukh, S.K., Verekar, S.A., Bhave, S. V, 2014. Endophytic fungi: A reservoir of antibacterials. Front. Microbiol. https://doi.org/10.3389/fmicb.2014.00715

Dev, A., Adil, M.T., Kumar, P., 2020. In Silico Based Approach to Identify Mura as A Potential Drug Target for Leprosy 3, 1–7.

Druzhinina, I., Kubicek, C.P., 2005. Species concepts and biodiversity in Trichoderma and Hypocrea: From aggregate species to species clusters. J. Zhejiang Univ. Sci. 6 B, 100–

112. https://doi.org/10.1631/jzus.2005.B0100

Du, X., Li, Y., Xia, Y.L., Ai, S.M., Liang, J., Sang, P., Ji, X.L., Liu, S.Q., 2016. Insights into protein–ligand interactions: Mechanisms, models, and methods. Int. J. Mol. Sci. 17, 1–34. https://doi.org/10.3390/ijms17020144

El-Kalyoubi, S., Agili, F., 2016. A novel synthesis of fused uracils: Indenopyrimidopyridazines, pyrimidopyridazines, and pyrazolopyrimidines for antimicrobial and antitumor evalution. Molecules 21, 1–14. https://doi.org/10.3390/molecules21121714

Erbaş, A., 2018. Effects of electrostatic interactions on ligand dissociation kinetics. Phys Rev E. 97. https://doi.org/10.1103/PhysRevE.97.022405.

Eyre, A.W., Wang, M., Oh, Y., Dean, R.A., 2019. Identi fi cation and Characterization of the Core Rice Seed Microbiome 148–157. https://doi.org/10.1094/PBIOMES-01-19-0009-R

Eze, P.M., Nnanna, J.C., Okezie, U., Buzugbe, H.S., Abba, C.C., Chukwunwejim, C.R., Okoye, F.B.C., Esimone, C.O., 2019. Screening of metabolites from endophytic fungi of some Nigerian medicinal plants for antimicrobial activities. EuroBiotech J. 3, 10–18. https://doi.org/10.2478/ebtj-2019-0002

Fajardo, S., García-Galvan, R., F., Barranco, V., Galvan, J.C., Batlle, S.F., 2016. Introductory Chapter: Terpenes and Terpenoids. Intech i, 13. https://doi.org/http://dx.doi.org/10.5772/57353

Famuyide, I.M., Aro, A.O., Fasina, F.O., Eloff, J.N., McGaw, L.J., 2019a. Antibacterial and antibiofilm activity of acetone leaf extracts of nine under-investigated south African Eugenia and Syzygium (Myrtaceae) species and their selectivity indices. BMC Complement. Altern. Med. 19, 1–13. https://doi.org/10.1186/s12906-019-2547-z

Famuyide, I.M., Aro, A.O., Fasina, F.O., Eloff, J.N., McGaw, L.J., 2019b. Antibacterial activity and mode of action of acetone crude leaf extracts of under-investigated Syzygium and Eugenia (Myrtaceae) species on multidrug resistant porcine diarrhoeagenic Escherichia coli. BMC Vet. Res. 15, 1–14. https://doi.org/10.1186/s12917-019-1914-9

Farombi, E.O., Owoeye, O., 2011. Antioxidative and chemopreventive properties of Vernonia amygdalina and Garcinia biflavonoid. Int. J. Environ. Res. Public Health 8, 2533–2555. https://doi.org/10.3390/ijerph8062533

Figueiredo, J.E.F., Gomes, E.A., Guimarães, C.T., Lana, U.G. de P., Teixeira, M.A., Lima, G.V.C., Bressan, W., 2009. Molecular analysis of endophytic bacteria from the genus Bacillus isolated from tropical maize (Zea mays L.). Brazilian J. Microbiol. 40, 522–534. https://doi.org/10.1590/s1517-83822009000300014

Finkel, O.M., Castrillo, G., Herrera Paredes, S., Salas González, I., Dangl, J.L., 2017. Understanding and exploiting plant beneficial microbes. Curr. Opin. Plant Biol. 38, 155–163. https://doi.org/10.1016/j.pbi.2017.04.018

Fotio, A.L., Dimo, T., Nguelefack, T.B., Dzeufiet, P.D.D., Ngo Lemba, E., Temdie, R.J., Ngueguim, F., Olleros, M.L., Vesin, D., Dongo, E., Kamtchouing, P., Garcia, I., 2009. Acute and chronic anti-inflammatory properties of the stem bark aqueous and methanol extracts of Sclerocarya birrea (Anacardiaceae). Inflammopharmacology 17, 229–237. https://doi.org/10.1007/s10787-009-0011-2

Fouda, A.H., Hassan, S.E.D., Eid, A.M., Ewais, E.E.D., 2015. Biotechnological applications of fungal endophytes associated with medicinal plant Asclepias sinaica (Bioss.). Ann. Agric. Sci. 60, 95–104. https://doi.org/10.1016/j.aoas.2015.04.001

Gadd, M.E., 2002. The impact of elephants on the marula tree Sclerocarya birrea. Afr. J. Ecol. 40, 328–336. https://doi.org/10.1046/j.1365-2028.2002.00385.x

Gaertin, L., Kéita, O., Dianka, B., Coulibaly, S.S., 2020. Chromatographic Analyses of Anti diabetic plants: Sclerocarya birrea (A. Rich) Hochst, Balanites aegyptiaca (L) Del, Ceiba pentandra (L) Gaertin. Int. J. Adv. Res. Chem. Sci. 7, 22–26. https://doi.org/10.20431/2349-0403.0701004

Gajdács, M., Albericio, F., 2019. Antibiotic resistance: from the bench to patients. Antibiotics 8, 8–11. https://doi.org/10.3390/antibiotics8030129

Garcia-Vallve, S., Palan, J., Romeu, A., 1999. Horizontal gene transfer in glycosyl hydrolases inferred from codon usage in Escherichia coli and Bacillus subtilis. Mol. Biol. Evololution 16, 1125–1134.

Glasauer, A., Sena, L.A., Diebold, L.P., Mazar, A.P., Chandel, N.S., 2014. Targeting SOD1 reduces experimental non-small-cell lung cancer. J. Clin. Invest. 124, 117–128. https://doi.org/10.1172/JCI71714

Gouwakinnou, G.N., Lykke, A.M., Assogbadjo, A.E., Sinsin, B., 2011. Local knowledge, pattern and diversity of use of Sclerocarya birrea. J. Ethnobiol. Ethnomed. 7, 1–9. https://doi.org/10.1186/1746-4269-7-8

Goyena, R., 2019. Microbial Root Endophytes, Journal of Chemical Information and Modeling. https://doi.org/10.1017/CBO9781107415324.004

Grey, M.S., 2019. Accessing seasonal weather forecasts and drought prediction information for rural households in Chirumhanzu district, Zimbabwe. Jàmbá J. Disaster Risk Stud. 11, 1–9. https://doi.org/10.4102/jamba.v11i1.777

Grosch, R., Zachow, C., Berg, G., 2018. Tomato Seeds Preferably Transmit Plant Bene fi cial Endophytes 2, 183–193. https://doi.org/10.1094/PBIOMES-06-18-0029-R

Guclu-Ustundag, Ö., Mazza, G., 2007. Saponins: Properties, applications and processing. Crit.

Rev. Food Sci. Nutr. 47, 231–258. https://doi.org/10.1080/10408390600698197

Hall, J.B., O'Brien, E.M., Sinclar, F.. ., 2002. Sclerocarya birrea: a monograph 157.

Hao, D., Xiao, P., 2020. Pharmaceutical resource discovery from traditional medicinal plants: Pharmacophylogeny and pharmacophylogenomics. Chinese Herb. Med. https://doi.org/10.1016/j.chmed.2020.03.002

Hardoim, P.R., 2019. Endophytes and Secondary Metabolites 3–31. https://doi.org/10.1007/978-3-319-76900-4

Hardoim, P.R., van Overbeek, L.S., Berg, G., Pirttilä, A.M., Compant, S., Campisano, A., Döring, M., Sessitsch, A., 2015. The Hidden World within Plants: Ecological and Evolutionary Considerations for Defining Functioning of Microbial Endophytes. Microbiol. Mol. Biol. Rev. 79, 293–320. https://doi.org/10.1128/mmbr.00050-14

Harrison, J.G., Beltran, L.P., Buerkle, C.A., Cook, D., Gardner, D.R., Parchman, T.L., Forister, M.L., 2019. A suite of rare microbes interacts with a dominant, heritable, fungal endophyte to influence plant trait expression. bioRxiv 608729. https://doi.org/10.1101/608729

Hernández Bautista, R.J., Mahmoud, A.M., Königsberg, M., López Díaz Guerrero, N.E., 2019. Obesity: Pathophysiology, monosodium glutamate-induced model and anti-obesity medicinal plants. Biomed. Pharmacother. 111, 503–516. https://doi.org/10.1016/j.biopha.2018.12.108

Hinterdobler, W., Schinnerl, J., 2019. Chemical diversity and richness of fungal endophytes from Costa Rican Palicourea and Psychotria species (Rubiaceae). Acta Zoobot Austria.

Hudzicki, J., 2009. Kirby-Bauer Disk Diffusion Susceptibility Test Protocol 1–23.

Husain, F.M., 2013. IN VITRO INTERFERENCE OF BACTERIAL QUORUM SENSING

AND VIRULENCE FACTORS BY CERTAIN BIOACTIVE NATURAL PRODUCTS 202002.

Ibanez, F., Tonelli, M.L., Munoz, V., Figueredo, M.S., Fabra, A., 2017. Endophytes: Biology and Biotechnology. Endophytes Biol. Biotechnol. Sustain. Dev. Biodivers. 15, 25–41. https://doi.org/10.1007/978-3-319-66541-2

Isa, A.I., Awouafack, M.D., Dzoyem, J.P., Aliyu, M., Magaji, R.A.S., Ayo, J.O., Eloff, J.N., 2014. Some Strychnos spinosa (Loganiaceae) leaf extracts and fractions have good antimicrobial activities and low cytotoxicities. BMC Complement. Altern. Med. 14. https://doi.org/10.1186/1472-6882-14-456

Jamshidi-Kia, F., Lorigooini, Z., Amini-Khoei, H., 2018. Medicinal plants: Past history and future perspective. J. HerbMed Pharmacol. 7, 1–7. https://doi.org/10.15171/jhp.2018.01

Jiménez-Luna, J., Cuzzolin, A., Bolcato, G., Sturlese, M., Moro, S., 2020. A deep-learning approach toward rational molecular docking protocol selection. Molecules 25, 1–12. https://doi.org/10.3390/molecules25112487

Jiménez, A., García, P., De La Puente, S., Madrona, A., Camarasa, M.J., Pérez-Pérez, M.J., Quintela, J.C., García-del Portillo, F., San-Félix, A., 2018. A novel class of cationic and non-peptidic small molecules as hits for the development of antimicrobial agents. Molecules 23. https://doi.org/10.3390/molecules23071513

Jin, Z., Gao, L., Zhang, L., Liu, T., Yu, F., Zhang, Z., Guo, Q., Wang, B., 2017. Antimicrobial activity of saponins produced by two novel endophytic fungi from Panax notoginseng. Nat. Prod. Res. 31, 2700–2703. https://doi.org/10.1080/14786419.2017.1292265

Juboi, H., 2017. EVALUATION OF THE ANTIBIOTICS AND SECONDARY METABOLITES BIOSYNTHETIC POTENTIAL OF Plantactinospora sp . KBS50 , A

RARE MARINE-DERIVED ACTINOMYCETE Master of Science (Research).

K.G. Ramawat, 2008. Herbal Drugs: Ethnomedicine to Modern MedicinNo Title.

Kadiri, O., Olawoye, B., 2016. Vernonia amygdalina: An Underutilized Vegetable with Nutraceutical Potentials – A Review. Turkish J. Agric. - Food Sci. Technol. 4, 763. https://doi.org/10.24925/turjaf.v4i9.763-768.570

Kassim, A., Omuse, G., Premji, Z., Revathi, G., 2016. Comparison of Clinical Laboratory Standards Institute and European Committee on Antimicrobial Susceptibility Testing guidelines for the interpretation of antibiotic susceptibility at a University teaching hospital in Nairobi , Kenya : a cross - sectional . Ann. Clin. Microbiol. Antimicrob. 1–7. https://doi.org/10.1186/s12941-016-0135-3

Kaul, S., Gupta, S., Ahmed, M., Dhar, M.K., 2012. Endophytic fungi from medicinal plants: A treasure hunt for bioactive metabolites. Phytochem. Rev. 11, 487–505. https://doi.org/10.1007/s11101-012-9260-6

Kemal, J., Zerihun, T., Alemu, S., Sali, K., Nasir, M., Abraha, A., Feyera, T., 2020. In Vitro Acaricidal Activity of Selected Medicinal Plants Traditionally Used against Ticks in Eastern Ethiopia. J. Parasitol. Res. 2020. https://doi.org/10.1155/2020/7834026

Khan, Shahid Ullah, Anjum, S.I., Ansari, M.J., Khan, M.H.U., Kamal, S., Rahman, K., Shoaib, M., Man, S., Khan, A.J., Khan, Salim Ullah, Khan, D., 2019. Antimicrobial potentials of medicinal plant’s extract and their derived silver nanoparticles: A focus on honey bee pathogen. Saudi J. Biol. Sci. 26, 1815–1834. https://doi.org/10.1016/j.sjbs.2018.02.010

Kim, H., Mohanta, T.K., Park, Y.H., Park, S.C., Shanmugam, G., Park, J.S., Jeon, J., Bae, H., 2020. Complete genome sequence of the mountain-cultivated ginseng endophyte Burkholderia stabilis and its antimicrobial compounds against ginseng root rot disease.

Biol. Control 140, 104126. https://doi.org/10.1016/j.biocontrol.2019.104126

Kishimoto, S., Sato, M., Tsunematsu, Y., Watanabe, K., 2016. Evaluation of biosynthetic pathway and engineered biosynthesis of alkaloids. Molecules 21. https://doi.org/10.3390/molecules21081078

Kowalski, K.P., Kingsley, K.L., Butterworth, S., Elmore, M.T., Brindisi, L., White, J.F., 2018. 'Endobiome Interference ' as a Strategy to Curtail Aggressiveness in Invasive Plant Species Ultimate Goal is to Control Invasive Phragmites australis by Targeting its Growth Promotional Microbiome .

Kozubek, A., Zarnowski, R., Stasiuk, M., Gubernator, J., 2001. Natural amphiphilic phenols as bioactive compounds. Cell. Mol. Biol. Lett. 06, 351–355.

Kusari, S., Hertweck, C., Spiteller, M., 2012. Chemical ecology of endophytic fungi: Origins of secondary metabolites. Chem. Biol. 19, 792–798. https://doi.org/10.1016/j.chembiol.2012.06.004

Li, L.Y., Sun, B.D., Zhang, G.S., Deng, H., Wang, M.H., Tan, X.M., Zhang, X.Y., Jia, H.M., Zhang, H.W., Zhang, T., Zou, Z.M., Ding, G., 2018. Polyketides with different post-modifications from desert endophytic fungus Paraphoma sp. Nat. Prod. Res. 32, 939–943. https://doi.org/10.1080/14786419.2017.1371166

Ma, X.Y., Yang, F.X., Su, C., Yan, Y., Huang, S.X., 2019. A new 2,2′-dipyridine and its analogues from endophytic streptomyces sp. KIB H017c with potent cytotoxicity. Rec. Nat. Prod. 14, 98–104. https://doi.org/10.25135/rnp.147.19.05.1268

Madzibane, J., Potgieter, M.J., 1999. Uses of Colophospermum mopane (Leguminosae : Caesalpinioideae) by the Vhavenda. South African J. Bot. 65, 440–444. https://doi.org/10.1016/S0254-6299(15)31039-5

Mahizan, N.A., Yang, S.K., Moo, C.L., Song, A.A.L., Chong, C.M., Chong, C.W., Abushelaibi, A., Erin Lim, S.H., Lai, K.S., 2019. Terpene derivatives as a potential agent against antimicrobial resistance (AMR) pathogens. Molecules 24, 1–21. https://doi.org/10.3390/molecules24142631

Makhado, R.A., Potgieter, M.J., Policy, F., Resources, N., 2009. Colophospermum mopane Wood Utilisation in the Northeast of the Limpopo Province , South Africa.

Malfanova, N. V., 2013. Endophytic bacteria with Thesis_Malfanova.

Manganyi, M.C., Tchatchouang, C.D.K., Regnier, T., Bezuidenhout, C.C., Ateba, C.N., 2019. Bioactive Compound Produced by Endophytic Fungi Isolated From Pelargonium sidoides Against Selected Bacteria of Clinical Importance. Mycobiology 47, 335–339. https://doi.org/10.1080/12298093.2019.1631121

Mantravadi, P.K., Kalesh, K.A., Dobson, R.C.J., Hudson, A.O., Parthasarathy, A., 2019. The quest for novel antimicrobial compounds: Emerging trends in research, development, and technologies. Antibiotics 8, 1–34. https://doi.org/10.3390/antibiotics8010008

Maroyi, A., 2019. Review of ethnomedicinal, phytochemical and pharmacological properties of lannea schweinfurthii (Engl.) Engl. Molecules 24. https://doi.org/10.3390/molecules24040732

Maroyi, A., 2013. Traditional use of medicinal plants in south-central Zimbabwe: Review and perspectives. J. Ethnobiol. Ethnomed. 9. https://doi.org/10.1186/1746-4269-9-31

Martinuz, A., Schouten, A., Sikora, R.A., 2011. Systemically Induced Resistance and Microbial Competitive Exclusion : Implications on Biological Control.

Mashe, T., Gudza-Mugabe, M., Tarupiwa, A., Munemo, E., Mtapuri-Zinyowera, S., Smouse, S.L., Sooka, A., Stray-Pedersen, B., Smith, A.M., Mbanga, J., 2019. Laboratory

characterisation of Salmonella enterica serotype Typhi isolates from Zimbabwe, 2009-2017. BMC Infect. Dis. 19. https://doi.org/10.1186/s12879-019-4114-0

Mast, Y., Stegmann, E., 2019. Actinomycetes: The antibiotics producers. Antibiotics 8, 10–13. https://doi.org/10.3390/antibiotics8030105

Matar, G.M., Andremont, A., Bazzi, W., 2020. Editorial: Combating Antimicrobial Resistance - A One Health Approach. Front. Cell. Infect. Microbiol. 9, 10–13. https://doi.org/10.3389/fcimb.2019.00458

McLean, T.C., Wilkinson, B., Hutchings, M.I., Devine, R., 2019. Dissolution of the disparate: Co-ordinate regulation in antibiotic biosynthesis. Antibiotics 8. https://doi.org/10.3390/antibiotics8020083

Meade, E., Slattery, M.A., Garvey, M., 2020. Bacteriocins, potent antimicrobial peptides and the fight against multi drug resistant species: Resistance is futile? Antibiotics 9. https://doi.org/10.3390/antibiotics9010032

Mhondoro, M., Ndlovu, N., Bangure, D., Juru, T., Gombe, N.T., Shambira, G., Nsubuga, P., Tshimanga, M., 2019. Trends in antimicrobial resistance of bacterial pathogens in Harare, Zimbabwe, 2012-2017: A secondary dataset analysis. BMC Infect. Dis. 19, 1–9. https://doi.org/10.1186/s12879-019-4295-6

Microbiology, A.S., 2020. A Comparative Study on the Antioxidant Activity of Four Different Fungal Endophytes 3, 33–41.

Ministry of Health and Child Care, Ministry of Agriculture, Mechanisation and Irrigation, Ministry of Environment, Water, and Climate, 2017. Zimbabwe One Health Antimicrobial Resistance National Action Plan 2017-2021.

Mohamed, G.A., Ibrahim, S.R.M., Asfour, H.Z., 2020. Antimicrobial metabolites from the

endophytic fungus Aspergillus versicolor. Phytochem. Lett. 35, 152–155. https://doi.org/10.1016/j.phytol.2019.12.003

Mohotti, S., Rajendran, S., Muhammad, T., Strömstedt, A.A., Adhikari, A., Burman, R., de Silva, E.D., Göransson, U., Hettiarachchi, C.M., Gunasekera, S., 2020. Screening for bioactive secondary metabolites in Sri Lankan medicinal plants by microfractionation and targeted isolation of antimicrobial flavonoids from Derris scandens. J. Ethnopharmacol. 246, 112158. https://doi.org/10.1016/j.jep.2019.112158

Mudzengi, C.P., Murwira, A., Tivapasi, M., Murungweni, C., Burumu, J. V, Halimani, T., Mudzengi, C.P., Murwira, A., Tivapasi, M., Murungweni, C., 2017. Antibacterial activity of aqueous and methanol extracts of selected species used in livestock health management. Pharm. Biol. 0, 000. https://doi.org/10.1080/13880209.2017.1287744

Naama-amar, A., Gitman, S., Shoshana, N., Bahar, O., Naor, V., Zchori-fein, E., Iasur-kruh, L., 2020. Antimicrobial activity of metabolites secreted by the endophytic bacterium frateuria defendens. Plants 9, 1–13. https://doi.org/10.3390/plants9010072

Nan, Z.B., 2018. The Interaction Between Symbiosis and Pathogenic Fungi 2061–2073. https://doi.org/10.1094/PDIS-05-18-0762-FE

Nankaya, J., Gichuki, N., Lukhoba, C., Balslev, H., 2020. Medicinal plants of the Maasai of Kenya: A review. Plants 9, 1–17. https://doi.org/10.3390/plants9010044

Ndihokubwayo, J., Yahaya, A., Desta, A., Ki-Zerbo, G., Odei, E., Keita, B., Pana, A., Nkhoma, W., 2013. Antimicrobial resistance in the African Region: issues, challenges and actions proposed. WHO Press 16, 27–30.

Ngarivhume, T., Van'T Klooster, C.I.E.A., De Jong, J.T.V.M., Van Der Westhuizen, J.H., 2015. Medicinal plants used by traditional healers for the treatment of malaria in the

Chipinge district in Zimbabwe. J. Ethnopharmacol. 159, 224–237. https://doi.org/10.1016/j.jep.2014.11.011

Nguyen, H.T., Pokhrel, A.R., Nguyen, C.T., Pham, V.T.T., Dhakal, D., Lim, H.N., Jung, H.J., Kim, T.-S., Yamaguchi, T., Sohng, J.K., 2020. Streptomyces sp. VN1, a producer of diverse metabolites including non-natural furan-type anticancer compound. Sci. Rep. 10, 1756. https://doi.org/10.1038/s41598-020-58623-1

Nguyen, Q.H., Nguyen, H. Van, Vu, T.H.N., Chu-Ky, S., Vu, T.T., Hoang, H., Quach, N.T., Bui, T.L., Chu, H.H., Khieu, T.N., Sarter, S., Li, W.J., Phi, Q.T., 2019. Characterization of endophytic Streptomyces griseorubens MPT42 and assessment of antimicrobial synergistic interactions of its extract and essential oil from host plant Litsea cubeba. Antibiotics 8. https://doi.org/10.3390/antibiotics8040197

Nielsen, J.C., Nielsen, J., 2017. Development of fungal cell factories for the production of secondary metabolites: Linking genomics and metabolism. Synth. Syst. Biotechnol. 2, 5–12. https://doi.org/10.1016/j.synbio.2017.02.002

Nishiumi, S., Miyamoto, S., Kawabata, K., Ohnishi, K., Mukai, R., Murakami, A., Ashida, H., Terao, J., 2011. Dietary flavonoids as cancer-preventive and therapeutic biofactors. Front. Biosci. - Sch. 3 S, 1332–1362. https://doi.org/10.2741/s229

Nitcheu Ngemakwe, P.H., Remize, F., Thaoge, M.L., Sivakumar, D., 2017. Phytochemical and nutritional properties of underutilised fruits in the southern African region. South African J. Bot. 113, 137–149. https://doi.org/10.1016/j.sajb.2017.08.006

Noor, A., Gunasekaran, S., Vijayalakshmi, M.A., 2018. Article in Pharmacognosy Research · October 2017. Pharmacognosy Res. 10, 24–30. https://doi.org/10.4103/pr.pr

Nuankeaw, K., Chaiyosang, B., Suebrasri, T., Kanokmedhakul, S., Lumyong, S., Boonlue, S.,

2020. First report of secondary metabolites, Violaceol I and Violaceol II produced by endophytic fungus, Trichoderma polyalthiae and their antimicrobial activity. Mycoscience 61, 16–21. https://doi.org/10.1016/j.myc.2019.10.001

Obasa, K., White, F.F., Pathology, P., 2017. A Dimorphic and Virulence-Enhancing Endosymbiont Bacterium Discovered in Rhizoctonia solani 14–23.

Ojewole, J.A.O., 2004. Evaluation of the analgesic, anti-inflammatory and anti-diabetic properties of Sclerocarya birrea (A. Rich.) Hochst. stem-bark aqueous extract in mice and rats. Phyther. Res. 18, 601–608. https://doi.org/10.1002/ptr.1503

Ojewole, J.A.O., Mawoza, T., Chiwororo, W.D.H., Owira, P.M.O., 2010. Sclerocarya birrea (A. Rich) Hochst. ['Marula'] (Anacardiaceae): A review of its phytochemistry, pharmacology and toxicology and its ethnomedicinal uses. Phyther. Res. 24, 633–639. https://doi.org/10.1002/ptr.3080

Olakunle Ajiboye, T., 2011. In vivo antioxidant potentials of Piliostigma thonningii (Schum) leaves: Studies on hepatic marker enzyme, antioxidant system, drug detoxifying enzyme and lipid peroxidation. Hum. Exp. Toxicol. 30, 55–62. https://doi.org/10.1177/0960327110366785

Packer, J., Turpin, G., Ens, E., Venkataya, B., Hunter, J., 2019. Building partnerships for linking biomedical science with traditional knowledge of customary medicines: A case study with two Australian Indigenous communities. J. Ethnobiol. Ethnomed. 15, 1–11. https://doi.org/10.1186/s13002-019-0348-6

Palanichamy, P., Krishnamoorthy, G., Kannan, S., Marudhamuthu, M., 2018. Bioactive potential of secondary metabolites derived from medicinal plant endophytes. Egypt. J. Basic Appl. Sci. 5, 303–312. https://doi.org/10.1016/j.ejbas.2018.07.002

Paniculata, A., 2015. ACTIVITY SPECTRA OF EXTRACT OF PHOMOPSIS SP . ISOLATED FROM World Journal of Pharmaceutical Research.

Pansanit, A., Pripdeevech, P., 2018. Antibacterial secondary metabolites from an endophytic fungus, Arthrinium sp. MFLUCC16-1053 isolated from Zingiber cassumunar. Mycology 9, 264–272. https://doi.org/10.1080/21501203.2018.1481154

Pavithra, N., Sathish, L., Ananda, K., 2014. Antimicrobial and Enzyme Activity of Endophytic Fungi Isolated from Tulsi Antimicrobial and Enzyme Activity of Endophytic Fungi Isolated from Tulsi Abstract : Introduction : Isolation of endophytic fungi.

Pelo, S., Mavumengwana, V., Green, E., 2020. Diversity and Antimicrobial Activity of Culturable Fungal Endophytes in Solanum mauritianum. Int. J. Environ. Res. Public Health 17. https://doi.org/10.3390/ijerph17020439

Photolo, M.M., Mavumengwana, V., Sitole, L., Tlou, M.G., 2020. Antimicrobial and Antioxidant Properties of a Bacterial Endophyte , Methylobacterium radiotolerans MAMP 4754 , Isolated from Combretum erythrophyllum Seeds 2020.

Porras-alfaro, A., Bayman, P., 2011. Hidden Fungi , Emergent Properties : Endophytes and Microbiomes. https://doi.org/10.1146/annurev-phyto-080508-081831

Praptiwi, Fathoni, A., Ilyas, M., 2020. Diversity of endophytic fungi from Vernonia amygdalina, their phenolic and flavonoid contents and bioactivities. Biodiversitas 21, 436–441. https://doi.org/10.13057/biodiv/d210202

Primrose, S.B., Twyman, R.M., 2006. Principles of Gene Manipulation and Genomics, Gene. https://doi.org/10.1136/jmg.19.5.397-a

Rajesh, P., Kannan, V., Latha, S., Selvamani, P., 2011. Phytochemical and pharmacological profile of plants belonging to Strychnos genus: a review. Carbon N. Y. 250, 4.

Rasooly, R., Molnar, A., Choi, H., Do, P., Racicot, K., 2019. In-Vitro Inhibition of Staphylococcal Pathogenesis by Witch-Hazel and Green Tea Extracts 1–13. https://doi.org/10.3390/antibiotics8040244

Robertsen, H.L., Musiol-Kroll, E.M., 2019. Actinomycete-derived polyketides as a source of antibiotics and lead structures for the development of new antimicrobial drugs. Antibiotics 8. https://doi.org/10.3390/antibiotics8040157

Rosenblueth, M., Martínez-romero, E., 2006. Bacterial Endophytes and Their Interactions with Hosts 19, 827–837.

Saeed, A., Ahsan, F., Nawaz, M., Iqbal, K., Rehman, K.U., Ijaz, T., 2020. Incidence of vancomycin resistant phenotype of the methicillin resistant staphylococcus aureus isolated from a tertiary care hospital in Lahore. Antibiotics 9. https://doi.org/10.3390/antibiotics9010003

Sanchez, S., Demain, A.L., 2011. Secondary Metabolites. Compr. Biotechnol. Second Ed. 1, 155–167. https://doi.org/10.1016/B978-0-08-088504-9.00018-0

Sessitsch, A., Hardoim, P., Döring, J., Weilharter, A., Krause, A., Woyke, T., Mitter, B., Friedrich, F., Rahalkar, M., Hurek, T., Sarkar, A., Bodrossy, L., Overbeek, L. Van, Brar, D., Elsas, J.D. Van, 2012. Functional Characteristics of an Endophyte Community Colonizing Rice Roots as Revealed by Metagenomic Analysis 25, 28–36.

Shaaban, M., Nasr, H., Hassan, A.Z., Asker, M.S., 2013. Bioactive secondary metabolites from endophytic aspergillus fumigatus: Structural elucidation and bioactivity studies. Rev. Latinoam. Quim. 41, 50–60.

Shang, X.-F., Morris-Natschke, S.L., Yang, G.-Z., Liu, Y.-Q., Guo, X., Xu, X.-S.X., Goto, M., Li, J.-C., Lee, K.-H., 2018. Biologically Active Quinoline and Quinazoline Alkaloids Part

II. Med Res Rev 38, 1614–1660. https://doi.org/10.1002/med.21492

Shoko, T., 2018. Traditional Herbal Medicine and Healing in Zimbabwe. J. Tradit. Med. Clin. Naturop. 07, 7–9. https://doi.org/10.4172/2573-4555.1000254

Sibanda, E., Mabandla, M.V., 2018. Antioxidant activity of fungal endophytes isolated from Kigelia africana, Annona senegalensis and Vitex payos. https://doi.org/10.13140/RG.2.2.25592.96008

Simhadri, N., Muniappan, M., Kannan, I., Viswanathan, S., 2017. Phytochemical analysis and docking study of compounds present in a polyherbal preparation used in the treatment of dermatophytosis. Curr. Med. Mycol. 3, 6–14. https://doi.org/10.29252/cmm.3.4.6

Singh, N., Shreshtha, A.K., Thakur, M.S., Patra, S., 2018. Xanthine scaffold: scope and potential in drug development. Heliyon 4, e00829. https://doi.org/10.1016/j.heliyon.2018.e00829

Singh, S., 2015. PHYTOCHEMICAL AND MOLECULAR DOCKING ANALYSES OF PROSOPIS JULIFLORA DERIVED PHYTOCHEMICALS AGAINST ANTI-APOPTOTIC PROTEIN BCL-2. World J. Pharm. Res. 4.

Spengler, G., 2019. The Role of Drug Repurposing in the Development of Novel Antimicrobial Drugs : Non-Antibiotic Pharmacological Agents as Quorum Sensing-Inhibitors.

Supuran, C.T., 2011. Bacterial carbonic anhydrases as drug targets: Toward novel antibiotics? Front. Pharmacol. JUL, 1–6. https://doi.org/10.3389/fphar.2011.00034

Takarova, T., 2018. Determination of Antimicrobial Properties and Characterisation of Endophytes from Eight Indiginous trees in Zimbabwe. Univ. Zimbabwe.

Tan, S., Moore, G., Nodwell, J., 2019. Put a bow on it: Knotted antibiotics take center stage. Antibiotics 8. https://doi.org/10.3390/antibiotics8030117

Taganna, J. C., Quanico, J. P., Perono, R. M. G., Amor, E. C., Rivera, W. L., 2011. Tannin-rich fraction from Terminalia catappa inhibits quorum sensing (QS) in Chromobacterium violaceum and the QS-controlled biofilm maturation and LasA staphylolytic activity in Pseudomonas aeruginosa. Journal of Ethnopharmacology 134, 865–871.

Tijjani, M.A., 2018. Phytochemistry, isolationsand some pharmacological studies of ethanol leaf extract of piliostigma thonningii 1 10, 20–62.

Tkacz, A., Poole, P., 2015. Role of root microbiota in plant productivity 66, 2167–2175. https://doi.org/10.1093/jxb/erv157

Torres, C., Sturla, M., Romero, A., Judis, M., 2019. Bioguided isolation of antimicrobial polyphenols from Cuspidaria convoluta leaves and their synergistic effect with antibiotics. Asian Pac. J. Trop. Biomed. 9, 434–442. https://doi.org/10.4103/2221-1691.269525

Traoré, L., Yaro, V.S.O., Soudré, A., Ouédraogo-Koné, S., Ouédraogo, D., Yougbaré, B., Zoma, B.L., Hien, M., Guissou, M.L., Traoré, A., Mészáros, G., Wurzinger, M., Burger, P., Okeyo, A.M., Thiombiano, A., Sölkner, J., 2020. Indigenous knowledge of veterinary medicinal plant use in cattle treatment in southwestern Burkina Faso (West Africa). South African J. Bot. 128, 189–199. https://doi.org/10.1016/j.sajb.2019.09.015

Troisi, J., Pulvento, C., National, I., Vega-galvez, A., 2015. Saponins.

Turner, T.R., James, E.K., Poole, P.S., 2013. The plant microbiome. https://doi.org/10.1186/gb-2013-14-6-209

Uche-Okereafor, N., Sebola, T., Tapfuma, K., Mekuto, L., Green, E., Mavumengwana, V., 2019. Antibacterial activities of crude secondary metabolite extracts from pantoea species obtained from the stem of solanum mauritianum and their effects on two cancer cell lines. Int. J. Environ. Res. Public Health 16. https://doi.org/10.3390/ijerph16040602

Ullah, A., Prottoy, N.I., Araf, Y., Hossain, S., Sarkar, B., Saha, A., 2019. Molecular Docking and Pharmacological Property Analysis of Phytochemicals from <i>Clitoria ternatea</i> as Potent Inhibitors of Cell Cycle Checkpoint Proteins in the Cyclin/CDK Pathway in Cancer Cells. Comput. Mol. Biosci. 09, 81–94. https://doi.org/10.4236/cmb.2019.93007

UNICEF, 2019. Unicef technical Note on AMR.

Uzma, F., Konappa, N.M., Chowdappa, S., 2016. Diversity and extracellular enzyme activities of fungal endophytes isolated from medicinal plants of Western Ghats, Karnataka. Egypt. J. Basic Appl. Sci. 3, 335–342. https://doi.org/10.1016/j.ejbas.2016.08.007

Valgas, C., De Souza, S.M., Smânia, E.F.A., Smânia, A., 2007. Screening methods to determine antibacterial activity of natural products. Brazilian J. Microbiol. 38, 369–380. https://doi.org/10.1590/S1517-83822007000200034

Verma, V.C., Gange, A.C., 2014. Advances in Endophytic Research.

Vogel, C., Bai, Y., 2016. The Plant Microbiota : Systems-Level Insights and Perspectives. https://doi.org/10.1146/annurev-genet-120215-034952

Wang, F.W., Jiao, R.H., Cheng, A.B., Tan, S.H., Song, Y.C., 2007. Antimicrobial potentials of endophytic fungi residing in Quercus variabilis and brefeldin A obtained from Cladosporium sp. World J. Microbiol. Biotechnol. 23, 79–83. https://doi.org/10.1007/s11274-006-9195-4

Wang, S.S., Liu, J.M., Sun, J., Sun, Y.F., Liu, J.N., Jia, N., Fan, B., Dai, X.F., 2019. Diversity of culture-independent bacteria and antimicrobial activity of culturable endophytic bacteria isolated from different Dendrobium stems. Sci. Rep. 9, 1–12. https://doi.org/10.1038/s41598-019-46863-9

Wang, T., Li, Q., Bi, K., 2018. Bioactive flavonoids in medicinal plants: Structure, activity and biological fate. Asian J. Pharm. Sci. 13, 12–23. https://doi.org/10.1016/j.ajps.2017.08.004

Wang, W., Arshad, M.I., Khurshid, M., Rasool, M.H., Nisar, M.A., Aslam, M.A., Qamar, M.U., 2018. Antibiotic resistance : a rundown of a global crisis. Infect. Drug Resist. 1645–1658.

Wang, Z.R., Yang, H.X., Peng, X.P., Li, G., Lou, H.X., 2020. Induced production of zinniol analogues by co-cultivation of two endophytic fungi in the same ecological niche. Phytochem. Lett. 35, 206–210. https://doi.org/10.1016/j.phytol.2019.12.007

Weng, A., Thakur, Melzig, Fuchs, 2011. Chemistry and pharmacology of saponins: special focus on cytotoxic properties. Bot. Targets Ther. 19. https://doi.org/10.2147/btat.s17261

White, James F, Brindisi, L., Verma, S.K., Yao, X., 2019. Seed Endophytes. Seed Endophytes. https://doi.org/10.1007/978-3-030-10504-4

White, James F., Kingsley, K.L., Zhang, Q., Verma, R., Obi, N., Dvinskikh, S., Elmore, M.T., Verma, S.K., Gond, S.K., Kowalski, K.P., 2019. Review: Endophytic microbes and their potential applications in crop management. Pest Manag. Sci. 75, 2558–2565. https://doi.org/10.1002/ps.5527

WHO, 2017. Global Antimicrobial Resistance Surveillance System (GLASS) Report, Who. https://doi.org/ISBN 978-92-4-151344-9

Wink, M., 2010. Functions and Biotechnology of Plant Secondary Metabolites., second edi. ed, Willey-Blackwell. wiley-blackwell, germany.

Wu, F., Yang, D., Zhang, L., Chen, Y., Hu, X., Li, L., Liang, J., 2019. Diversity estimation and antimicrobial activity of culturable endophytic fungi from Litsea cubeba (Lour.) Pers. in China. Forests 10, 1–12. https://doi.org/10.3390/f10010033.

Wu, H., Yang, H.Y., You, X.L., Li, Y.H., 2013. Diversity of endophytic fungi from roots of Panax ginseng and their saponin yield capacities. Springerplus 2, 1–9. https://doi.org/10.1186/2193-1801-2-107.

Yasser, M.M., Mousa, A.S.M., Marzouk Marym, A., Tagyan, A.I., 2019. Molecular Identification, Extracellular Enzyme Production and Antimicrobial Activity of Endophytic Fungi Isolated from Solanum tuberosum L. in Egypt. Biosci. Biotechnol. Res. Asia 16, 135–142. https://doi.org/10.13005/bbra/2731.

Yuan, Z., Tian, Y., He, F., Zhou, H., 2019. Endophytes from Ginkgo biloba and their secondary metabolites. Chinese Med. (United Kingdom) 14. https://doi.org/10.1186/s13020-019-0271-8.

Zaferanloo, B., 2014. Endophytes from Australian native plants as novel sources of bioactive compounds for industrial , environmental and medicinal applications Bita Zaferanloo.

Zeng, Y., He, X., Jiang, W., Kou, J., Yu, B., 2020. Ten Representative Saponins on Tissue Factor Expression in Human Monocytes: Structure–Activity Relationships and Molecular Docking. Nat. Prod. Commun. 15, 1934578X2091368. https://doi.org/10.1177/1934578x20913684.

Zhang, T., Zhong, S., Li, T., Zhang, J., 2020. Saponins as modulators of nuclear receptors. Crit. Rev. Food Sci. Nutr. 60, 94–107. https://doi.org/10.1080/10408398.2018.1514580

Zin, N.M., Zakaria, N., Ismail, A., Ahmad, S.J., Mohd Sarmin, N.I., 2020. Genotypic and phenotypic characterization of endophytic microbispora SUK 14 from Labisia pumila. Res. J. Biotechnol. 15, 136–143.

Zipfel, P.F., Wiech, T., Rudnick, R., Afonso, S., Person, F., Skerka, C., 2019. Complement inhibitors in clinical trials for glomerular diseases. Front. Immunol. 10.

https://doi.org/10.3389/fimmu.2019.02166.

Zomorodian, K., Saeidi, D., Fani, D., Tazarvi, F., Hajinezhad, M.R., Hashemi, S.A., Amani, A.M., Mousavi, S.M., 2019. Investigation the antioxidant, antibacterial and insecticidal activities of cuscuta epithymum and pyrethrum roseum plants using polydimethylsiloxane (CAR/PDMS). J. Environ. Treat. Tech. 7, 234–244.

Zouaoui, N., Chenchouni, H., Bouguerra, A., Massouras, T., Barkat, M., 2020. Characterization of volatile organic compounds from six aromatic and medicinal plant species growing wild in North African drylands. NFS J. 18, 19–28. https://doi.org/10.1016/j.nfs.2019.12.001.

Appendices

Appendix I: Constituents of endophytic sample 17 GC-MS of endophytes.

Sample Name: Sample 17
Sample Type: Endophytic acetone extracts
AcqMethodFile: Endophyte screen method
AcqMethodPath D:\MassHunter\GCMS
Instrument: EMA GCMS Dilution:1

RT	Compound Name	Area	Match	CAS#	Formula
3.179	1,4-Dioxane-2,6-dione	1141023	92.9	4480-83-5	C4H4O4
3.302	Osmium, [methyl 2-(1,1-dimethylethyl)-4,5-dihyd	505718	89.1	116842-31-0	C19H25N3O7Os
3.820	2,3-Butanediol	15175681	95.0	513-85-9	C4H10O2
3.536	Tetramethyl silicate	422053	93.8	681-84-5	C4H12O4Si
3.984	2,3-Butanediol, [R-(R*,R*)]-	43737272	96.3	24347-58-8	C4H10O2
4.129	acetic acid, 2- methyl-propyl ester	6067825	93.6	110-19-0	C6H12O2
3.582	(1S,2R,4S)-N-[2'-(N',N'-Dimethylamino)ethyl]-2-h	931465	93.9	2000527-65-3	C14H28N2O3S
4.497	2-methyl pyrazine	2177404	89.0	109-08-0	C5H6N2
4.501	Pyridine, 2,3,4,5-tetrahydro-	8307594	92.4	505-18-0	C5H9N
4.808	2-Pentanone, 4-methoxy-	1287739	89.7	13122-52-6	C6H12O2
6.178	1-Butylpyrrolidine	4018499	95.1	767-10-2	C8H17N
4.337	1-Phenyl-4,4-ethylenedioxy-3-pentanone	868339	90.8	2000259-88-7	C13H16O3
8.490	Trisulfide, dimethyl	3163117	97.6	3658-80-8	C2H6S3
12.495	Benzeneethanamine	47450016	94.0	64-04-0	C8H11N
4.581	(1S,5S,7R)-(3-(2-Fluoroethyl)-6,8-dioxa-3-azabicy	78710	90.0	2000171-90-9	C8H14FNO3
6.796	Pyrazine, 2,5-dimethyl-	3737710	95.9	123-32-0	C6H8N2
9.236	Decane	10355884	89.1	124-18-5	C10H22
4.848	3-Methylamino-3-cyclobuten-1,2-dione	1207262	89.2	2000018-04-7	C5H5NO2
9.543	Pyrazine, trimethyl-	7963515	97.2	14667-55-1	C7H10N2

RT	Compound Name	Area	Match	CAS#	Formula
7.419	3-Buten-1-amine, N,N,2,3-tetramethyl-	3617317	94.0	65149-80-6	C8H17N
4.932	N-trimethylammonio-2-hydroxypropanamidate	195393	91.8	0-00-0	C6H4N2O2
5.103	1H-Pyrrole, 2-methyl-	248880	92.3	636-41-9	C5H7N
18.582	2H-Pyrrol-2-one, 1,5-dihydro-4-methoxy-	14623773	89.1	69778-83-2	C5H7NO2
11.994	Pyrazine, 5-ethyl-2,3-dimethyl-	3262309	90.1	15707-34-3	C8H12N2
19.659	Tetradecane	36638241	97.2	629-59-4	C14H30
6.996	2,3-dihydroxypyrazine	306019	92.8	2000018-44-1	C4H4N2O2
10.450	Butanedioic acid, dimethyl ester	2543009	97.9	106-65-0	C6H10O4
7.373	3,4-Dimethyl-1H-pyrrole	389952	92.8	822-51-5	C6H9N
10.570	L-Proline, ethyl ester	2978365	91.8	5817-26-5	C7H13NO2
14.955	Dodecane	8472056	98.0	112-40-3	C12H26
7.727	L-Valine, methyl ester	487549	92.0	4070-48-8	C6H13NO2
16.364	Benzene, 1,3-bis(1,1-dimethylethyl)-	3027710	95.8	1014-60-4	C14H22
16.934	Hexadecane	1428403	91.1	544-76-3	C16H34
27.426	Octadecane	61655978	97.7	593-45-3	C18H38
12.210	1-(Ethoxycarbonyl)-2-(1'-deuteriooctylidene)cyclo	18723010	92.4	2000409-33-2	C16H25DO3
12.341	(3',5'-Dimethyl-1'-prop-2'-ynyl)-1H-pyrazole	281750	91.7	2000044-23-2	C8H10N2
9.189	18-Norpregna-4,8,11,13-tetraen-3-one, 20,21-dih	214121	93.2	71379-35-6	C21H26O3
9.257	(E)-5,5-Difluoro-4-hydroxy-3-methyl-2-dodecen-6	2271336	93.8	2000349-88-8	C13H22F2O2
29.906	3-ISOBUTYLHEXAHYDROPYRROLO[1,2-A]PYRAZI	35826317	89.3	5654-86-4	C11H18N2O2
10.027	1-(1'-pyrrolidinyl)-2-butanone	7224268	91.3	2000056-30-4	C8H15NO
10.097	1-Hexanol, 2-ethyl-	129514	94.5	104-76-7	C8H18O
10.439	16-Methoxy-1-trimethylsilyloxy-8,9-secofusicocca-	1519861	95.7	2000741-24-0	C24H42O2Si
23.616	3-Hexadecene, (Z)-	8936302	96.8	34303-81-6	C16H32
16.285	2-Isopentyl-3-methylpyrazine	350706	89.6	0-00-0	C10H16N2
23.757	Hexadecane	62750709	98.7	544-76-3	C16H34
11.147	N-Pentylpyrrole	450344	89.2	2000049-64-6	C9H15N
38.008	Pyrrolo[1,2-a]pyrazine-1,4-dione, hexahydro-3-(p	25903492	93.4	14705-60-3	C14H16N2O2
38.577	Deferoxamine	45056717	95.8	70-51-9	C25H48N6O8

RT	Compound Name	Area	Match	CAS#	Formula
17.835	2-(3-Methylbutyl)-3,5-dimethylpyrazine	2413519	93.6	111150-30-2	C11H18N2
11.755	Disulfide, dipentyl	35214418	89.2	112-51-6	C10H22S2
39.315	Pyrrolo[1,2-a]pyrazine-1,4-dione, hexahydro-3-(p	40832556	94.3	14705-60-3	C14H16N2O2
27.130	Pyrrolo[1,2-a]pyrazine-1,4-dione, hexahydro-	54196660	92.9	19179-12-5	C7H10N2O2
27.307	9-Octadecene, (E)-	9949395	94.3	7206-25-9	C18H36
11.872	5.alpha.[16,16.-2H2]-Androst-2-en-17.beta.-ol	2243435	92.4	0-00-0	C19H27D2O4S
19.437	(+)-Sedridine [2-(2-hydroxypropyl)piperdine]	11582663	98.2	2000059-96-7	C8H17NO
12.592	Hexanoyl(tert-butyldimethyl)silane	773592	92.0	2000242-11-1	C12H26OSi
13.140	2-(Nitromethyl)piperidine	352943	89.3	2000060-75-3	C6H12N2O2
30.752	Eicosane	37785278	98.4	112-95-8	C20H42
21.696	(+-)-(5S,9S)-5,9-Dimethylpentadecane	633655	89.0	2000327-27-7	C17H36
21.766	pentadecane	2903231	92.1	629-62-9	C15H32
14.007	5-Acetylthio-6,7-dihydro-2(3H)-oxepinone	826189	97.3	2000158-41-1	C8H10O3S
32.112	1-Hexadecanol	2858784	94.6	36653-82-4	C16H34O
22.845	2-(1H-Imidazol-2-yl)acetic acid	3644570	91.5	2000032-64-8	C5H6N2O2
22.967	(1S,2R,4S)-N-[2'-(Morpholin-4-yl)ethyl]-2-hydroxy	13281098	89.7	2000645-11-8	C16H30N2O4S
23.485	2-Ethylhexyl 3-Methyl-4,7-dioxo-4,7-dihydrobenzo	8010516	92.4	2000614-88-6	C18H22O4S
34.103	1-Docosene	4127152	95.5	1599-67-3	C22H44
34.218	Docosane	18298132	93.3	629-97-0	C22H46
16.542	Undecane, 4,7-dimethyl-	739523	90.3	17301-32-5	C13H28
25.635	Heptacosane	1559004	90.5	593-49-7	C27H56
17.161	1-Octyne	638799	93.2	629-05-0	C8H14
39.771	Tetracosane	5612817	92.9	646-31-1	C24H50
17.675	(1R,2R)-2,4,4-trimethyl-5-methylene-1-cyclohexa	279293	95.6	2000082-56-5	C10H18O
17.775	(E)-O-1-(Caprolactam-N-yl)ethyl-4-methylbenzald	76416	92.5	2000435-33-7	C16H22N2O2
18.225	Ethyl (2S,4S)-1-tert-Butoxycarbonyl-4-(dimethyla	5649373	92.1	2000557-67-7	C15H26N2O5
19.354	1-(3',4'-Methylenedioxyphenyl)-2-propaneamine	84738	90.3	2000140-36-1	C10H13NO2
29.124	Heptadecane	2188150	91.2	629-78-7	C17H36
19.695	Formamide, N-1-adamantyl-	133519	93.9	3405-48-9	C11H17NO
30.655	3-Octadecene, (E)-	7397657	96.2	7206-19-1	C18H36
21.166	Pyridine, 2-phenyl-	753269	91.3	1008-89-5	C11H9N

RT	Compound Name	Area	Match	CAS#	Formula
30.839	1-Propanone, 1-(1-methyl-4-phenyl-1H-pyrrol-3-y	709363	89.2	131940-03-9	C14H15NO
32.113	1-Octadecanol	2645054	94.9	112-92-5	C18H38O
22.634	Benzyl Acetate	934487	98.9	2000071-64-2	C9H10O2
22.644	6-Chloro-2-(1,1-dimethylethyl)indole	125589	91.5	2000220-44-9	C12H14ClN
22.808	2-Isoxazolidinepropanenitrile, 4-cyano-3-(1-meth	192263	90.1	89903-13-9	C10H15N3O
23.008	trans-2,3-Bis(iodomethyl)-1,4-dioxane	1009936	89.5	2000695-05-0	C6H10I2O2
23.009	(4-Fluorobenzoyl)(tert-butyl)dimethylsilane	1020732	94.5	0-00-0	C18H19FOSi
23.321	endo-2,3-di(methoxycarbonyl)-benzo[e]bicyclo[2.	135863	91.7	121917-11-1	C18H22O4
23.321	2,3,3a,4,5,6-hexahydro-1H-benzo[de][1,6]naphth	135416	91.6	105400-84-8	C11H14N2
23.566	Diethyl 2-(m-methoxybenzyl)malonate	290775	92.5	2000459-47-6	C15H22O5
23.642	1H-Pyrrolo[1,2-a]indole, 2,3-dihydro-	8090400	91.7	1421-19-8	C11H11N
23.881	3-(2'-Hydroxy-4'-methyl-3'-pentenyl)thia-2-cyclop	693020	90.2	2000246-30-3	C10H16O3S
23.997	Benzoic acid, 2-hydroxy-4-methoxy-6-[(2-propyl-1	369799	91.7	127743-32-2	C22H26O6
25.097	3-Amino-2,2,4-trimethylhexane	106840849	97.8	2000060-10-4	C9H21N
36.772	(+-)1-(4-Methylacridine-9-yl)-3-((tetrahydrofuran-	444975	89.2	2000658-15-5	C20H21N3OS
25.634	n-Cetyl thiocyanate	1070219	93.9	2000463-69-1	C17H33NS
25.763	Isopropyl N-benzoylaziridine-2-carboxylate	67306	91.8	2000301-95-4	C13H15NO3
25.843	5-(t-Butyl)-4-methyltthiophen-2(5H)-one	2265486	92.5	2000117-97-8	C9H14OS
26.321	1-butyloctylbenzene	90867	92.9	2000345-69-3	C18H30
26.394	1-Propanol, 3-(p-hydroxyphenyl)-	101914	90.4	10210-17-0	C9H12O2
27.305	(1RS,7RS)-1,4,7,10-Tetramethyl-2,8-dioxatricyclo	1170081	90.6	2000260-99-2	C14H20O2
28.154	Undecane, 5-methyl-	270422	89.2	1632-70-8	C12H26
28.417	Hexadecane, 1-iodo-	1406523	89.4	544-77-4	C16H33I
28.487	Cyclo(L-Pro-L-Leu)	17529514	90.4	2000229-34-9	C11H18N2O2
28.710	1,2-Benzenedicarboxylic acid, dibutyl ester	839987	92.3	84-74-2	C16H22O4
29.992	6,7,8-Trihydroxybenzo[b]pyran-2(2H)-one	3262287	90.3	2000179-94-4	C9H6O5
30.267	1,2-Benzenedicarboxylic acid, butyl 2-methylprop	651509	92.7	17851-53-5	C16H22O4
30.368	1-Methyl-3-(methylthio)-5-(mesityloxy)-1,3-dihyd	71543	92.5	2000433-09-7	C11H14O4S2
30.599	3-exo-methyl- and 3-endo-methyl-cis-3,3a,4,5,6,6	2757645	98.0	77481-55-1	C8H10N2
30.750	3-Hydroxy-3-methylcyclopentanone	126078	89.3	2000021-11-0	C6H10O2
30.767	(4aRS,7RS,9aRS,9bRS)-octahydro-7-[(3RS,4RS)-t	655015	93.9	2000506-39-7	C14H19NO6

RT	Compound Name	Area	Match	CAS#	Formula
32.029	1,2-Dichloro-1,1-difluoro-2-nonen-4-one	188323	96.3	2000336-01-2	C9H12Cl2F2O
32.656	Diphenylmethyl (2E,4E,7R,12Z)-14-Hydroxy-3,5,7	148800	92.0	2000820-23-6	C30H38O3
33.195	trifluoroethyl phenylacetate	1522249	98.7	2000252-03-6	C10H9F3O2
33.880	3-Benzoyl-5-cyclopropyl-4,5-dihydroisoxazole 2-o	686036	91.1	2000295-81-3	C13H13NO3
33.890	7-t-Butyl-3,4,5-trimethoxybicyclo[4.2.0]octa-1,3,5	250817	93.7	2000408-53-0	C15H22O4
34.221	cis-3,5-[di(t-Butyl)silanedioxy]cyclopent-1-ene	342824	89.7	2000325-10-7	C13H24O2Si
34.437	N-Benzyl-N-allyl-N-phenylidenehydroxyamine	1210050	90.8	0-00-0	C16H23NO
35.249	4-Phenyl-5-hexen-1-ol	787155	91.7	2000134-13-3	C12H16O
35.382	(S)-1-[.alpha.-(N-Methyl-N-phenylamino)benzyl]-2	456918	91.1	0-00-0	C25H23NO
35.781	1H-Pyrazole-4-carboxamide, 1-methyl-3-(methyla	965033	95.0	78416-38-3	C6H10N4O
35.782	1-Benzylidene-2,4-cyclopentadiene	1039781	93.9	2000083-61-4	C12H10
37.214	1-(6'-Methoxy-7'-methyl-1',2',3',4'-tetrahydronap	41541	91.0	2000260-49-9	C14H20O2
37.526	(2E,7E)-2,7-Nondienyl 1,9-bis(2,2,4,4-tetramethy	46936	89.6	2000838-16-4	C25H42N2O6
37.676	Cyclohexanone, 2-acetyl-2-(3-ethoxy-2-propenyl)-	659655	91.0	87698-12-2	C13H20O3
37.676	2-Acetoxyethyl trimethyl acetate	669312	91.7	2000164-01-3	C9H16O4
37.811	o-(N,N-Diacylamino)neopentanophenone	151065	90.1	2000392-45-3	C15H19NO3
39.584	(E)-1-Bromotridec-1-ene	777955	89.1	2000388-45-3	C13H25Br

Appendix II: Constituents of endophytic sample 9.

SampleName:	sample 9
Sample Type:	Endophytic acetone extracts
AcqMethodFile	Endophyte screen method
AcqMethodPath	D:\MassHunter\GCMS\1\methods\
Acq Time	7/8/20 2:48 PM
Operator	P.CHAGONDA

RT	Compound Name	Area	Match	CAS#	Formula
3.351	Carbamic acid, methyl ester	1406535	96.2	598-55-0	C2H5NO2
3.502	Methyl (2R,3S)-3-hydroxy-2-methylbutanoate	911181	93.9	2000041-70-2	C6H12O3
4.672	Pyridine, 2,3,4,5-tetrahydro-	12567496	95.8	505-18-0	C5H9N
3.596	Ethane, 1-methoxy-1-[[(methylsulfonyl)methyl]th	97471	90.7	74705-14-9	C5H12O3S2
3.797	2-oxo-propanoic acid, methyl ester	2221679	92.8	600-22-6	C4H6O3
3.932	Furan, 2-methoxy-	292181	90.9	25414-22-6	C5H6O2
11.993	2-Pyrrolidinone	23239473	96.3	616-45-5	C4H7NO
6.811	Pyrazine, 2,5-dimethyl-	727632	96.1	123-32-0	C6H8N2
4.053	Benzoic acid, 2,4-dimethoxy-6-propyl-, 4-carboxy	848194	95.4	104307-58-6	C24H30O7
4.132	Acetic acid, butyl ester	1847567	95.2	123-86-4	C6H12O2
8.480	Trisulfide, dimethyl	1172613	94.2	3658-80-8	C2H6S3
4.807	anti-3,5-Diethyl-1-hepten-4-ol	146591	90.3	2000119-97-5	C11H22O
9.230	Heptane, 3,4-dimethyl-	24366239	91.6	922-28-1	C9H20
4.927	1-acetoxy-4-ethoxybutan-2-one	137232	90.7	114250-53-2	C8H14O4
5.088	1H-Pyrrole, 2-methyl-	80551	90.0	636-41-9	C5H7N
5.269	4'-Methylenespiro[cyclopropane-1,3'-tricyclo[5.2.1	1009791	91.5	2000125-37-4	C13H16
5.514	2-Pyridinecarboxylic acid, 5-methyl-	212989	94.8	4434-13-3	C7H7NO2
12.253	Undecane	12564597	93.2	1120-21-4	C11H24
14.952	Dodecane	7762175	98.9	112-40-3	C12H26
22.207	Phenol, 2,4-bis(1,1-dimethylethyl)-	4215172	93.0	96-76-4	C14H22O

RT	Compound Name	Area	Match	CAS#	Formula
6.896	2(3H)-Furanone, dihydro-	1432378	90.4	96-48-0	C4H6O2
15.959	1-BENZOFURAN-2(3H)-ONE	1103071	94.0	553-86-6	C8H6O2
16.362	Benzene, 1,3-bis(1,1-dimethylethyl)-	2778619	96.1	1014-60-4	C14H22
10.451	Butanedioic acid, dimethyl ester	1311164	98.9	106-65-0	C6H10O4
16.930	pentadecane	1578763	91.9	629-62-9	C15H32
8.072	Hexacosane	194558	89.9	630-01-3	C26H54
27.053	Pyrrolo[1,2-a]pyrazine-1,4-dione, hexahydro-	54239803	90.4	19179-12-5	C7H10N2O2
19.654	Tetradecane	25937460	99.1	629-59-4	C14H30
9.230	2-Butanone, 1,1-dichloro-3,3-dimethyl-	14379473	93.0	22591-21-5	C6H10Cl2O
9.303	1-(4-Amino-3-hexyloxyphenyl)ethanone	66948	89.3	2000308-81-6	C14H21NO2
9.445	Dimethyl 4-[(4'-nitrophenyl)ethynyl]pyridine-2,6-d	527065	90.7	2000629-71-5	C17H12N2O6
9.493	1-(4-Methoxybenzyloxy)-2-allylbenzene	182605	93.1	2000371-45-7	C17H18O2
23.553	Cyclopropane, 1-ethenyl-2-(fluoromethyl)-, cis-	3292839	95.3	107557-15-3	C6H9F
23.751	Hexadecane	31709817	96.3	544-76-3	C16H34
10.515	(RS)-3,4-Dihydro-4-isopropyl-2-pyridone	1470753	89.5	2000052-74-2	C8H13NO
37.958	Pyrrolo[1,2-a]pyrazine-1,4-dione, hexahydro-3-(p	29606934	91.7	14705-60-3	C14H16N2O2
39.276	Pyrrolo[1,2-a]pyrazine-1,4-dione, hexahydro-3-(p	10305524	93.2	14705-60-3	C14H16N2O2
11.196	Undecane, 5-methyl-	811835	91.4	1632-70-8	C12H26
27.303	1-Dodecene	3674243	90.2	112-41-4	C12H24
18.006	Dodecane	572394	90.0	112-40-3	C12H26
27.419	Octadecane	23153653	97.6	593-45-3	C18H38
11.762	5-(2-Bromotetrafluoroethyl)-5-hydroxy-3-methyl-	626529	91.4	2000449-07-8	C6H6BrF4NO2
12.015	(3R*,5S*,6R*)-3-Isopropyl-6-methyl-6-phenyl-5-(	322625	91.0	2000596-36-8	C20H25NO3
21.173	Pyridine, 3-phenyl-	392366	89.0	1008-88-4	C11H9N
13.326	Propanenitrile, 2,2-dimethyl-	1112730	94.6	630-18-2	C5H9N
30.649	1-Docosene	2456566	90.8	1599-67-3	C22H44
30.746	Eicosane	11339346	98.2	112-95-8	C20H42
22.306	(S)-(-)-2-Acetylaminopropan-1-ol	12848727	93.8	2000024-91-2	C5H11NO2
14.469	2,4,6-Cycloheptatriene-1-carboxylic acid, ethyl es	1639820	93.9	27332-37-2	C10H12O2
34.094	1-Docosene	2023181	92.6	1599-67-3	C22H44

RT	Compound Name	Area	Match	CAS#	Formula
24.851	2,4(1H,3H)-Pyrimidinedione	17200797	92.9	66-22-8	C4H4N2O2
25.018	Cyclohexanone-4,4-d2, 2,2-dimethyl-	1264874	91.3	79640-11-2	C8H12D2O
16.059	Hexadecane	214475	92.8	544-76-3	C16H34
16.538	Undecane, 4,4-dimethyl-	577463	92.0	17312-68-4	C13H28
17.132	Hexadecane, 7,9-dimethyl-	452418	90.8	21164-95-4	C18H38
26.702	2-[1'-(Diisopropylaminoethyl)cyclopentyl]cyclopen	3025630	93.8	2000451-05-2	C18H33NO
17.262	Pentadecane	208310	96.7	629-62-9	C15H32
17.399	Octadecane	838374	96.0	593-45-3	C18H38
18.006	Tricosane	548585	94.4	638-67-5	C23H48
18.221	syn-7,9-Dimethylhexadecane	148522	94.5	2000371-94-8	C18H38
19.343	cis-1-((E)-3-Carbethoxy-2-propenyl)-2-(1-cyanopr	578833	95.2	2000353-83-9	C15H23NO2
29.587	Cyclo(L-Pro-L-Leu)	4676638	89.3	2000229-34-9	C11H18N2O2
29.767	prolylleucyl anhydride	2088779	89.4	2000229-35-2	C11H18N2O2
20.130	Hexadecane	211527	91.0	544-76-3	C16H34
29.980	5H,10H-Dipyrrolo[1,2-a:1',2'-d]pyrazine-5,10-dion	100936317	93.2	19943-27-2	C10H14N2O2
20.602	1-[1-(Bromomethyl)-2-(2,2,2-trichloroethyl)cyclop	401920	92.8	2000781-56-9	C13H16BrCl3N2O2
30.649	pentadecene	2309487	92.3	27251-68-9	C15H30
20.895	Undecane	533112	97.1	1120-21-4	C11H24
21.174	N-But-3-enyl-N-butylformamide	258581	90.7	2000084-65-2	C9H17NO
32.105	1-Octadecanol	520580	89.3	112-92-5	C18H38O
32.650	(1S,1'S,2R,2'R,4S,4'S,5R,5'R) 4,4'-Bis[2-phenyl-3,	1004680	89.9	2000767-59-9	C24H22O6
34.095	1-tridecanol	1365110	92.4	112-70-9	C13H28O
34.209	Eicosane	5065765	92.5	112-95-8	C20H42
24.434	Tridecane	113974	89.3	629-50-5	C13H28
25.144	Cyclopropanemethanamine, .alpha.-(1,1-dimethyl	1036504	91.1	99113-50-5	C12H25N
25.273	Aminoacetonitrile	750524	93.6	540-61-4	C2H4N2
25.632	Neopentyl 2-oxobutanoate	678506	92.8	2000123-55-1	C9H16O3
25.752	4,4-Difluoro-3-hydroxy-2,2-dimethyl-5-undecanon	1069753	93.1	2000356-39-1	C13H24F2O2
25.769	1-Decyn-4-ol	953084	89.4	27907-00-2	C10H18O

RT	Compound Name	Area	Match	CAS#	Formula
26.431	2-Acetyl-4-ethyl-2H-1,4-thiazin-3(4H)-one	184005	93.9	2000156-80-4	C8H11NO2S
27.170	trans-3-Chloro-1-cyclohexyl-4-phenylazetidin-2-on	316466	89.8	2000398-79-8	C15H18ClNO
27.184	Bicyclo[3.2.2]non-6-en-2-one, 1-methoxy-	908125	91.8	53922-08-0	C10H14O2
27.425	4-Hexen-1-ol, 4-methyl-	3226367	89.7	59518-07-9	C7H14O
28.481	1-[(1E,3R)-3,4,4-Trimethyl-1-pentenyl]cyclohexan	208930	93.1	2000183-45-7	C14H26
28.519	(R)-N-Butyl-.alpha.-methylsuccinimide	161371	91.1	2000116-08-4	C9H15NO2
28.702	1,2-Benzenedicarboxylic acid, butyl 2-methylprop	877623	89.2	17851-53-5	C16H22O4
28.760	2-Ethyl-1-(4'-methoxyphenyl)-3-buten-1-ol	235762	94.0	2000217-76-4	C13H18O2
29.120	Undecane	321031	93.7	1120-21-4	C11H24
29.873	anti-O,O'-dibenzene	1802333	89.3	2000087-97-8	C12H12
29.915	4-(5-Phenyl-1H-3-pyrazolyl)benzonitrile	46337	89.4	2000341-31-6	C16H11N3
30.070	(+)-Ethyl 4,6-dimethyl-3,6-dihydro-2H-pyran-2-ca	773544	96.1	2000154-22-1	C10H16O3
30.112	2-Piperidinecarboxylic acid, 1-methyl-, methyl est	709760	89.5	1690-74-0	C8H15NO2
30.513	4-(2-Nitrophenyl)but-3-en-2-ol	320758	97.2	2000177-79-2	C10H11NO3
31.146	2H-Pyrrol-2-one, 3-acetyl-1,5-dihydro-4-hydroxy-	137299	93.4	128892-52-4	C9H13NO3
31.186	1H-Pyrazole-4-carboxamide, 1-methyl-3-(methyla	2517234	95.7	78416-38-3	C6H10N4O
33.009	Pentadecane	407624	89.0	629-62-9	C15H32
34.145	l,l-4a,5,6,7,8,8a-hexahydro-4-phenyl-8a-[(trimeth	533560	96.1	99437-96-4	C17H25NO3Si
36.854	(-)-6(S)-Phenyl-5,6-dihydro-2H-pyran-2-one	126493	89.5	2000128-72-5	C11H10O2
40.333	1-Allyl-3-(2-(2-methoxybenzylidene)hydrazinyl)qu	11461	89.6	2000615-19-6	C19H18N4O2

Appendix III: Constituents of endophytic sample 3.

SampleName:	Sample3
SampleType:	Endophytic acetone extracts
AcqMethodFile:	Endophyte screen method
AcqMethodPath	: D:\MassHunter\GCMS
Instrument: EMA GCMS	Dilution:1

RT	Compound Name	Area	Match	CAS#	Formula
4.574	Pyridine, 2,3,4,5-tetrahydro-	2816845	91.8	505-18-0	C5H9N
3.932	3-Penten-2-one, 4-methyl-	5432275	89.4	141-79-7	C6H10O
3.937	Urea, hydroxy-	2912957	94.6	127-07-1	CH4N2O2
4.131	Acetic acid, butyl ester	2320099	92.5	123-86-4	C6H12O2
4.326	N-ETHYLPYRROLIDINE	6467814	94.2	2000010-65-1	C6H13N
3.873	(2E)-1-O-Acetyl-3,7-dimethyl-6,7-dihydroxy-2-oct	1020069	92.1	2000292-57-5	C12H22O4
3.938	Acetonitrile-d3	1802292	90.4	2206-26-0	C2D3N
4.330	2H-1,2-Oxazine, 3,6-dihydro-3-methyl-	4233244	96.0	107468-64-4	C5H9NO
4.574	4,4-Dimethylhepta-1,6-diene	1853363	92.3	2000031-68-4	C9H16
11.933	2-Pyrrolidinone	13403793	96.7	616-45-5	C4H7NO
8.485	Trisulfide, dimethyl	10217502	98.6	3658-80-8	C2H6S3
4.806	2-Pentanone, 4-methoxy-	792995	92.9	13122-52-6	C6H12O2
12.806	Benzeneethanamine	82788841	92.4	64-04-0	C8H11N
9.234	Decane	12747878	94.6	124-18-5	C10H22
16.363	Benzene, 1,3-bis(1,1-dimethylethyl)-	3228361	94.7	1014-60-4	C14H22
5.509	2-Pyridinecarboxylic acid, 5-methyl-	141988	94.6	4434-13-3	C7H7NO2
18.156	Ornithine	42794565	92.0	70-26-8	C5H12N2O2
6.034	Ethanone, 1-(2-nitrophenyl)-	163052	93.9	577-59-3	C8H7NO3
12.254	Undecane	9940777	97.1	1120-21-4	C11H24
20.181	5-(4-Fluorophenyl)tetrazole	232115610	89.0	2000101-56-6	C7H5FN4
9.551	Pyrazine, trimethyl-	1779305	94.4	14667-55-1	C7H10N2
6.806	Pyrazine, 2,5-dimethyl-	511418	89.3	123-32-0	C6H8N2

RT	Compound Name	Area	Match	CAS#	Formula
15.032	2-Piperidinone	344080639	96.1	675-20-7	C5H9NO
6.894	2(3H)-Furanone, dihydro-	984887	92.2	96-48-0	C4H6O2
10.453	Butanedioic acid, dimethyl ester	1450946	96.0	106-65-0	C6H10O4
22.446	Formamide, (2-acetylphenyl)-	6306388	91.1	2000100-40-0	C9H9NO2
22.657	Carbon dioxide	383890554	89.7	124-38-9	CO2
7.443	Pyridine, 3,5-dimethyl-	1328636	92.7	591-22-0	C7H9N
8.284	1,2,3-tri(t-Butyl)cyclopropenylium tribromide	839828	89.8	142634-81-9	C15H27Br3
26.021	4a,8b-trans-9-methylperhydro-4,5,8a,9a-tetraazaf	47147574	93.9	122872-64-4	C10H20N4
20.188	1,2,4-Trioxolane, 3-(4-chlorophenyl)-5-(4-methox	182601739	92.7	107245-94-3	C15H13ClO4
20.241	Tricyclo[4.4.1.1(2,5)]dodeca-3,7,9-triene, (1.alph	1379679	93.6	76024-05-0	C12H14
27.142	Pyrrolo[1,2-a]pyrazine-1,4-dione, hexahydro-	24726626	91.5	19179-12-5	C7H10N2O2
8.870	2,3-Dihydro-2-phenyl-4-quinolone	280824	90.5	2000271-66-8	C15H13NO
15.002	1-chloro-4-ethoxybutan-2-one	2256889	96.8	57429-13-7	C6H11ClO2
15.505	(4R*,5R*,6R*)-1,7-dioxaspiro[5.5]undecan-4,5-di	1925867	89.8	2000163-81-3	C9H16O4
10.648	2-(Prop-2'-enyl)pyrrolidine	3834943	94.0	2000018-29-2	C7H13N
16.931	Nonadecane	1058432	90.3	629-92-5	C19H40
10.905	5,5-Dideuteriomethoxycyclohexane	1547306	93.2	2000021-95-7	C7H12D2O
34.210	Eicosane	9266646	94.7	112-95-8	C20H42
17.601	o-Ethynylaniline	3625247	92.6	2000025-07-9	C8H7N
17.621	5-Acetyl-2-methylpyridine	1948607	91.2	42972-46-3	C8H9NO
27.173	Tryptophol	5615238	89.7	526-55-6	C10H11NO
11.788	Pyrazine, 2-ethyl-3,5-dimethyl-	565042	94.9	13925-07-0	C8H12N2
18.573	4-methylquinazoline	638189	90.5	2000062-33-1	C9H8N2
27.421	Octadecane	29809138	97.7	593-45-3	C18H38
37.994	Pyrrolo[1,2-a]pyrazine-1,4-dione, hexahydro-3-(p	25966162	91.4	14705-60-3	C14H16N2O2
38.555	Deferoxamine	27525861	96.2	70-51-9	C25H48N6O8
39.318	Pyrrolo[1,2-a]pyrazine-1,4-dione, hexahydro-3-(p	54890235	94.5	14705-60-3	C14H16N2O2
19.655	Tetradecane	27482361	91.8	629-59-4	C14H30
12.252	4-Hexen-3-ol, 2,2-dichloro-1,1,1-trifluoro-5-methy	3258064	91.5	103654-93-9	C7H9Cl2F3O

RT	Compound Name	Area	Match	CAS#	Formula
20.066	1-(3,5-Dibenzyloxyphenyl)hexane-1,3,5-trione	70909519	97.3	2000782-92-5	C26H24O5
20.066	2-Pentenal, 5-phenyl-	70887569	95.3	33046-84-3	C11H12O
12.826	2-Deuterio-N-[2-(deuteriomethyl)hexyl)benzylami	11062708	91.5	2000214-68-7	C14H21D2N
21.174	Pyridine, 2-phenyl-	461769	90.0	1008-89-5	C11H9N
21.360	Benzeneethanol, 4-hydroxy-	10275421	90.5	501-94-0	C8H10O2
30.746	Eicosane	18428905	98.2	112-95-8	C20H42
22.059	2-Fluorobenzoic acid, 4-nitrophenyl ester	1623491	89.2	2000391-57-8	C13H8FNO4
22.205	5-Isopropyl-4-(trifluoromethyl)-1H-pyrimidin-2-on	1999267	90.0	2000215-21-3	C8H9F3N2O
13.924	Butanoic acid, 4-amino-2-methyl-	608757	89.6	42453-21-4	C5H11NO2
23.613	1-Tridecene	2581556	89.8	2437-56-1	C13H26
14.484	Phenylacetic acid - methyl ester	783125	94.1	2000071-36-1	C9H10O2
23.753	Hexadecane	27948387	98.7	544-76-3	C16H34
34.095	1-Nonadecene	1960233	95.5	18435-45-5	C19H38
24.690	1,3,3-Trimethylazetidine-2,4-dione	46331672	96.1	74255-30-4	C6H9NO2
26.398	(3-Nitro-4-methylphenyl)ammonium hydrogenesu	30736151	93.1	2000075-12-9	C7H8N2O2
16.329	3-Pentanone, 2,2-dichloro-4-methyl-	688576	92.9	66250-08-6	C6H10Cl2O
26.418	anti-2-Methyl-1-phenyl-3-buten-1-ol	81780808	95.5	2000098-89-3	C11H14O
26.811	5-Ethyl-5-cyclohexylcarbamoylimidazole-2,4-dione	5054052	93.2	2000366-39-3	C12H19N3O3
16.931	Pentadecane	878488	94.4	629-62-9	C15H32
17.131	Octadecane	303841	95.8	593-45-3	C18H38
17.399	1-Methylbutyl nitrite	479287	90.1	0-00-0	C5H11NO2
17.918	.alpha.-Cyclopentyl-4-methoxyacetophenone	145241	89.2	2000254-44-9	C14H18O2
28.706	3-[4'-(t-Butyl)phenyl]furan-2,5-dione	813676	90.3	2000293-44-2	C14H14O3
28.875	1,2,4-Trihydroxy-6-n-pentylbenzene	448047	89.8	2000187-49-5	C11H16O3
18.186	4-Penten-1-ol, 4-ethyl-	3834212	95.0	59518-08-0	C7H14O
29.106	1H-Purine-2,6-dione, 3,7-dihydro-7-[(4-hydroxy-3	1006278	91.8	92014-27-2	C14H13N5O5
19.655	PENTADECANE	22945563	95.5	629-62-9	C15H32
30.649	1-Hexadecanol	3278777	96.0	36653-82-4	C16H34O
20.000	3-Methyl-5-phenyl-2(5H)-furanone	79073	93.8	2000128-71-6	C11H10O2
20.132	Undecane	242889	93.3	1120-21-4	C11H24

RT	Compound Name	Area	Match	CAS#	Formula
20.163	3,4-Dihydroxybenzaldehyde	2363936	92.9	2000050-12-4	C7H6O3
20.980	Tetradecane	343993	89.9	2000195-31-3	C14H30
21.241	2-Octanone	1155622	90.3	111-13-7	C8H16O
32.528	N-[(4'-Hydroxyphenyl)ethyl)]tetradeca-5,8,11-trie	6441905	91.4	2000633-99-6	C22H31NO2
21.693	(3R,13R)-3,13-Dimethylheptadecane	635770	91.7	2000417-21-8	C19H40
32.659	(1S)-6-O-acetyl-1,5-anhydro-3,4-dideoxy-1-(1,2-p	1045319	90.4	2000229-01-9	C11H14O4
21.763	Neopentyl 2-oxobutanoate	1006593	90.4	2000123-55-1	C9H16O3
22.197	methyl-(3R)-(-)-3-ethyl-5-oxopentanoate	1194460	91.4	107985-93-3	C8H14O3
22.204	(+)-(E)-(R)-N,N-Di-tert-butoxycarbonyl-1,3-diphe	586329	91.2	2000771-82-5	C25H31NO4
33.833	(S)-O-Benzyl-N,N-dibenzylserine - benzylester	2018283	92.2	2000837-60-6	C31H31NO3
22.931	3-[N-(Ethoxycarbonyl)amino]-3-(1-acetoxyethyl)-t	847338	98.1	2000385-06-3	C11H17NO6
23.078	cis-3-fluoro-6,6-dimethlbicyclo[3.1.0]hexan-2-one	2919830	90.9	130549-02-9	C8H11FO
25.385	3H-furazano[3,4-d]pyrimidine-5,7-quinone	2345330	90.4	135396-33-7	C4H2N4O3
25.833	Nonadecane	1023420	93.5	629-92-5	C19H40
39.757	Pentatriacontane	2784673	91.9	630-07-9	C35H72
40.705	2-(6-Amino-9H-purin-9-yl)-6-O-[(1,1-dimethyl)eth	264674	90.5	2000685-71-1	C17H29N5O2Si
26.716	6-Hydroxy-endo-tricyclo[5.2.1.0(2,6)]dec-8-en-3-	659907	95.9	2000102-95-0	C10H12O2
26.883	1,4-Xylylene-1,4-phenylenediacetate	799618	90.4	2000895-06-5	C36H32O8
27.007	Bis(pentamethylcyclopentadienyl)titaniumnitrogen	113050	96.7	0-00-0	C20H32NTi
27.990	(1S,2S)-N-Methyl-1-methoxy-1-phenylprop-2-ylam	126979	92.6	2000140-68-4	C11H17NO
28.415	Hexadecane, 1-iodo-	577802	89.6	544-77-4	C16H33I
28.519	Isopropylpent-4-enylamine	1576378	89.0	20576-73-2	C8H17N
28.593	1,2-dimethyl-5-nitro-1H-imidazol-4-amine	1348898	93.0	2000084-99-4	C5H8N4O2
29.121	Hexadecane	830189	94.0	544-76-3	C16H34
29.165	Benzene, (1,6-dimethyl-1,3,5-heptatrienyl-3-d)-	973193	92.1	59193-35-0	C15H17D
29.374	Molokinenone	208869	91.0	2000655-87-6	C20H27ClO3
29.517	6-Benzyl-3-methoxypyridazine	192810	92.8	136489-62-8	C12H12N2O
29.518	2-Benzoyl-3-methylcyclopent-2-enone	179666	90.0	2000199-92-6	C13H12O2
29.979	Propane, 2,2-dimethyl-1-nitro-	639942	93.8	34715-98-5	C5H11NO2
30.261	(Z)-2-((2-Methylthio)styrylthio)aniline	441377	91.9	2000431-72-8	C15H15NS2

RT	Compound Name	Area	Match	CAS#	Formula
30.355	Methyl (E/Z)-3-Iodo-4-methoxybut-2-enoate	786666	96.0	2000374-37-1	C6H9IO3
30.740	1,2,3,3a,6,9-Hexaaza-cyclopenta[a]naphthalene	331234	89.7	2000122-34-6	C7H4N6
30.962	trans-9-Methylthioxanthene	48362	92.6	69381-65-3	C21H19NO2S2
31.050	(S)-(-)-N-Octyl-2-bromopropionamide	477951	94.4	2000397-92-2	C11H22BrNO
31.616	N,N,N',N'-Tetraisopropyl-1,2-dimethylethylenedia	1779735	90.5	2000377-97-0	C16H36N2
31.650	Octadecane	939640	89.5	593-45-3	C18H38
32.076	Dimethyl 3,3,4-trimethyl-1,4-pentadiene-1,2-dicar	70694	95.1	2000280-21-3	C12H18O4
32.334	Heptacosane	370852	91.9	593-49-7	C27H56
33.164	Alanine, N-carboxy-3-phenyl-, N-benzyl ester, L-	937519	92.6	1161-13-3	C17H17NO4
33.431	1-Piperidinecarboxylic acid, 2-methyl-6-(3-oxohep	318247	93.1	107539-57-1	C15H27NO3
33.825	(-)-2R,3R)-2,3-epoxy-1-(tert-butyldimethylsiloxy)-	1367676	97.4	117326-73-5	C24H34O3SSi
35.185	4-Hydroxy-3,5-bis([2H3]methoxy)cinnamyl alcoho	1000544	91.6	2000229-10-5	C11H8D6O4
35.779	N-But-3-enyl-N-butylformamide	942	90.4	2000084-65-2	C9H17NO
35.826	4-Butyl-2-(phenylsulfonyl)hept-3-en-5-one	211394	93.2	2000540-30-1	C17H24O3S
36.759	3-Methyl-N-(4-pyridyl)indole	482401	94.2	2000224-90-7	C14H12N2
36.762	endo 1-methyl 2-ethoxycarbonyl-3(Z)-ethylidene-	289263	91.7	130930-50-6	C12H16O3
38.230	3-Benzyl-2-[(4-hydroxybenzyl)amido]-5-(3-fluoro-	85542	91.1	2000800-19-4	C25H20FN3O3
38.546	1,4-Dihydroxy-2-[(2H3)methyl]-3-methylbenzene	1246792	92.1	2000050-43-4	C8H7D3O2
39.947	Dimethyl 1-(N-Trifluoroacetylamino)-2-phenylethy	34716	97.4	2000589-02-0	C12H15F3NO4P

Appendix IV: Constituents from GC-MS for endophytic sample 1.

SampleName:	Sample 1
SampleType:	Endophytic acetone extracts
AcqMethodFile:	Endophyte screen method
AcqMethodPath:	D:\MassHunter\GCMS
Acq Time	7/8/20 1:15 PM
Instrument: EMA GCMS	Dilution

RT	Compound Name	Area	Match	CAS#	Formula
3.349	Carbamic acid, methyl ester	601924	93.6	598-55-0	C2H5NO2
3.531	Tetramethyl silicate	514840	90.1	681-84-5	C4H12O4Si
4.487	Pyridine, 2,3,4,5-tetrahydro-	13208702	95.3	505-18-0	C5H9N
4.074	cis- and trans-2,2-Dimethyl-3-(2-methyl-1-propyl)	278405	92.0	78715-42-1	C11H23NO
8.484	Trisulfide, dimethyl	2010300	96.0	3658-80-8	C2H6S3
4.123	Acetic acid, butyl ester	4269600	93.5	123-86-4	C6H12O2
5.249	Benzene, ethyl-	2717715	92.1	100-41-4	C8H10
9.229	Decane	12253665	89.8	124-18-5	C10H22
9.545	Pyrazine, trimethyl-	3965517	96.3	14667-55-1	C7H10N2
12.538	Benzeneethanamine	72771092	95.3	64-04-0	C8H11N
10.444	Butanedioic acid, dimethyl ester	1413024	98.5	106-65-0	C6H10O4
6.168	1-(1'-pyrrolidinyl)-2-propanone	1159430	90.6	2000035-13-1	C7H13NO
4.879	Pyridine, 2,3,4,5-tetrahydro-	4420524	90.2	505-18-0	C5H9N
6.802	Pyrazine, 2,5-dimethyl-	1418344	90.2	123-32-0	C6H8N2
16.357	Benzene, 1,3-bis(1,1-dimethylethyl)-	2830660	94.8	1014-60-4	C14H22
7.351	3-Acetyl-1,3-dimethyltriazene	6116261	90.0	2000022-61-7	C4H9N3O
12.249	Undecane	7136161	93.8	1120-21-4	C11H24
18.562	2H-Pyrrol-2-one, 1,5-dihydro-4-methoxy-	23993745	92.7	69778-83-2	C5H7NO2
6.369	3-Cyclopropyl-2-butanone	201693	91.8	2000019-41-1	C7H12O
6.646	(-)-4-endo-Amino-2-oxabicyclo[3.3.0]oct-7-en-3-o	113556	89.9	2000052-44-7	C7H9NO2
14.948	Dodecane	8010158	96.2	112-40-3	C12H26

RT	Compound Name	Area	Match	CAS#	Formula
7.079	5-Hexen-2-amine, N-methyl-, (.+-.)-	1812668	90.2	113579-68-3	C7H15N
7.079	2-Hexanone	1894211	95.0	591-78-6	C6H12O
22.206	Phenol, 2,4-bis(1,1-dimethylethyl)-	3137654	90.3	96-76-4	C14H22O
9.668	Methyl 4-methyl-2-(2'-nitrophenyl)-5-oxo-5,7-dihy	450656	94.3	2000597-49-7	C16H12N2O6
7.364	3,4-Dimethyl-1H-pyrrole	176377	93.8	822-51-5	C6H9N
23.642	3-Methyl-4-phenyl-1H-pyrrole	3363901	89.6	2000089-07-0	C11H11N
7.723	L-Valine, methyl ester	767113	93.3	4070-48-8	C6H13NO2
10.528	L-Proline, ethyl ester	3217456	91.6	5817-26-5	C7H13NO2
8.063	2,2-Dimethoxy-5,5-di-n-propyl-1,3,4-.deta.(3)-ox	3676252	97.0	2000246-47-5	C10H20N2O3
8.083	1-Ammonium 3-aza-4-oxo-7-heptanoate	2348006	90.7	2000093-11-0	C6H12N2O3
27.111	Pyrrolo[1,2-a]pyrazine-1,4-dione, hexahydro-	59763297	90.5	19179-12-5	C7H10N2O2
19.652	Tetradecane	26615161	98.7	629-59-4	C14H30
11.769	Pyrazine, 2-ethyl-3,5-dimethyl-	983545	90.3	13925-07-0	C8H12N2
8.916	1-Phenyl-1,2,3,4-tetrahydro-.beta.-carboline	90664	91.9	2000351-98-4	C17H16N2
20.193	l-Phenylalanine, methyl ester	2007628	91.8	2577-90-4	C10H13NO2
9.228	4-Heptanone, 2,6-dimethyl-	9758968	91.7	108-83-8	C9H18O
29.616	Pyrrolo[1,2-a]pyrazine-1,4-dione, hexahydro-3-(2	42489553	89.3	5654-86-4	C11H18N2O2
9.493	1-((6-Formyl-2-pyridyl)methyl)hexahydro-1,4-diaz	272601	91.9	2000301-66-0	C12H15N3O2
21.878	.alpha.-(Methoxycarbonyl)-1,3-dioxolan-2-ylidene	13275059	90.5	2000163-20-4	C7H8O6
23.607	1-TETRADECENE	7163804	93.1	1120-36-1	C14H28
23.749	Hexadecane	34766126	98.5	544-76-3	C16H34
10.794	(E)-5,9-Dimethyl-2-nitrodeca-4,8-dienyl acetate	270072	91.1	2000418-28-3	C14H23NO4
10.944	5,5-Dideuteriomethoxycyclohexane	3727070	95.2	2000021-95-7	C7H12D2O
10.978	O-Acetyl-N-2-butenylhydroxylamine	1082341	89.8	2000037-92-4	C6H11NO2
16.927	pentadecane	1405852	91.8	629-62-9	C15H32
37.987	Pyrrolo[1,2-a]pyrazine-1,4-dione, hexahydro-3-(p	21563698	93.6	14705-60-3	C14H16N2O2
17.602	o-Ethynylaniline	1896771	92.7	2000025-07-9	C8H7N
38.565	Deferoxamine	58029161	96.3	70-51-9	C25H48N6O8
39.312	Pyrrolo[1,2-a]pyrazine-1,4-dione, hexahydro-3-(p	42807186	93.5	14705-60-3	C14H16N2O2
27.417	Octadecane	27115339	97.2	593-45-3	C18H38

RT	Compound Name	Area	Match	CAS#	Formula
17.829	2-(3-Methylbutyl)-3,5-dimethylpyrazine	682044	92.7	111150-30-2	C11H18N2
11.738	2-Pyrrolidinone	6948445	96.5	616-45-5	C4H7NO
29.980	5H,10H-Dipyrrolo[1,2-a:1',2'-d]pyrazine-5,10-dion	32860588	89.4	19943-27-2	C10H14N2O2
30.645	1-Nonadecene	2987669	95.2	18435-45-5	C19H38
30.742	Eicosane	15791511	98.1	112-95-8	C20H42
34.203	Triacontane	10663813	89.7	638-68-6	C30H62
25.411	2,4(1H,3H)-Pyrimidinedione	78591534	90.9	66-22-8	C4H4N2O2
16.058	Hexadecane	240400	94.1	544-76-3	C16H34
25.774	4-Fluoro-2-nicotinoylbenzoic acid	2791939	89.4	2000340-35-1	C13H8FNO3
25.808	5-(t-Butyl)-4-methyltthiophen-2(5H)-one	1807598	99.5	2000117-97-8	C9H14OS
25.921	Methyl 2-methyl-3-[N-(phenethylamino)]propiona	335785	92.6	2000263-84-7	C13H19NO2
26.292	5-(t-Butyl)-2(5H)-thiophenone	7139592	89.1	17171-84-5	C8H12OS
26.739	2,5,5-Trimethyl-[2-13C]-1-pyrroline-N-oxide	6717728	99.0	2000034-99-1	C7H13NO
26.786	2-Pentenal, (Z)-	15519970	94.6	1576-86-9	C5H8O
26.881	N,N-dibutyl-trifluoroacetamide	1763094	94.8	2000277-00-4	C10H18F3NO
17.351	1H-Pyrazole-4-carboxamide, 1-methyl-3-(methyla	68195	91.7	78416-38-3	C6H10N4O
17.394	Undecane, 4-methyl-	660364	90.2	2980-69-0	C12H26
27.512	4-Hexen-1-ol, 4-methyl-	4867236	98.2	59518-07-9	C7H14O
18.051	1-Diethylamino-2,5-dihydro-3,4-dimethyl-1-H-bor	50696	91.8	2000105-98-0	C10H20BN
28.702	1,2-Benzenedicarboxylic acid, bis(2-methylpropyl)	898674	90.2	84-69-5	C16H22O4
19.330	methyl 2,3,6-trideoxy-.alpha.-DL-threo-hex-2-enp	670280	90.6	58525-44-3	C7H12O3
19.656	1,2-Dicyano-4,5-bis(ethoxymethyl)benzene	405545	95.3	2000338-11-6	C14H16N2O2
30.258	1,2-benzene-dicarboxylic acid, 2-butoxy-2-oxoeth	789160	92.3	85-70-1	C18H24O6
19.937	1-Isopropylamino-4-hydroxy-4-methyl-1-penten-3	192700	90.0	2000121-42-0	C9H17NO2
20.389	2-cyclohexen-1-ol, 3-chloro-2-methyl-	242097	90.6	108035-76-3	C7H11ClO
31.010	Diethyl [2-(t-butyl)-5-methyl-4-oxohexyl]phospho	150307	93.6	2000533-83-6	C15H31O4P
20.499	[2-(1,2-dimethyl-3-oxocyclopentyl)ethyl]acetate	161201	90.7	124318-67-8	C11H18O3
31.110	Cyclohexanone, decamethyl-	1481113	90.4	92406-77-4	C16H30O
20.965	Sesquiterpene Lactone	84777	90.5	2000313-03-7	C15H24O2
20.975	Dodecane, 5,8-dimethyl-	585039	95.4	90600-89-8	C14H30

RT	Compound Name	Area	Match	CAS#	Formula
32.102	1-Octadecanol	756334	89.1	112-92-5	C18H38O
21.687	Undecane	746979	94.7	1120-21-4	C11H24
21.759	Undecane, 4-methyl-	1151876	94.5	2980-69-0	C12H26
21.878	5-Amino-2-methylhexan-2-ol	11628604	90.2	2000040-90-2	C7H17NO
22.111	1-Heptene, 5-methyl-	490520	98.2	13151-04-7	C8H16
22.638	1-(p-Nitrophenyl)-4-(ethylselanyl)but-2-en-1-ol	235091	89.9	2000518-67-4	C12H15NO3Se
22.898	7-Hydroxy-7-phenyl-3,9-diisopropyl-2,10-dioxadis	2704865	90.1	2000706-02-7	C22H28O5
34.091	9-Eicosene, (E)-	1366114	92.5	74685-29-3	C20H40
23.560	Ethanone, 1-(2,4-dimethyl-1H-pyrrol-3-yl)-	93695	93.5	2386-25-6	C8H11NO
24.012	1-Methoxy-3-[methoxy(trimethylsilyloxymethylen	52590	97.1	2000763-45-1	C17H36O5Si3
25.115	tert-Octyldiethylamine	785837	96.0	2000157-68-8	C12H27N
38.044	2,3,5-triacetoxy-8-hydroxy-1,4-naphthoquinone	428848	90.1	2000649-90-5	C16H12O9
25.629	Tetradecane	687741	94.3	629-59-4	C14H30
39.747	Eicosane	2192073	90.9	112-95-8	C20H42
26.229	(1R,2S)-2-(N,N-Dimethylamino)-1-phenylpropyl p	13062631	95.9	2000251-07-2	C14H19NO
26.669	2-Pyrrolidinepropanoic acid, (S)-	3731581	98.1	63328-10-9	C7H13NO2
26.679	2-(1-Fluorovinyl)-5-nitropyridine	3272623	95.4	2000111-72-6	C7H5FN2O2
27.307	2-Pentenal, (Z)-	198609	90.4	1576-86-9	C5H8O
27.411	1-Aza-5-(2-oxopropyl)bicyclo[4.4.0]decane-4,10-d	498324	93.2	2000270-94-5	C12H17NO3
28.413	2-Butanone, 4-(tetrahydro-2-furanyl)-	1528937	90.9	5059-25-6	C8H14O2
28.750	(2,3-Dihydroxyphenyl) Propyl Ketone	1027170	89.2	2000142-98-3	C10H12O3
29.079	6,8-Diethyl-5-allyl-indolizidine	886533	92.9	2000264-41-7	C15H27N
29.116	Pentadecane	638697	91.6	629-62-9	C15H32
29.455	1-[1-(Toluene-4-sulfonyl)-4,5-dihydro-1H-pyrrol-2	358460	92.1	2000487-91-3	C15H17NO3S
29.899	Cyclo(L-Leucyl-L-prolyl)	23293976	90.4	2000229-35-1	C11H18N2O2
29.903	5-Amino-8-chloronona-1,4-dien-3-one	2493828	90.8	141346-20-5	C9H14ClNO
30.081	2-Tetrazolin-5-one	1263875	90.8	16421-52-6	CH2N4O
30.173	2-(diphenylmethyl)-4,4,5,5-tetrafluoro-1,3,2-dithi	314444	91.5	119639-14-4	C15H11F4NS2
30.334	DEBROMO-WOODININE	515897	94.4	2000419-28-7	C17H23N3
30.447	Silane, trimethyl[1-(phenylsulfonyl)propyl]-	948818	90.2	91787-37-0	C12H20O2SSi

RT	Compound Name	Area	Match	CAS#	Formula
30.664	(E)-3-Iodo-3-undecenoic acid	76320	94.8	2000544-75-5	C11H19IO2
30.825	2-Butoxy-3-cyanomethylquinoline	524488	91.5	2000326-17-7	C15H16N2O
31.592	Pyridine-2,6-d2	259970	90.3	17265-96-2	C5H3D2N
32.329	trans-2,3-di(methoxycarbonyl)-3-methylbicyclo[2.	235697	91.2	117203-64-2	C13H18O4
32.566	Acenaphtho[1,2-c]furan	767407	89.2	2000176-94-6	C14H8O
33.181	5-exo-Phenylthio-4-(p-nitroanilino)furan-2(5H)-on	194928	91.1	2000597-48-0	C16H12N2O4S
33.785	(1RS,6RS,8SR)-2-Methyltricyclo[6.3.1.0(1,6)]dode	483240	90.7	2000306-04-5	C15H22O2
33.836	Spiro[cyclopropane-1,12'-pentacyclo[7.2.1.02,7.0	3100653	92.9	78365-80-7	C14H16
34.449	1-(Trifluoromethoxy)-2,4,6-trimethylbenzene	200829	91.9	2000209-20-0	C10H11F3O
35.588	(E)-4-Amino-5-(2-hydroxy-3,3-dimethyl-4-penteny	1718881	89.1	2000226-68-0	C11H15NO3

Appendix V: Dendrogram of nine endophytic bacterial isolates.

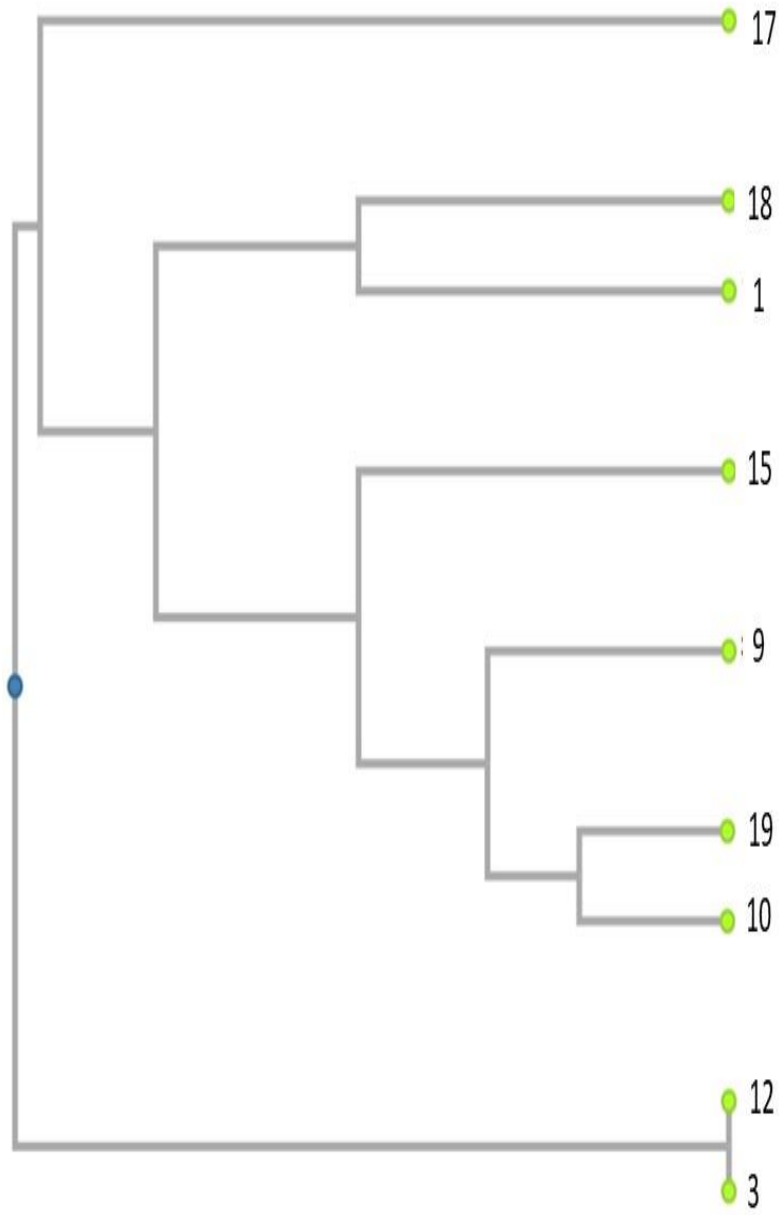

Appendix VI: Pharmacokinetic drug-likeness and medicinal chemistry properties of (+-)1-(4-Methylacridine-9-yl)-3-((tetrahydrofuran-2-yl)methyl)thiourea.

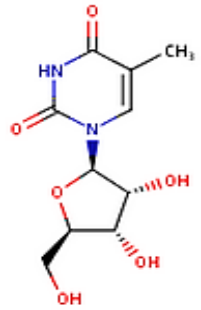

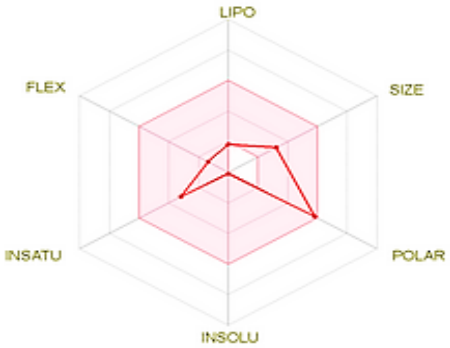

SMILES OC[C@H]1O[C@H]([C@@H]([C@@H]1O)O)n1cc(C)c(=O)[nH]c1=O

Physicochemical Properties	
Formula	C10H14N2O6
Molecular weight	258.23 g/mol
Num. heavy atoms	18
Num. arom. heavy atoms	6
Fraction Csp3	0.60
Num. rotatable bonds	2
Num. H-bond acceptors	6
Num. H-bond donors	4
Molar Refractivity	59.24
TPSA	124.78 Å²

Lipophilicity	
Log $P_{o/w}$ (iLOGP)	0.93
Log $P_{o/w}$ (XLOGP3)	-2.33
Log $P_{o/w}$ (WLOGP)	-2.87
Log $P_{o/w}$ (MLOGP)	-1.94
Log $P_{o/w}$ (SILICOS-IT)	-0.93
Consensus Log $P_{o/w}$	-1.43

Water Solubility	
Log *S* (ESOL)	-0.09
Solubility	2.11e+02 mg/ml ; 8.17e-01 mol/l
Class	Very soluble
Log *S* (Ali)	0.25
Solubility	4.55e+02 mg/ml ; 1.76e+00 mol/l
Class	Highly soluble
Log *S* (SILICOS-IT)	0.36
Solubility	5.92e+02 mg/ml ; 2.29e+00 mol/l
Class	Soluble

Pharmacokinetics	
GI absorption	Low
BBB permeant	No
P-gp substrate	No
CYP1A2 inhibitor	No
CYP2C19 inhibitor	No
CYP2C9 inhibitor	No
CYP2D6 inhibitor	No
CYP3A4 inhibitor	No
Log K_p (skin permeation)	-9.53 cm/s

Druglikeness	
Lipinski	Yes; 0 violation
Ghose	No; 1 violation: WLOGP<-0.4
Veber	Yes
Egan	Yes
Muegge	No; 1 violation: XLOGP3<-2
Bioavailability Score	0.55

Medicinal Chemistry	
PAINS	0 alert
Brenk	0 alert
Leadlikeness	Yes
Synthetic accessibility	3.96

Appendix VII: Pharmacokinetic drug-likeness and medicinal chemistry properties of 3-Amino-2,2,4-trimethylhexane.

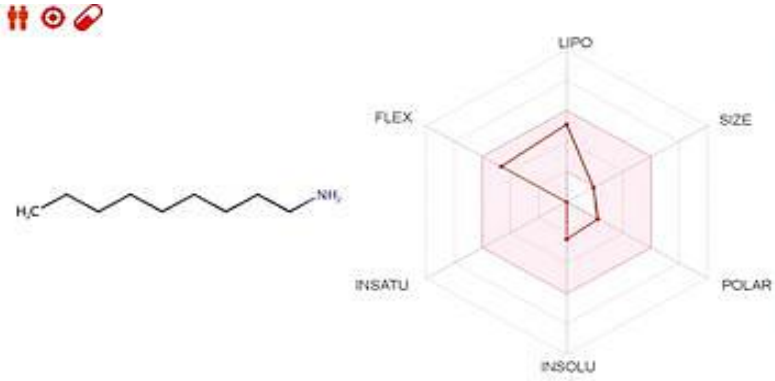

SMILES CCCCCCCCCN

Physicochemical Properties	
Formula	C9H21N
Molecular weight	143.27 g/mol
Num. heavy atoms	10
Num. arom. heavy atoms	0
Fraction Csp3	1.00
Num. rotatable bonds	7
Num. H-bond acceptors	1
Num. H-bond donors	1
Molar Refractivity	48.08
TPSA	26.02 Å²
Lipophilicity	
Log $P_{o/w}$ (iLOGP)	2.78
Log $P_{o/w}$ (XLOGP3)	3.44
Log $P_{o/w}$ (WLOGP)	2.70
Log $P_{o/w}$ (MLOGP)	2.54
Log $P_{o/w}$ (SILICOS-IT)	2.34
Consensus Log $P_{o/w}$	2.76

Water Solubility	
Log *S* (ESOL)	-2.43
Solubility	5.28e-01 mg/ml ; 3.69e-03 mol/l
Class	Soluble
Log *S* (Ali)	-3.67
Solubility	3.08e-02 mg/ml ; 2.15e-04 mol/l
Class	Soluble
Log *S* (SILICOS-IT)	-3.12
Solubility	1.08e-01 mg/ml ; 7.55e-04 mol/l
Class	Soluble
Pharmacokinetics	
GI absorption	High
BBB permeant	Yes
P-gp substrate	No
CYP1A2 inhibitor	No
CYP2C19 inhibitor	No
CYP2C9 inhibitor	No
CYP2D6 inhibitor	No
CYP3A4 inhibitor	No
Log K_p (skin permeation)	-4.73 cm/s
Druglikeness	
Lipinski	Yes; 0 violation
Ghose	No; 1 violation: MW<160
Veber	Yes
Egan	Yes
Muegge	No; 2 violations: MW<200, Heteroatoms<2
Bioavailability Score	0.55
Medicinal Chemistry	
PAINS	0 alert
Brenk	0 alert
Leadlikeness	No; 1 violation: MW<250
Synthetic accessibility	1.32

Appendix VIII: Pharmacokinetic drug-likeness and medicinal chemistry properties of 2-Piperidinone.

Molecule 1

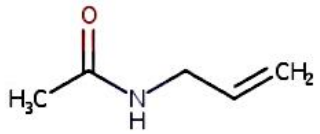

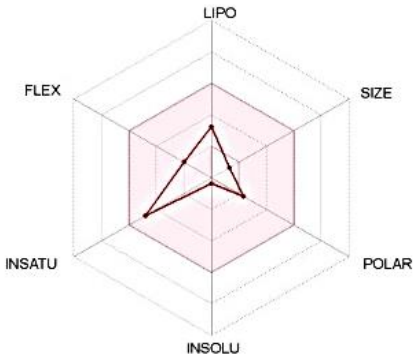

SMILES CC(=O)NCC=C

Physicochemical Properties	
Formula	C5H9NO
Molecular weight	99.13 g/mol
Num. heavy atoms	7
Num. arom. heavy atoms	0
Fraction Csp3	0.40
Num. rotatable bonds	3
Num. H-bond acceptors	1
Num. H-bond donors	1
Molar Refractivity	28.68
TPSA	29.10 Å²
Lipophilicity	
Log $P_{o/w}$ (iLOGP)	1.52
Log $P_{o/w}$ (XLOGP3)	0.18
Log $P_{o/w}$ (WLOGP)	0.31
Log $P_{o/w}$ (MLOGP)	0.38
Log $P_{o/w}$ (SILICOS-IT)	0.34
Consensus Log $P_{o/w}$	0.55

Water Solubility	
Log *S* (ESOL)	-0.37
Solubility	4.23e+01 mg/ml ; 4.27e-01 mol/l
Class	Very soluble
Log *S* (Ali)	-0.35
Solubility	4.44e+01 mg/ml ; 4.48e-01 mol/l
Class	Very soluble
Log *S* (SILICOS-IT)	-1.04
Solubility	9.08e+00 mg/ml ; 9.16e-02 mol/l
Class	Soluble
Pharmacokinetics	
GI absorption	High
BBB permeant	No
P-gp substrate	No
CYP1A2 inhibitor	No
CYP2C19 inhibitor	No
CYP2C9 inhibitor	No
CYP2D6 inhibitor	No
CYP3A4 inhibitor	No
Log K_p (skin permeation)	-6.78 cm/s
Druglikeness	
Lipinski	Yes; 0 violation
Ghose	No; 3 violations: MW<160, MR<40, #atoms<20
Veber	Yes
Egan	Yes
Muegge	No; 1 violation: MW<200
Bioavailability Score	0.55
Medicinal Chemistry	
PAINS	0 alert
Brenk	1 alert: isolated_alkene
Leadlikeness	No; 1 violation: MW<250
Synthetic accessibility	1.10

Appendix IX: Pharmacokinetic drug-likeness and medicinal chemistry properties of 2-(1H-Imidazol-2-yl)acetic acid.

Molecule 1

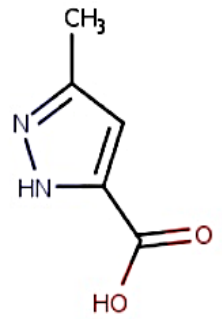

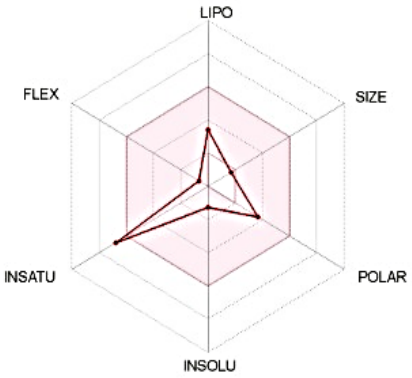

SMILES Cc1cc([nH]n1)C(=O)O

Physicochemical Properties	
Formula	C5H6N2O2
Molecular weight	126.11 g/mol
Num. heavy atoms	9
Num. arom. heavy atoms	5
Fraction Csp3	0.20
Num. rotatable bonds	1
Num. H-bond acceptors	3
Num. H-bond donors	2
Molar Refractivity	30.51
TPSA	65.98 Å²

Lipophilicity	
Log $P_{o/w}$ (iLOGP)	0.46
Log $P_{o/w}$ (XLOGP3)	0.48
Log $P_{o/w}$ (WLOGP)	0.42
Log $P_{o/w}$ (MLOGP)	-0.40
Log $P_{o/w}$ (SILICOS-IT)	0.78
Consensus Log $P_{o/w}$	0.35

Water Solubility	
Log *S* (ESOL)	-1.27
Solubility	6.78e+00 mg/ml ; 5.38e-02 mol/l
Class	Very soluble
Log *S* (Ali)	-1.43
Solubility	4.63e+00 mg/ml ; 3.67e-02 mol/l
Class	Very soluble
Log *S* (SILICOS-IT)	-0.95
Solubility	1.40e+01 mg/ml ; 1.11e-01 mol/l
Class	Soluble

Pharmacokinetics	
GI absorption	High
BBB permeant	No
P-gp substrate	No
CYP1A2 inhibitor	No
CYP2C19 inhibitor	No
CYP2C9 inhibitor	No
CYP2D6 inhibitor	No
CYP3A4 inhibitor	No
Log K_p (skin permeation)	-6.73 cm/s

Druglikeness	
Lipinski	Yes; 0 violation
Ghose	No; 3 violations: MW<160, MR<40, #atoms<20
Veber	Yes
Egan	Yes
Muegge	No; 1 violation: MW<200
Bioavailability Score	0.56

Medicinal Chemistry	
PAINS	0 alert
Brenk	0 alert
Leadlikeness	No; 1 violation: MW<250
Synthetic accessibility	1.53

Appendix X: Pharmacokinetic, drug-likeness and medicinal chemistry properties of octadecane.

Molecule 1

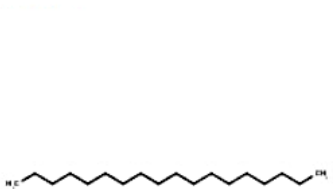

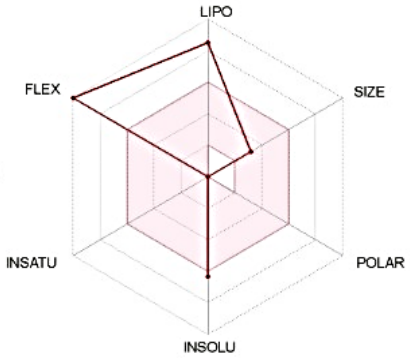

SMILES CCCCCCCCCCCCCCCCCC

Physicochemical Properties	
Formula	C18H38
Molecular weight	254.49 g/mol
Num. heavy atoms	18
Num. arom. heavy atoms	0
Fraction Csp3	1.00
Num. rotatable bonds	15
Num. H-bond acceptors	0
Num. H-bond donors	0
Molar Refractivity	88.64
TPSA	0.00 Å²

Lipophilicity	
Log $P_{o/w}$ (iLOGP)	5.23
Log $P_{o/w}$ (XLOGP3)	9.37
Log $P_{o/w}$ (WLOGP)	7.27
Log $P_{o/w}$ (MLOGP)	6.92
Log $P_{o/w}$ (SILICOS-IT)	7.10
Consensus Log $P_{o/w}$	7.18

Water Solubility	
Log *S* (ESOL)	-6.33
Solubility	1.19e-04 mg/ml ; 4.67e-07 mol/l
Class	Poorly soluble
Log *S* (Ali)	-9.27
Solubility	1.35e-07 mg/ml ; 5.32e-10 mol/l
Class	Poorly soluble
Log *S* (SILICOS-IT)	-7.13
Solubility	1.86e-05 mg/ml ; 7.33e-08 mol/l
Class	Poorly soluble

Pharmacokinetics	
GI absorption	Low
BBB permeant	No
P-gp substrate	No
CYP1A2 inhibitor	Yes
CYP2C19 inhibitor	No
CYP2C9 inhibitor	No
CYP2D6 inhibitor	No
CYP3A4 inhibitor	No
Log K_p (skin permeation)	-1.20 cm/s

Druglikeness	
Lipinski	Yes; 1 violation: MLOGP>4.15
Ghose	No; 1 violation: WLOGP>5.6
Veber	No; 1 violation: Rotors>10
Egan	No; 1 violation: WLOGP>5.88
Muegge	No; 2 violations: XLOGP3>5, Heteroatoms<2
Bioavailability Score	0.55

Medicinal Chemistry	
PAINS	0 alert
Brenk	0 alert
Leadlikeness	No; 2 violations: Rotors>7, XLOGP3>3.5
Synthetic accessibility	2.49

Appendix XI: Pharmacokinetic, drug-likeness and medicinal chemistry properties 5H,10H-Dipyrrolo[1,2-a:1',2'-d]pyrazine-5,10-dione, octahydro-, (5aS,10aS)-.

Molecule 1

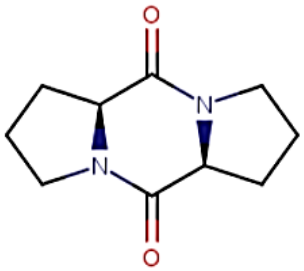

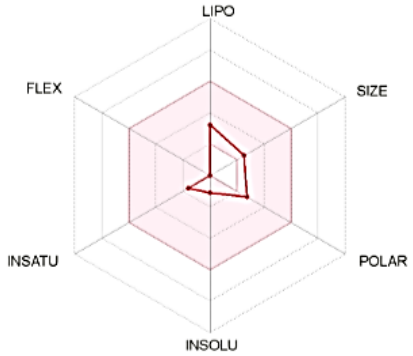

SMILES O=C1[C@@H]2CCCN2C(=O)[C@H]2N1CCC2

Physicochemical Properties	
Formula	C10H14N2O2
Molecular weight	194.23 g/mol
Num. heavy atoms	14
Num. arom. heavy atoms	0
Fraction Csp3	0.80
Num. rotatable bonds	0
Num. H-bond acceptors	2
Num. H-bond donors	0
Molar Refractivity	57.86
TPSA	40.62 Å²

Lipophilicity	
Log $P_{o/w}$ (iLOGP)	1.90
Log $P_{o/w}$ (XLOGP3)	0.10
Log $P_{o/w}$ (WLOGP)	-0.78
Log $P_{o/w}$ (MLOGP)	0.35
Log $P_{o/w}$ (SILICOS-IT)	0.28
Consensus Log $P_{o/w}$	0.37

Water Solubility	
Log *S* (ESOL)	-1.11
Solubility	1.52e+01 mg/ml ; 7.81e-02 mol/l
Class	Very soluble
Log *S* (Ali)	-0.51
Solubility	6.03e+01 mg/ml ; 3.10e-01 mol/l
Class	Very soluble
Log *S* (SILICOS-IT)	-0.64
Solubility	4.43e+01 mg/ml ; 2.28e-01 mol/l
Class	Soluble

Pharmacokinetics	
GI absorption	High
BBB permeant	No
P-gp substrate	No
CYP1A2 inhibitor	No
CYP2C19 inhibitor	No
CYP2C9 inhibitor	No
CYP2D6 inhibitor	No
CYP3A4 inhibitor	No
Log K_p (skin permeation)	-7.41 cm/s

Druglikeness	
Lipinski	Yes; 0 violation
Ghose	No; 1 violation: WLOGP<-0.4
Veber	Yes
Egan	Yes
Muegge	No; 1 violation: MW<200
Bioavailability Score	0.55

Medicinal Chemistry	
PAINS	0 alert
Brenk	0 alert
Leadlikeness	No; 1 violation: MW<250
Synthetic accessibility	2.28

Appendix XII: Constants of Acids and bases: Commercial Concentrated Reagent.

Substance	Formula	Molecular weight	Specific gravity	Molarity
Sulphuric acid	H_2SO_4	98.1	1.84	18.0
Hydrochloric acid	HCL	36.46	1.18	11.65
DMSO	C_2H_6OS	78.13		14.1

Appendix XIII: Preparation of lysis buffer.

Constituent	Stock	Final Conc	10 ml	50 ml
Tris-HCL	1 M	100 mM	1 ml	5 ml
EDTA	0.5 %	60 mM	1.2 ml	6 ml
NaCl	5 M	150 mM	300 µl	1.5 ml
SDS	10 %	1 %	1 ml	5 ml
H_20			6.5 ml	32.5 ml

Appendix XIV: Calculation of concentration

Sample No.	Endophyhte Isolate	Mass of empty weigh boat(g) **[WBM]**	Mass of weigh boat plus extract(g) **[GEM]**	Mass of Extract(g) **[EM]**	Mass of Extract(mg)	Concentration(mg/µl) **C**	Concentration(mg/µl) **C**	Concentration(mg/µl) **C**
				EM=GEM-WBM	g -» mg x1000	C=Mass(mg)/Vol(µl) Volume=50µl	C=Mass(mg)/Vol(µl) Volume=85µl	C=Mass(mg)/Vol(µl) Volume=100µl
1	A8[1]	2.03	2.26	0.23	230.00	4.60	2.71	2.30
2	A8[2]	2.03	2.24	0.21	210.00	4.20	2.47	2.10
3	A9[1]	2.03	2.18	0.15	150.00	3.00	1.76	1.50
4	A9[2]	2.03	2.27	0.24	240.00	4.80	2.82	2.40
5	B1	2.03	2.28	0.25	250.00	5.00	2.94	2.50
6	B3	2.03	2.18	0.15	150.00	3.00	1.76	1.50
7	B6	2.03	2.16	0.13	130.00	2.60	1.53	1.30
8	B10[1]	2.03	2.18	0.15	150.00	3.00	1.76	1.50
9	B10[2]	2.03	2.25	0.22	220.00	4.40	2.59	2.20
10	C5[1]	2.03	2.24	0.21	210.00	4.20	2.47	2.10
11	C5[2]	2.03	2.30	0.27	270.00	5.40	3.18	2.70
12	D8	2.03	2.17	0.14	140.00	2.80	1.65	1.40
13	E4	2.03	2.24	0.21	210.00	4.20	2.47	2.10
14	E7[1]	2.03	2.26	0.23	230.00	4.60	2.71	2.30
15	E7[2]	2.03	2.26	0.23	230.00	4.60	2.71	2.30
16	E8[1]	2.03	2.21	0.18	180.00	3.60	2.12	1.80

Sample No.	Endophyhte Isolate	Mass of empty weigh boat(g) **[WBM]**	Mass of weigh boat plus extract(g) **[GEM]**	Mass of Extract(g) **[EM]**	Mass of Extract(mg)	Concentration(mg/µl) **C**	Concentration(mg/µl) **C**	Concentration(mg/µl) **C**
				EM=GEM-WBM	g -» mg x1000	C=Mass(mg)/Vol(µl) Volume=50µl	C=Mass(mg)/Vol(µl) Volume=85µl	C=Mass(mg)/Vol(µl) Volume=100µl
19	F^2	2.03	2.22	0.19	190.00	3.80	2.24	1.90
20	G^1	2.03	2.25	0.22	220.00	4.40	2.59	2.20
21	G^3	2.03	2.24	0.21	210.00	4.20	2.47	2.10
22	H^1	2.03	2.31	0.28	280.00	5.60	3.29	2.80
23	H^3	2.03	2.29	0.26	260.00	5.20	3.06	2.60